Universidade Federal de São João Del-Rei
Programa de Pós-Graduação em Bioengenharia

BÁRBARA FRANÇA NEGRI

Caracterização funcional dos genes de milho homólogos ao *Phosphorus Starvation Tolerance 1*, responsável por aumentar a superfície radicular, a aquisição de fósforo e a produção de grãos em arroz

SÃO JOÃO DEL REI
MINAS GERAIS - BRASIL
MARÇO 2019

BÁRBARA FRANÇA NEGRI

Caracterização funcional dos genes de milho homólogos ao *Phosphorus Starvation Tolerance 1*, responsável por aumentar a superfície radicular, a aquisição de fósforo e a produção de grãos em arroz

TESE SUBMETIDA AO PROGRAMA DE PÓS-GRADUAÇÃO EM BIOENGENHARIA, DA UNIVERSIDADE FEDERAL DE SÃO JOÃO DEL REI COMO PARTE DOS REQUISITOS NECESSÁRIOS PARA A OBTENÇÃO DO TÍTULO DE *DOCTOR SCIENTIAE.*

SÃO JOÃO DEL REI
MINAS GERAIS - BRASIL
MARÇO 2019

BÁRBARA FRANÇA NEGRI

CARACTERIZAÇÃO FUNCIONAL DOS GENES DE MILHO HOMÓLOGOS AO *PHOSPHORUS STARVATION TOLERANCE 1*, RESPONSÁVEL POR AUMENTAR A SUPERFÍCIE RADICULAR, A AQUISIÇÃO DE FÓSFORO E A PRODUÇÃO DE GRÃOS EM ARROZ

Tese submetida ao Programa de Pós-graduação em Bioengenharia, da Universidade Federal de são João del-Rei como parte dos requisitos necessários para a obtenção do título de *Doctor Scientiae.*

Aprovada: 27 de março de 2019

Profa. Dra. Janaína de Oliveira Melo
UFVJM

Prof. Dr. Leonardo Lucas Carnevalli Dias
UFSJ

Prof. Dr. Luiz Eduardo Vieira Del Bem
UFMG

Profa. Dra. Cláudia Teixeira Guimarães
Embrapa/UFSJ

Profa. Dra. Sylvia Morais de Sousa Tinoco
Orientadora – Embrapa/UFSJ

Dedico este trabalho à minha doce e querida irmã, Nana.

AGRADECIMENTOS

Aos meus queridos pais, Vera Lúcia e José Negri, que com muito carinho dedicaram à vida deles em prol dos filhos, mesmo que isso significasse muitas vezes abdicarem dos seus próprios desejos. Obrigada por me ensinarem os valores da vida, pelos incentivos, pela dedicação e pelas sábias palavras nos momentos mais difíceis. Aos meus amados irmãos, Danielle e Tiago, por compreenderem a minha ausência e por me amarem mesmo assim. Ao Christian, pelo incentivo, companheirismo e pela compreensão.

A minha orientadora, Dra. Sylvia Morais, que foi e é a verdadeira mãe acadêmica. Obrigada por me mostrar a existência desse mundo acadêmico, por acreditar no meu potencial e por ter me incentivado a seguir por esse caminho que antes achava inacessível. Obrigada por me fazer acreditar que é possível alcançar os sonhos tão desejados. Os meus mais sinceros agradecimentos por ter depositado em mim tamanha confiança.

Ao Gabriel, pelos incentivos, auxílios, contribuições e ensinamentos. A Laiane, minha companheira de jornada acadêmica. Obrigada por me ensinar tanto, por ser tão amável e prestativa. As minhas queridas companheiras de jornada, Denise, Mariana, Simara e Karine obrigada por todos os auxílios, contribuições e por todas as risadas.

Aos meus co-orientadores, Dra. Claudia Teixeira Guimarães e Dr. Jurandir Vieira Magalhães, pelos ensinamentos, assim como a Dra. Andrea Almeida Carneiro e Dra. Maria Marta Pastina, que sempre me ajudaram. Aos analistas e técnicos dos laboratórios da Embrapa Milho e Sorgo, Ubiraci, Beatriz, Meire, Célio, Gislene e Miguel, pelos grandes ensinamentos. Ao pessoal da casa de vegetação: José Neto, Célio e Geraldo pela ajuda constante nos experimentos nas casas de vegetação.

Aos colegas de trabalho, funcionários e estudantes do Núcleo de Biologia Aplicada da Embrapa Milho e Sorgo, que de alguma forma contribuíram para o meu crescimento profissional e pessoal.

A UFSJ pela oportunidade e à Coordenação de Aperfeiçoamento de Pessoal de Nível Superior (CAPES) pela concessão da bolsa de estudos.

O meu sincero agradecimento a todos.

“A mente que se abre a uma nova ideia, jamais voltará ao seu tamanho original”

(Albert Einstein)

SUMÁRIO

RESUMO ... 12
ABSTRACT ... 14
DELINEAMENTO DA TESE ... 16
1 INTRODUÇÃO ... 17
1.1 A CULTURA DO MILHO ... 17
1.2 FÓSFORO – UM ELEMENTO ESSENCIAL ... 19
1.3 MECANISMOS DE EFICIÊNCIA DE AQUISIÇÃO DE P ... 20
1.4 SISTEMA RADICULAR DO MILHO ... 22
1.5 RAÍZES EMBRIONÁRIAS DO MILHO ... 22
1.6 RAÍZES PÓS-EMBRIONÁRIAS DO MILHO ... 23
1.7 ZONAS DE CRESCIMENTO E DESENVOLVIMENTO DAS RAÍZES ... 24
1.8 REGULAÇÃO DA EXPRESSÃO DE GENES ENVOLVIDOS NA MORFOLOGIA DO SISTEMA RADICULAR E NA TOLERÂNCIA AO ESTRESSE DE P ... 25
1.9 GENES *PHOSPHORUS-STARVATION TOLERANCE 1* (*PSTOL1*) ... 27
1.9.1 *OsPSTOL1* ... 27
1.9.2 *TaPSTOL* ... 28
1.9.3 *SbPSTOL1* ... 29
1.9.4 *ZmPSTOL1* ... 30
2 OBJETIVOS ... 32
3 REFERÊNCIAS BIBLIOGRÁFICAS ... 33
CAPÍTULO 1 ... 44
ABSTRACT ... 44
INTRODUCTION ... 45
MATERIALS AND METHODS ... 48
Maize transformation via *Agrobacterium tumefaciens* with rice, maize and sorghum *PSTOL1* ... 48
Phenotypic assessment of root morphology in hydroponics ... 49
Expression analysis of *PSTOL1* genes under low-P ... 50
Phenotypic assessment of maize biomass accumulation and plant height under low and high P concentrations in the soil ... 50
Statistical analyses ... 51
RESULTS ... 51
Root morphology of non-transgenic lines ... 51

Selection of transgenic events 52

Phenotypic characterization of maize events overexpressing *PSTOL1* for root morphology in nutrient solution with low-P 53

Overexpression of *PSTOL1* genes increases shoot dry matter accumulation in a low P soil 54

DISCUSSION 55

ACKNOWLEDGEMENTS 57

REFERENCES 59

TABLES 64

FIGURE LEGENDS 68

FIGURES 70

CAPÍTULO 2 75

ABSTRACT 75

INTRODUÇÃO 76

MATERIAL E MÉTODOS 79

Análise da expressão gênica em genótipos contrastantes para eficiência no uso de P 79

Análise de *expression Genome*-W*ide* Association *Study* (*eGWAS*) ... 80

Sequenciamento da região promotora de *ZmPSTOL1_3.06* e obtenção de eventos *ZmPSTOL1_3.06*::*Gus* 82

Análise *in silico* da região promotora 83

Ensaios fluorimétrico e histoquímico 83

Obtenção das plantas transgênicas superexpressando *ZmPSTOL1_3.06* 84

Comprimento dos pelos radiculares 84

RESULTADOS 84

***ZmPSTOL1_3.06* é mais expresso na zona de diferenciação celular da raiz primária do genótipo eficiente ao uso de P** 84

Análise de eGWAS com linhagens de milho contrastantes para morfologia radicular 86

Caracterização da região promotora de *ZmPSTOL1_3.06* 89

DISCUSSÃO 95

***ZmPSTOL1_3.06* é uma quinase expressa preferencialmente na raiz em diferentes estágios da planta** 95

A região promotora de *ZmPSTOL1_3.06* possui elementos cis-regulatórios relacionados com P e formação de pelos radiculares 97

A superexpressão de *ZmPSTOL1_3.06* aumenta o comprimento dos pelos radiculares em milho..... 98
REFERÊNCIAS..... 101
4 CONCLUSÃO GERAL..... 109
5 ANEXO..... 110

LISTA DE FIGURAS

CAPÍTULO 1

Figure 1: Phenotypic characterization of non-transgenic maize lines in low P conditions. (A) Images of the B104, L3 and L22 root systems……70

Figure 2: Schematic structure of pMCG1005-*PSTOL1* cassette…....……...71

Figure 3: Correlation analysis of root morphology traits, shoot dry weight and shoot P content traits and *PSTOL1* expression (ΔCt)……...……72

Figure 4: Phenotypic characterization of wild type B104 and transgenic lines *PSTOL1* (*OsPSTOL1, SbPSTOL1* and *ZmPSTOL1*) in nutrient solution with low-P.....73

Figure 5: Phenotypic characterization of wild type B104 and transgenic lines PSTOL1 (*OsPSTOL1, SbPSTOL1* and *ZmPSTOL1*) grown in a low P soil.....74

CAPÍTULO 2

Figura 1: Perfil de expressão do gene *ZmPSTOL1_3.06* nas linhagens L3 e L22 crescidas em solução nutritiva com baixo P (2,5 µM).....86

Figura 2: Expressão dos genes candidatos no sistema radicular de linhagens de milho contrastantes quanto ao comprimento total de raízes.....88

Figura 3: Esquema da sequência do gene *ZmPSTOL1_3.06* das linhagens L3 e L22.....90

Figura 4: Perfil da atividade de GUS sob regulação do promotor *ZmPSTOL1_3.06*(L3).....92

Figura 5: Análise de expressão gênica dos genes (**A**) *ZmPSTOL1_3.06*, (**B**) *Rth1,* (**C**) *Rth3* e imagem de raiz selvagem – B104 (**E**) e de eventos *UBI::ZmPSTOL1_3.06* (**F**).....94

Figura 6: Quantificação dos pelos radiculares (mm) das linhagens L3 e L22...95

LISTA DE TABELAS

CAPÍTULO 1

Table 1: Analysis of variance for three quantitative traits of transgenic maize grown in greenhouse conditions with low and high P……64
Supplemental Table S1: Primers used for PCR and RT-qPCR assays……66
Supplemental Table S2: Description of maize transgenic events overexpressing *OsPSTOL1*, *SbPSTOL1* and *ZmPSTOL1* genes……...67

CAPÍTULO 2

Tabela 1: Lista dos genótipos de milho pertencentes ao Banco de Germoplasma e Programa de Melhoramento da Embrapa Milho e Sorgo utilizados nos experimentos de expressão gênica.....81

Tabela 2: Posição, distância e p-valor dos marcadores significativos na análise de
eGWAS.....89

Tabela 3: Elementos cis regulatórios localizados na região promotora do gene *ZmPSTOL1_3.06* (L3) (-2282 pb) e *ZmPSTOL1_3.06* (L22) (-2613 pb) envolvidos na formação de raiz e estresse de P.....91

NEGRI, Bárbara França (DS). Universidade Federal de São João del Rei, março de 2019. Título: **Caracterização funcional dos genes de milho homólogos ao *Phosphorus Starvation Tolerance 1*, responsável por aumentar a superfície radicular, a aquisição de fósforo e a produção de grãos em arroz**. Orientadora: Dra. Sylvia Morais de Sousa Tinoco. Co-orientadores: Dra. Claudia Teixeira Guimarães e Dr. Jurandir Vieira Magalhães.

RESUMO

A baixa disponibilidade de fósforo (P) é uma das principais limitações para produtividade de cereais em solos tropicais. A modificação na morfologia radicular é o principal mecanismo de adaptação ao baixo P pelas plantas, uma vez que proporcionam maior aquisição do nutriente, através de uma maior exploração do solo. O gene *Phosphorus-starvation tolerance 1* (*PSTOL1*) foi identificado como o responsável pelo lócus *Phosphorus Uptake 1* (*Pup1)*, e codifica uma proteína quinase responsável pelo aumento do crescimento precoce das raízes, absorção de P e, produção de grãos em arroz. Homólogos do *OsPSTOL1* em sorgo (*Sorghum bicolor, SbPSTOL1*) e em milho (*Zea mays, ZmPSTOL1*) foram identificados via mapeamento associativo e de lócus de característica quantitativa (QTLs) na modulação da morfologia do sistema radicular e aumento de produção sob condições de baixo P. Este trabalho teve como objetivo caracterizar funcionalmente os genes de arroz *OsPSTOL1*, sorgo *(Sb03g006765*, *Sb03g031690* e *Sb07g002840)* e milho *(ZmPSTOL1_8.05*, *ZmPSTOL1_3.06* e *ZmPSTOL1_8.02)*. Para tanto, os genes *OsPSTOL1*, *SbPSTOL1* e *ZmPSTOL1* foram superexpressos na linhagem de milho B104*.* Os eventos transgênicos foram analisados em solução nutritiva sob baixo P e em solo sob baixo P e alto. Os eventos *OsPSTOL1* e *SbPSTOL1* tiveram um incremento de raízes superfinas, o que levou a um aumento da área de superfície radicular e de biomassa vegetal, tanto em câmara de crescimento quanto em casa de vegetação. Apenas o evento superexpressando o gene *ZmPSTOL1_3.06* apresentou diferença significativa para altura da planta quando comparado com à linhagem selvagem B104. Além disso, foi feita a caracterização detalhada do gene de milho *ZmPSTOL1_3.06*, sendo analisada

a expressão e a regulação desse gene. A expressão de *ZmPSTOL1_3.06* ocorreu preferencialmente na zona de diferenciação da raiz primária, mais precisamente nos pelos radiculares, do genótipo eficiente na aquisição de P e foi modulada pela disponibilidade e P. A presença dos motivos de ligação relacionados a aquisição de P (*ZmPHR1)* e formação de pelos radiculares (*ZmLRL5)* na região promotora de *ZmPSTOL1_3.06*, junto ao fato das plantas transgênicas sob seu promotor apresentarem maior atividade de GUS sob baixo P e nos pelos radiculares indicaram uma potencial relação entre esses fatores de transcrição e *ZmPSTOL1_3.06.* Além disso, plantas transgênicas superexpressando *ZmPSTOL1_3.06* alteraram o alongamento dos pelos radiculares e a expressão de genes relacionados com a sua formação. Os resultados sugerem até o momento, que os genes *PSTOL1* tem um papel mais geral no desenvolvimento do sistema radicular, o que resulta no aumento da eficiência de P, que pode beneficiar a produção de cereais.

Palavras-chaves: Eficiência de P; raiz; quinase; expressão gênica.

NEGRI, Bárbara França (DS). Universidade Federal de São João del Rei, março de 2019. Título: **Functional characterization of maize genes homologous to *Phosphorus Starvation Tolerance 1*, responsible for increasing a root surface, phosphorus acquisition and grain yield in rice.** Orientadora: Dra. Sylvia Morais de Sousa Tinoco. Co-orientadores: Dra. Claudia Teixeira Guimarães e Dr. Jurandir Vieira Magalhães.

ABSTRACT

Low phosphorus (P) availability is a major constraint for cereal productivity in tropical soils. Modifications in root morphology are the major adaptation mechanism plant developed under P starvation, once provide greater nutrient acquisition through larger soil exploration. The *Phosphorus-starvation tolerance 1* (*PSTOL1*) gene was identified as responsible for the locus *Phosphorus Uptake 1* (*Pup1*), and encodes a protein kinase responsible for increased early root growth, P uptake, and grain yield in rice. Sorghum (*Sorghum bicolor*, *SbPSTOL1*) and maize (*Zea mays*, *ZmPSTOL1*) homologs to *OsPSTOL1* were identified via association and quantitative trait loci (QTLs) mapping of traits related to root system morphology modulation and yield increased under low P. This study aimed to characterize rice *OsPSTOL1*, sorghum (*Sb03g006765*, *Sb03g031690* and *Sb07g002840*) and maize (*ZmPSTOL1_8.05*, *ZmPSTOL1_3.06* and *ZmPSTOL1_8.02*) genes. For this, *OsPSTOL1*, *SbPSTOL1* e *ZmPSTOL1* genes were overexpressed in maize line B104. The events were analyzed in nutrient solution under low P and in soil under low and high P. *OsPSTOL1* and S*bPSTOL1* events presented an increase of superfine roots, which led to an increase in root surface area and plant biomass, both in the growing chamber and in the greenhouse conditions. Only the event overexpressing the gene *ZmPSTOL1_3.06* presented significant difference for plant height when compared to B104. In addition, we performed a detailed characterization of the

ZmPSTOL1_3.06 gene, analyzing its expression and regulation. *ZmPSTOL1_3.06* expression occurred preferentially in the differentiation zone of the primary root, more precisely in the root hairs of the P-efficient line and was modulated by P availability. The presence of the binding motifs related to the P acquisition (*ZmPHR1*) and the formation of root hairs (*ZmLRL5*) in *ZmPSTOL1_3.06* promoter region, together with the fact that the transgenic plants under its promoter showed higher GUS activity under low P and in root hairs, indicated a potential relationship between these transcription factors and *ZmPSTOL1_3.06*. Moreover, transgenic plants overexpressing *ZmPSTOL1_3.06* altered root hairs elongation the expression of genes related to their formation. Our results suggested so far, that the *PSTOL1* genes have a more general role in the root system development, which results in an increased P efficiency, which may benefit cereal production.

Keywords: P efficiency; root; kinase; gene expression.

DELINEAMENTO DA TESE

Esta tese é constituída por dois capítulos e está subdividida da seguinte maneira:

- Introdução Geral, contendo o referencial teórico sobre os principais temas abordados na tese: a cultura do milho; a importância do fósforo e os mecanismos de eficiência ligados à sua aquisição; sistema radicular do milho e a regulação da expressão de genes relacionados a sua formação e a tolerância ao estresse de P; e os genes *PSTOL1*.

- Capítulo 1, que corresponde a um artigo científico que será submetido à revista Journal of Experimental Botany: "Overexpression of *PSTOL1*_like genes increases root surface área and biomass accumulation for maize cultivated under low P availability".

- Capítulo 2, que corresponde a um artigo que será submetido à revista Plant Molecular Biology: "*Phosphorus-Starvation Tolerance 1* (*ZmPSTOL_3.06*) está associado a formação do pelo radicular e eficiência de fósforo em milho".

- Anexo, que contém o artigo científico de co-autoria publicado na revista BMC Plant Biology intitulado "Multiple interval QTL mapping and searching for *PSTOL1* homologs associated with root morphology, biomass accumulation and phosphorus content in maize seedlings under low-P".

1 INTRODUÇÃO

1.1 A CULTURA DO MILHO

O milho (*Zea mays* L.) é uma planta que pertence ao gênero *Zea*, família Poaceae e a ordem Cyperales. Dentre as espécies desse gênero*, Zea mays* L. é a espécie que possui maior interesse econômico e variabilidade quanto à composição química e estrutural dos grãos (Shah *et al*., 2016). O milho, juntamente com o arroz e o trigo, são os cereais mais cultivados no mundo e são parte da base alimentar humana. Estes cereais são consumidos de maneira direta, *in natura* ou farinhas, como também de forma indireta, através da alimentação de animais (FAO, 2015a; FAO, 2015b), constituindo cerca de 42,5% do total das calorias consumidas mundialmente (FAO, 2016). Além disso, podem ser utilizados na produção de biocombustíveis, que é uma alternativa para mitigar os impactos ambientais e atender novas demandas energéticas (Mohanty & Swain, 2019).

Com o aumento populacional, há uma crescente demanda por alimentos e consequentemente uma maior necessidade de aumentar a produtividade do milho. Estima-se que foram produzidos na safra de 2017/2018 1076,2 milhões de toneladas de milho, o que corresponde a 48% do total de cereais. Os três maiores produtores mundiais de milho são os Estados Unidos, a China e o Brasil com uma produção estimada da safra de 2017/2018 de aproximadamente 371, 259 e 82 milhões de toneladas, respectivamente. O Brasil também participa do mercado internacional, tendo exportado cerca 23,5 milhões de toneladas da sua produção, o que corresponde a 29% do total (USDA, 2018).

De acordo os dados da Companhia Nacional de Abastecimento (CONAB), a região Centro-Sul do Brasil foi a que mais produziu milho na safra de 2017/2018 com 71.817,1 milhões de toneladas, enquanto a região Norte/Nordeste produziu 8.968,9 milhões de toneladas (CONAB, 2019). O milho é cultivado principalmente na região do Cerrado, que ocupa uma área de 204,7

milhões de hectares da porção central do Brasil (Sano *et al*., 2008), cujo 46% do solo é do tipo latossolo, que apresenta baixa fertilidade e alta acidez.

O melhoramento genético do milho seja por método convencional ou transgenia, juntamente com práticas agrícolas associadas, tais como: métodos de cultivo, fertilizantes, maquinário e mecanização, armazenamento de grãos e sementes, entre outros, garantem a produtividade e minimizam a exploração de novas áreas de cultivo (Sariningpuri *et al*., 2017). Dentro desse contexto, os transgênicos ganharam destaque nos últimos 20 anos, uma vez que a produtividade e o rendimento das lavouras geneticamente modificadas foram, em média, maiores do que em plantios convencionais, devido à redução na aplicação de defensivos por hectare e diminuição das perdas em virtude do ataque de pragas (CIB, 2018). No ano de 2017, cerca de 189,8 mi/ha foram usados para cultivo de transgênicos no mundo (ISAAA, 2018). O Brasil foi o segundo país que mais plantou transgênico, ficando atrás somente dos Estados Unidos (ISAAA, 2018). Em 2017, dos cerca de 50,2 mi/ha plantados de transgênicos no Brasil, 31% corresponde a produção de milho (ISAAA, 2018), que é a espécie que possui mais eventos regulamentados no mundo (232 aprovações em 30 países) (ISAAA, 2018).

Recentemente, diversos genótipos de milho (B104, B73, Mo17, CML247, PH207 e W22) que vem sendo utilizados como modelos para estudos genético-moleculares relacionados a tolerância à estresses bióticos, como resistência a bactérias, fungos e viroses (Singh *et al*., 2016; Rossi *et al*., 2018; Ladejobi *et al*., 2018), estresses abióticos, tais como hídrico, metais e fósforo (Azevedo *et al*., 2015; Zhao *et al*., 2018a; Zhao *et al*., 2018b) tiveram seu genoma completamente sequenciado *(https://www.maizegdb.org/*). O genótipo B104, é derivado da mesma população do B73 (genoma referência) e apesar de muito similares (93% de similaridade, como definido por Romay *et al.* 2013), o B104 é facilmente transformável, enquanto o B73 não é. Essa característica permite que ele seja utilizado como uma ferramenta biotecnológica, tanto para estudos relacionados à caracterização funcional de genes quanto para introdução de genes de interesse agronômico para o melhoramento genético (Anami *et al*., 2010; Raji *et al*., 2018).

1.2 FÓSFORO – UM ELEMENTO ESSENCIAL

O fósforo (P) é um dos elementos essenciais para o crescimento das plantas, onde a sua concentração varia de 0,05 a 0,50% do peso seco (Bieleski, 1973; Schachtman *et al*., 1998). Este elemento tem uma participação em uma variedade de processos, incluindo a geração de energia, síntese de ácido nucléico, fotossíntese, glicólise, respiração, síntese de membrana e estabilidade de ativação e inativação de enzimas, reações redox, sinalização, metabolismo de carbono e de fixação de nitrogênio (Bieleski, 1973; Schachtman *et al*., 1998; Raghothama, 1999).

Embora encontrado com abundância em muitos solos, apenas uma pequena fração está na forma disponível para as plantas (Araújo & Machado, 2006). A forma inorgânica que as plantas absorvem, H_2PO^{4-} e HPO_4^{-2}, é encontrada nos solos em uma concentração de 0,1 a 10 µM, sendo que 50% se encontra na forma não assimilável pelas plantas, levando a uma condição sub-ótima para a produção de grãos (Bieleski, 1973; Schachtman *et al*., 1998; Hinsinger, 2001; Vance *et al*., 2003). Além disso, por causa da elevada capacidade de fixação com óxidos de ferro e alumínio em solos tropicais, o P acaba se tornando um nutriente insolúvel e limitando a produtividade da cultura nessas áreas (Lopes & Cox, 1979; Raij, 1991; Rheinheimer *et al*., 2003), com eficiência de uso em torno de <15% a 20% (Mitra, 2015).

A escassez do P pode ser exacerbada, uma vez que este elemento não é renovável, sendo que as reservas atuais de fosfato devem acabar entre 50 e 200 anos. Os preços dos alimentos tendem a dobrar ou triplicar, sem fontes fosfatadas de baixo custo, caso a demanda continue a mesma ou aumente (Cordell, 2014; Sattari *et al*., 2016). Portanto, os avanços biotecnológicos associados a técnicas de melhoramento genético e manejo sustentável se tornam uma alternativa para garantir a produção de alimentos e a proteção de recursos naturais.

As plantas adquirem o P do solo diretamente pelo sistema radicular ou indiretamente pelos fungos micorrízicos arbusculares (FMA) (Bucher, 2007; Jeong *et al*., 2015). Para que ocorra a absorção de P pelas plantas é necessário

um mecanismo de absorção eficiente uma vez que as raízes absorvem e concentram o P no xilema a partir de um baixo gradiente de concentração presente na solução do solo (Raghothama, 2000; Hinsinger, 2001; Smith, 2002; Kirkbly & Johnston, 2008). De forma geral, após ser absorvido pelo processo de difusão, o P move-se do córtex ao cilindro central das raízes pelo simplasto e depois de absorvido pelo simplasma radicular, o P pode tomar cinco possíveis destinos: 1) Ingressa no compartimento metabólico (citoplasma celular e suas organelas), onde a maior assimilação de P em compostos orgânicos ocorre via formação de uma ligação anidrido no ATP; 2) uma pequena fração de P ingressa nas vias biossintéticas de lipídeos, DNA e RNA, tornando-se um componente estrutural da célula; 3) uma quantidade de P é perdida pela célula via efluxo, particularmente em condições de alto suprimento de P; 4) ocorre o influxo e armazenamento de P no vacúolo para regular a homeostase de P no interior da célula; e 5) o P é transportado simplasticamente para as células do parênquima do xilema e, posteriormente, liberado no apoplasto do xilema para o transporte à longa distância para os tecidos da parte aérea (Rausch & Bucher, 2002).

1.3 MECANISMOS DE EFICIÊNCIA DE AQUISIÇÃO DE P

A capacidade de adaptação de uma planta a baixa disponibilidade de P no solo pode ser estabelecida de duas formas, por mecanismos internos, de forma que a planta otimize a utilização de P, e por mecanismos que melhoram a aquisição de P a partir do solo. A eficiência no uso de P em milho em condições de campo está mais associada com a capacidade da planta em adquirir P do solo (eficiência de aquisição) do que com a sua capacidade em utilizar mais eficientemente o P no interior da planta (eficiência de utilização interna) (Parentoni & Souza Jr. 2008). A eficiência na aquisição de P é de duas a três vezes mais importante do que a eficiência de utilização interna para genótipos de milho tropical em condições contrastantes de P (Parentoni *et al*., 2011). Além disso, 80% dos QTLs mapeados para eficiência de aquisição de P co-localizam com QTLs de eficiência de uso de P, indicando que a eficiência na aquisição é o

principal determinante da eficiência do uso em milho tropical (Mendes *et al*., 2014).

Os mecanismos adaptativos relacionados ao aumento da aquisição de P estão associados com alterações na morfologia e arquitetura do sistema radicular, interações com microrganismos e modificações químicas na rizosfera (Vance *et al*., 2003; Ramaekers *et al*., 2010; Lynch, 2011). O P é um elemento imóvel localizado principalmente na camada superior do solo, sendo que genótipos eficientes apresentam maior número de raízes adventícias, sistema radicular mais superficial e com menor diâmetro, raízes laterais mais dispersas, pelos radiculares mais longos e densos, maior exsudação de ácidos orgânicos e fosfatases, maior micorrização e maior biomassa radicular (Lynch, 2007; Ramaekers *et al*., 2010; Lynch, 2011). Em genótipos eficientes, as alterações da morfologia do sistema radicular levam ao aumento da aquisição de P com um custo metabólico mínimo (Lynch & Brown 2001; Lynch & Ho 2005; Lynch, 2011). Genótipos de milho com maior número de raízes coronais ou adventícias exploraram melhor a parte superficial do solo e melhoram a aquisição de P sob baixa disponibilidade deste nutriente, resultando em um melhor crescimento e rendimento de plantas (Sun *et al*., 2018).

Em plantas jovens com poucas raízes adventícias, a ramificação das raízes laterais pode aumentar a exploração de novos domínios do solo ainda não alcançados pelas raízes adventícias (Lynch, 2011). Linhagens de milho provenientes do cruzamento das linhagens B73 (P-ineficiente) e Mo17 (P-eficiente) apresentam uma maior densidade de raízes laterais (Trachsel *et al.*, 2011; Trachsel *et al.*, 2013; Zhan & Lynch, 2015; Zhan *et al.*, 2015), maior aquisição de P, maior biomassa e consequentemente, um aumento no rendimento de grãos (Jia *et al.,* 2018).

Em uma estratégia adaptativa para melhorar a eficiência metabólica do forrageamento do solo sob estresse, as raízes favorecem o crescimento primário (alongamento) em relação ao crescimento secundário (espessamento radial) para alcançar uma maior exploração dos domínios do solo (Lynch, 2007; Lynch e Brown, 2008; Lynch, 2011). Foi observada uma correlação negativa entre diâmetro médio e a área de superfície da raiz numa população de linhagens endogâmicas recombinantes (RILs) provenientes de um cruzamento de

genótipos contrastantes para eficiência de aquisição de P (L3 – eficiente e L22 – ineficiente) crescidas em solução nutritiva com baixo P (Azevedo *et al.,* 2015). Além disso, o diâmetro radicular exerce um efeito indireto sob o peso seco e o conteúdo de P da planta via área de superfície radicular (Azevedo *et al.,* 2015).

1.4 SISTEMA RADICULAR DO MILHO

O sistema radicular tem duas funções principais, a aquisição de água e nutrientes do solo, e de ancoragem. O estabelecimento adequado da arquitetura básica de todo o sistema radicular é de fundamental importância para o cumprimento destas funções. No milho a estrutura radicular é compreendida por raízes que são classificadas como embrionárias e pós-embrionárias (Hochholdinger *et al*., 2004; Atkinson *et al*., 2014). As raízes embrionárias são compostas por uma única raiz primária e raízes seminais embrionárias que emergem do nó escutelar do milho. Essas raízes são importantes para o vigor das plântulas nos estágios iniciais do desenvolvimento (Sanguineti *et al*., 1998). Já as raízes pós-embrionárias compõem o sistema radicular da planta adulta e compreendem nas raízes de primeira ordem, denominadas coronais, adventícias ou nodais, e pelas raízes chamadas de segunda ordem, que emergem de outras raízes, como as raízes laterais e os pelos radiculares, que permitem o aumento da exploração do solo e da superfície de absorção (Yu *et al.,* 2016).

1.5 RAÍZES EMBRIONÁRIAS DO MILHO

A primeira raiz a emergir é a primária que é derivada do tecido meristemático formado embrionariamente. A raiz primária é composta pelo xilema e floema dentro de uma coluna vascular e pelo periciclo, que constituem a estela, que é rodeada por camadas concêntricas de tecido da epiderme, do córtex e da endoderme (Smith & De Smet, 2012). A iniciação da raiz primária

ocorre durante a embriogênese através da especificação de uma única célula superior do suspensor, denominada hipófise. Essa célula gera o centro quiescente, através de divisão celular assimétrica, formando o meristema da raiz primária (De Smet *et al*., 2010). Esse meristema primário dá origem a todas as células e tecidos que compõem a raiz. A divisão celular, combinada com alongamento e diferenciação, é responsável pelo crescimento contínuo e desenvolvimento da raiz (Jiang & Feldman, 2005).

Ao contrário da raiz primária, as raízes seminais são de número variável e surgem da coleorriza e são visíveis apenas por um curto período de tempo após a germinação, sendo logo substituídas pelas raízes coronais (Imin *et al*., 2007). As raízes seminais de monocotiledôneas, como o milho e o arroz, são formadas embrionariamente e os primórdios emergem do nó escutelar em estágios tardios da embriogênese (Sass, 1977; Erdelska & Vidovencova, 1993; Feldman, 1994; Hochhildinger *et al.*, 2004).

1.6 RAÍZES PÓS-EMBRIONÁRIAS DO MILHO

As raízes coronais, também chamadas de raízes nodais e seminais pós-embrionárias surgem durante toda a vida da planta nos nós coleoptilares, podendo ser consideradas raízes de primeira ordem pelo fato de não emergirem de outra raiz (Hochholdinger & Tuberosa, 2009). Esse tipo de raiz é exclusivo das espécies de monocotiledôneas e proporcionam apoio mecânico necessário para a sustentação da planta adulta (Hochholdinger, 2009). Além disso, juntamente com as raízes laterais, são de grande importância para o fornecimento de água e nutrientes, compondo a maior parte do sistema radicular fibroso dos cereais nas plantas adultas (Hochholdinger *et al*., 2004).

Os primórdios das raízes laterais são originários de um subconjunto de células na periferia da parte vascular interna da raiz. Em milho, arroz, cevada e trigo, as células quiescentes originam-se do periciclo e células da endoderme opostas ao floema. Ao contrário das dicotiledôneas, como Arabidopsis, em que as raízes laterais são exclusivamente provenientes do periciclo e de células

opostas ao protoxilema (Casero *et al*., 1995; Demchenko & Demchenko, 2001). As raízes laterais contribuem significativamente para plasticidade do sistema radicular do milho e absorção de água e nutrientes (Yu *et al*., 2016).

O aumento na proliferação de pelos radiculares permite um grande aumento do volume de solo a ser explorado. Nas plantas cultivadas, os pelos radiculares contribuem com até 77% da área total de raiz, maximizando o volume de solo a ser explorado, com um mínimo de biomassa possível (Parker *et al.*, 2000). Eles são um instrumento para aquisição de nutrientes, água, ancoragem e interação com microrganismos (Gilroy & Jones, 2000). Os pelos radiculares são unicelulares e uma das poucas células nas plantas superiores que usam o crescimento no ápice para expandir (Kropf *et al.*, 1998). No milho (*Zea mays*), três mutantes, *roothairless1*, *2*, e *3* (*rth1*, *rth2*, *rth3*), foram identificados por afetar o alongamento dos pelos radiculares, porém exibem iniciação normal da sua formação (Wen e Schnable, 1994). Mutantes com defeitos na formação de pelos radiculares têm menor capacidade de adquirir P e crescem menos do que os selvagens (Hochholdinger & Tuberosa, 2009).

1.7 ZONAS DE CRESCIMENTO E DESENVOLVIMENTO DAS RAÍZES

Todas as raízes do milho, apresentam uma estrutura longitudinal caracterizada por uma coifa na extremidade terminal, uma zona meristemática subterminal (juntas denominadas de zona de divisão celular), seguida por zonas nas quais células recém-formadas se alongam (zona de alongamento celular) e se diferenciam (zona de diferenciação celular) (Ishikawa & Evans, 1995). A zona de diferenciação, na qual tipos celulares funcionalmente distintos são formados, pode ser identificada pela presença de pelos radiculares epidérmicos. Assim, as raízes representam um gradiente de diferenciação celular ao longo do eixo longitudinal, células jovens e indiferenciadas estão localizadas na extremidade distal perto da ponta da raiz, enquanto células diferenciadas estão localizadas em direção à extremidade proximal da raiz (Ishikawa & Evans, 1995).

1.8 REGULAÇÃO DA EXPRESSÃO DE GENES ENVOLVIDOS NA MORFOLOGIA DO SISTEMA RADICULAR E NA TOLERÂNCIA AO ESTRESSE DE P

As respostas genéticas aos estresses abióticos são complexas e multigênicas e as proteínas que compreendem a classe de fatores de transcrição (FT) desempenham um papel importante na regulação da transcrição de genes relacionados com a formação e desenvolvimento do sistema radicular e que compõem os mecanismos de resposta ao estresse de P. A região promotora ou regulatória dos genes, além de conter as sequências de sítio de ligação da RNA polimerase (TATA box e GC box), podem conter sítios de ligação para esses FT, ativando ou inibindo a síntese do RNA mensageiro do gene alvo.

Um dos exemplos de FT que estão relacionados com o desenvolvimento do sistema radicular são as proteínas *RTCS* e *RTCL*. As plantas mutantes com perda de função do *RTCS* não possuem raízes seminais embrionárias e raízes da coroa, enquanto o mutante com perda de função do *RTCL* possui um desenvolvimento radicular reduzido, indicando que o *RTCS* atua na iniciação e o *RTCL* atua no alongamento radicular (Taramino *et al*., 2007; Xu *et al*., 2015). Além disso, estudos demostram que *RTCS* pode atuar reprimindo a expressão de RTCL (Xu *et al.,* 2015). Tanto o gene *RTCS* quanto *RTCL* tem a sua expressão controlada por um FT, ARF 34, que é responsivo à auxina (Xu *et al*., 2015). ARF34 se liga a elementos *cis* presente na região promotora desses genes, ativando a transcrição de *RTCS* e *RTCL*. Por outro lado, a proteína RTCS atua na ativação da transcrição do gene *ARF34* (Majer *et al*., 2012).

O gene *RUM1* está relacionado com a formação de raízes laterais e codifica uma proteína da família AUX/IAA que participa das vias de sinalização de auxina (Woll *et al*., 2005; Von Behrens *et al*., 2011). Em situações em que ocorre baixas concentrações de auxina, o FT codificado por *RUM1* se liga aos fatores responsivos a auxina *ARF25* e *ARF34*, inibindo a transcrição desses genes e impedindo que as proteínas codificadas por esses genes, que também são FT, interajam com elementos responsivos a auxina. O cenário oposto ocorre

quando existem altos níveis de auxina, onde há uma estabilidade na interação entre AUX/IAA e o complexo de degradação SCF/TIR1 E3 ubiquitina-ligase, ocorrendo a degradação da proteína AUX/IAA pelo proteossomo 26S. A degradação do FT AUX/IAA possibilita a interação entre as ARFs e os elementos responsivos a auxinas, possibilitando a sua transcrição (Mockaitis & Estelle, 2008; Von Behrens *et al*., 2011; Zhang *et al*., 2014b).

O gene *ZmLRL5* é preferencialmente expresso nos pelos radiculares e codifica uma proteína do tipo FT pertencente à família bHLH (basic helix-loop-helix) (Wang *et al*., 2018). Esse FT controla a expressão de genes específicos de pelos radiculares e uma mutação no seu primeiro éxon causa a redução do comprimento dos pelos. Além disso, as análises realizadas na região promotora desses genes preferencialmente expressos nos pelos, incluindo *ZmLRL5,* revelam a presença de um motivo de ligação de DNA degenerado de 6 pb de comprimento de sequência 'GWACGW' (onde W = C/T) em 765 genes. O motivo CACGTG é estritamente conservado e é descrito nos promotores de dois genes específicos de pelo radicular de Arabidopsis, *AtEXPA7* e *AtEXPA18* (Kim *et al*., 2006; Won *et al.,* 2009).

Uma variedade de fatores de transcrição, que se ligam aos elementos *cis* regulatórios envolvidos na rede de sinalização de P foram identificados. Esses elementos são conhecidos por modular a expressão de genes envolvidos no desenvolvimento radicular, na absorção, assimilação, remobilização e no armazenamento de P (Chiou & Lin, 2011; Zhang *et al*., 2014a). Um desses exemplos é o fator de transcrição PHR1 que possui um papel central na rede de sinalização de P (Rubio *et al*., 2001; Chiou & Lin, 2011). PHR1 se liga ao elemento *cis* regulatório PBS1 que está presente em vários promotores de genes envolvidos com a sinalização de P (Rubio *et al.,* 2001). Os homólogos de *PHR1* em Arabidopsis e arroz regulam o desenvolvimento da raiz e a expressão de sete genes induzidos pela privação de P (Rubio *et al*., 2001; Nilsson *et al*., 2007; Zhou *et al*., 2008; Bustos *et al*., 2010). O seu homólogo em trigo (*TaPHR1*) estimula a ramificação lateral, aumenta a absorção de P e produção de grãos, e regula positivamente um subconjunto de genes de resposta à privação de P no trigo (Wang *et al*., 2013).

1.9 GENES *PHOSPHORUS-STARVATION TOLERANCE 1* (*PSTOL1*)

1.9.1 *OsPSTOL1*

A identificação de vias e de genes em diferentes espécies de plantas pode ajudar na compreensão do funcionamento da aquisição e sinalização de P e permite o desenvolvimento de culturas mais eficientes (Zhang *et al*., 2014a; Malhi *et al*., 2015). Um dos genes relacionados a adaptação da planta à baixa disponibilidade de P é o *Phosphorus Starvation Tolerance 1 (PSTOL1)*, descoberto em uma variedade de arroz *aus-type* (Kasalath) originária de uma região da Índia onde o solo é pobre nutricionalmente (Londo *et al.,* 2006; Haefele & Hijmans, 2007). Variedades dessa região tem sido utilizadas como fonte de genes ligados a tolerância a alagamento, seca, calor e baixa condição de P (Xu *et al.,* 2006; Manzanilla *et al*., 2011; Gowda *et al*., 2012; Gamuyao *et al*., 2012).

O loco de característica quantitativa (*Quantitative Trait Loci*, QTL) *Phosphorus uptake 1* (*Pup1*) localizado no cromossomo 12 explica 80% da variação fenotípica para tolerância a deficiência de P em arroz e está associado ao aumento da taxa de crescimento radicular (Ni *et al*., 1998; Wissuwa *et al*., 1998; Wissuwa & Ae, 2001; Wissuwa *et al*., 2002). Existe uma inserção/deleção de cerca de 90 kb na região do *Pup1*, quando comparado o genoma de referência Nipponbare com a variedade Kasalath, doadora do loco *Pup1* (Gamuyao *et al*., 2012). Essa região é rica em retransposons e outros elementos transponíveis e os 68 genes preditos em Kasalath são novos ou desconhecidos. Dentre esses genes, o *OsPupk46* codifica uma quinase serina/treonina do tipo receptora citoplasmática da subfamília LRK10L-2 e apresenta maior expressão sob baixo P. Esse gene foi clonado e denominado *Phosphorus Starvation Tolerance 1* (*PSTOL1*) (BAK26566). Quando o *OsPSTOL1* foi superexpresso nas variedades IR64 e Nipponbare, representando duas variedades distintas de arroz irrigado moderno (*indica* e *japonica*, respectivamente), que naturalmente

não possuem o gene, houve aumento da área de superfície radicular e da aquisição de P, o que levou a um aumento de rendimento de grãos de aproximadamente 30% em condição de baixa disponibilidade de P (Gamuyao *et al*., 2012). O desempenho superior do *OsPSTOL1* também foi confirmado em linhagens semi-isogênicas (NILs), criadas a partir do *background* genético da variedade IR64, que apresentaram um aumento significativo do crescimento radicular (Gamuyao et al., 2012).

Além disso, a análise da expressão do gene repórter ß-glucuronidase (*GUS*) sob o controle do promotor do *OsPSTOL1* mostra a presença de GUS na região meristemática, onde são formadas as raízes da coroa, mais precisamente nos primórdios das raízes coronais e nas células do parênquima. Nenhuma coloração do GUS é identificada em tecidos maduros, sugerindo que *PSTOL1* é um regulador do crescimento e desenvolvimento precoce das raízes da coroa (Gamuyao *et al.,* 2012).

1.9.2 *TaPSTOL*

Em trigo, a proteína *TaPSTOL* possui 74,2% de identidade e 92,7% de similaridade da sua sequência de aminoácidos com a sequência do *OsPSTOL1*, apresentando também o domínio quinase serina/treonina (Milner *et al*., 2018). A expressão de *TaPSTOL* é presente tanto na raiz quanto na parte aérea sendo suprimida sob altas concentrações de P. Os ensaios histoquímicos demonstram a presença de GUS controlado pelo promotor de *TaPSTOL* em vários tipos da raiz, porém mais fortemente nas pontas das raízes primárias e laterais, nos coleóptiles e nos pelos radiculares, e com maior intensidade em condição limitante de P. Além disso, *TaPSTOL* está relacionado com uma série de características agronômicas importantes, como tempo de florescimento e tamanho de grãos (Milner *et al*., 2018).

1.9.3 *SbPSTOL1*

Utilizando uma abordagem de genômica comparativa com mapeamento associativo e de QTL, foram identificados no genoma do sorgo seis homólogos (*Sb03g006765, Sb03g031670, Sb03g031680, Sb03g031690, Sb03g0311700, Sb07g002840*) ao gene *OsPSTOL1* (Hufnagel *et al*., 2014). A identidade da sequência dos aminoácidos das proteínas *SbPSTOL1* com *OsPSTOL1* é de 55% a 73% e a predição dos domínios demonstra que todas as proteínas compartilham o domínio serina/treonina quinase. O homólogo de sorgo com maior similaridade é o *Sb07g002840*, que está localizado no cromossomo 7, enquanto os outros cinco estão localizados no cromossomo 3 (Hufnagel *et al*., 2014). Uma peculiaridade das proteínas PSTOL1 de sorgo é a presença de um peptídeo sinal que sugere uma via secretória, um domínio transmembrana e de interação com parede celular. O domínio de associação com parede celular do tipo WAK na região C-terminal não são encontrados no *OsPSTOL1* e nem no *Sb07g002840,* mas estão presentes nas demais proteínas *PSTOL1* de sorgo. Já o domínio do tipo GUB_WAK é encontrado especificamente no *Sb03g006765* e *Sb03g031700* (Hufnagel *et al*., 2014).

Há uma associação significativa entre os genes *SbPSTOL1* e produção de grãos em campo no Brasil e morfologia e arquitetura radicular em solução nutritiva sob baixa disponibilidade de P (Hufnagel *et al*., 2014). Além disso, os genes são associados ao acúmulo de biomassa, conteúdo de P e produtividade de grãos em uma população originada da África, sugerindo uma estabilidade desses genes em diferentes ambientes e genótipos de sorgo. Quatro dos homólogos identificados em sorgo são, provavelmente, produtos de eventos de duplicação *in tandem*, o que pode ser um mecanismo adicional de amplificação dos efeitos do *SbPSTOL1* em baixo P. Hufnagel *et al*. (2014) sugerem que os homólogos *SbPSTOL1* possuem a capacidade de aumentar a absorção de P em condição de baixa disponibilidade deste nutriente por um mecanismo relacionado não somente pelo crescimento precoce da raiz, como é o caso de *OsPSTOL1*, mas também por meio da modulação da arquitetura radicular.

Além disso, os genes *SbPSTOL1* co-localizam com QTLs relacionados a características de morfologia radicular, aquisição de P e produtividade de grãos de sorgo em solo tropical com baixo P (Hufnagel *et al*., 2014; Bernardino *et al*., 2019). O gene *Sb03g006765* co-localiza com QTL relacionado com área de superfície de raízes finas (diâmetro entre 1 e 2 mm), assim como os genes *Sb03g031670*, *Sb03g031680*, *Sb03g031690* e *Sb03g031700*, que também co-localizam com um QTL de produtividade de grãos. O gene *Sb07g002840* co-localiza com QTLs relacionados à produtividade de grãos e diâmetro médio da raiz. A correlação significativa entre as características de eficiência na aquisição de P e produção de grãos de sorgo sob baixo P, indicam que a morfologia radicular deve ser um dos principais alvos para o melhoramento de cultivares de sorgo quanto ao aumento da eficiência de uso de P (Bernardino *et al*., 2019).

1.9.4 *ZmPSTOL1*

Por meio do mapeamento de QTL com uma população de RILs (*Recombinant Inbred Lines*) de milho, provenientes do cruzamento de duas linhagens caracterizadas em campo, como eficiente para uso de P (L3) e ineficiente (L22) (Parentoni *et al.,* 2010) e contrastantes para morfologia radicular (de Sousa *et al*., 2012), foi possível identificar QTLs de interesse agronômico e mostrar que a superfície radicular total é o componente que mais contribui para o peso seco e conteúdo de P de plântulas de milho crescidas sob baixo P (Azevedo *et al*., 2015). Neste estudo, foi usado um modelo de mapeamento para uma única característica (MIM), que permitiu a identificação de sete QTLs que controlam comprimento radicular, diâmetro médio, área de superfície radicular, razão de peso seco raiz:parte aérea. A proporção da variância fenotípica explicada por cada QTL (R^2) é de 6,84% a 15,12%. Quando utilizado um modelo de características múltiplas (MT-MIM) são encontrados dez QTLs com R^2 de 2,04% a 15,17% (Azevedo *et al*., 2015). Além disso alguns desses QTLs coincidem com QTLs de morfologia radicular e produção de grãos previamente mapeados, enquanto outros flanqueiam os genes *ZmPSTOL1*, com mais de 55%

de identidade e o domínio serina/treonina quinase conservado com *OsPSTOL1*. Dos seis genes candidatos, dois estão localizados no cromossomo 3 (*ZmPSTOL3.04* e *ZmPSTOL3.06*), um no cromossomo 4 (*ZmPSTOL4.05*) e três no cromossomo 8 (*ZmPSTOL8.02*, *ZmPSTOL8.05_1* e *ZmPSTOL8.05_2*). Desses, *ZmPSTOL3.06, ZmPSTOL4.05, ZmPSTOL8.05_1* e *ZmPSTOL8.05_2* co-localizam com QTLs para razão de peso seco raiz:parte aérea, diâmetro médio e comprimento radicular total, respectivamente. Desses seis genes, *ZmPSTOL3.06*, *ZmPSTOL8.02* e *ZmPSTOL8.05_1* apresentam maior expressão na raiz do que na parte aérea e *ZmPSTOL3.06* maior expressão sob baixo P. A expressão dos genes *ZmPSTOL1* é maior no parental que contribui com os alelos do fenótipo correspondente (Azevedo *et al*., 2015).

Considerando as informações apresentadas, torna-se de grande importância estudos mais aprofundados dos genes *PSTOL1*, devido ao seu potencial em aumentar a superfície radicular, a eficiência na aquisição de P e consequentemente a produção de cereais.

2 OBJETIVOS

2.1 OBJETIVO GERAL

Caracterizar funcionalmente os genes *PSTOL1* na modulação do sistema radicular de milho.

2.2 OBJETIVOS ESPECÍFICOS

2.2.1 Capítulo1

Avaliar as modificações morfológicas do sistema radicular, e a performance de plantas de milho transgênico com superexpressão dos genes *OsPSTOL1*, *SbPSTOL1* e *ZmPSTOL1* cultivados em condições de deficiência de P.

2.2.2 Capítulo 2

Caracterizar o perfil de expressão e a regulação transcricional do gene *ZmPSTOL1_3.06* no sistema radicular do milho

3 REFERÊNCIAS BIBLIOGRÁFICAS

ANAMI, S. E.; MGUTU, A. J.; TARACHA, C.; COUSSENS, G.; KARIMI, M.; HILSON, P.; LIJSEBETTENS, M.V.; MACHUKA, J. (2010). Somatic embryogenesis and plant regeneration of tropical maize genotypes. *Plant Cell Tiss Organ Cult*. 102:285–295.

ARAÚJO, A. P.; MACHADO, C. T. T. (2006). Fósforo. *In*: FERNANDES, M. S. (Ed.). *Nutrição mineral das plantas*. Viçosa: Sociedade Brasileira de Ciências do Solo, p. 253-280.

ATKINSON, A.; RASMUSSEN, A.; TRAINI, R.; VOB, U.; STURROCK, C.; MOONEY,S. H. J.; WELLS, D. M.; BENNETT, M. J. (2014). Branching Out in Roots: Uncovering Form, Function, and Regulation. *Plant Physiology* 166:538-550.

AZEVEDO, G. C.; CHEAVEGATTI-GIANOTTO, A.; NEGRI, B. F.; HUFNAGEL, B.; SILVA, L DA C.; MAGALHAES, J. V.; GARCIA, A.; LANA, U. G. P.; DE SOUSA, S. M.; GUIMARÃES, C. T. (2015). Multiple interval QTL mapping and searching for PSTOL1 homologs associated with root morphology, biomass accumulation and phosphorus content in maize seedlings under low-P. *BMC Plant Biol*. 15:172.

BERNARDINO, K. C.; PASTINA, M. M.; MENEZES, C. B.; DE SOUSA, S. M.; MACIEL, L. S.; CARVALHO JR, G.; GUIMARÃES, C. T.; BARROS, B. A.; COSTA e SLVA, L.; CARNEIRO, P. C. S.; SCHAFFERT, R. E.; KOCHIAN, L. V.; MAGALHÃES, J. V. (2019). The genetic architecture of phosphorus efficiency in sorghum involves pleiotropic QTL for root morphology and grain yield under low phosphorus availability in the soil. *BMC plant biology*, *19*(1), 87.

BIELESKI, R. L. (1973). Phosphate pools, phosphate transport, and phosphate availability. *Ann. Rev. Plant Physiol*., 24:225-252.

BUCHER, M. (2007). Functional biology of plant phosphate uptake at root and mycorrhiza interfaces. *New Phytol* 173:11–26.

BUSTOS, R.; CASTRILLO, G.; LINHARES, F.; PUGA, M. I.; RUBIO, V.; PEREZ-PEREZ, J.; SOLANO, R.; LEYVA, A.; PAZ-AREZ, J. (2010). A central

regulatory system largely controls transcriptional activation and repression responses to phosphate starvation in Arabidopsis. *PLoS Genet* 6: e1001102.

CASERO, P. J.; CASIMIRO, I.; LORET, P. G. (1995). Lateral root initiation by asymmetrical transverse divisions of pericycle cells in four plant species: *Raphanussativus, Helianthus annuus, Zea mays,* and *Daucuscarota*. *Protoplasma* 188:49-58.

CHIOU, T. J.; LIN, S. I. (2011). Signaling network in sensing phosphate availability in plants. *Annu Rev Plant Biol*., 62:185-206.

COMPANHIA NACIONAL DE ABASTECIMENTO – CONAB. <https://www.conab.gov.br/info-agro/safras/graos/boletim-da-safra-de-graos> Acesso em: 24 fev. 2019.

CONSELHO DE INFORMAÇÕES SOBRE BIOTECNOLOGIA – CIB. (2018). 20 anos de transgênicos: benefícios ambientais, econômicos e sociais no Brasil. <https://cib.org.br/20-anos-de-transgenicos/> Acesso em: 13 mar. 2019.

CORDELL D. (2014). Life's bottleneck: sustaining the world's phosphorus for a food secure future. *Annu Rev Environ and Resour* 39:161-88.

DEMCHENKO, N. P.; DEMCHENKO, K. N. (2001). Resumption of DNA synthesis and cell division in wheat roots as related to lateral root initiation. *Russian Journal of Plant Physiology* 48:755-764.

DE SMET, I.; LAU, S.; MAYER, U.; JÜRGENS, G. (2010). Embryogenesis– the humble beginnings of plant life. *The Plant Journal* 61:959-970.

DE SOUSA, S. M.; CLARK, R. T.; MENDES, F. F.; DE OLIVEIRA, A. C.; VASCONCELOS, M. J. V.; PARENTONI, S. N.; KOCHIAN, L. V.; GUIMARÃES, C. T.; MAGALHÃES, J. V. (2012) A role root morphology candidates genes in P acquisition efficiency in maize. *Functional Plant Biology* 39:925-935.

ERDELSKA, O.; VIDOVENCOVA, Z. (1993). Development of adventitious seminal root primordia during embryogenesis. *Biology* 48:85-88.

FELDMAN, L. The maize root. In: FREELING, M.; WALBOT, V. (Ed.). The maize handbook. New York: Springer, 1994. p. 29-37.

FOOD AND AGRICULTURE ORGANIZATION OF THE UNITED NATIONS - FAO. 2015 a. FAOSTAT. Online statistical database: production. <http://faostat3. fao.org/download/Q/QC/E> Acesso em: 24 fev. 2019.

FOOD AND AGRICULTURE ORGANIZATION OF THE UNITED NATIONS - FAO. 2015 b. FAOSTAT. Online statistical database: Food balance<http:// faostat3.fao.org/download/FB/*/E> Acesso em: 24 fev. 2019.

FOOD AND AGRICULTURE ORGANIZATION OF THE UNITED NATIONS - FAO. (2016). Save and grow in practice – Maize – Rice – Wheat. FAO, Roma.

GAMUYAO, R.; CHIN, J. H.; TANAKA, J. P. PESARESI, P.; CATAUSAN, S.; DALID, C. LOEDIN, I. S.; MENDOZA, E. M. T.; WISSUWA, M.; HEUER, S. (2012). The protein kinase Pstol1 from traditional rice confers tolerance of phosphorus deficiency. *Nature* 488: 535–539.

GILROY, S.; JONES, D. L. (2000). Through form to function: root hair development and nutrient uptake. *Trends in Plant Sciences* 5:56-60.

GOWDA, V. R.; HENRY, A.; VADEZ, V.; SHASHIDHAR, H. E.; SERRAJ, R. (2012). Water uptake dynamics under progressive drought stress in diverse accessions of the OryzaSNP panel of rice (*Oryza sativa*). *Functional Plant Biology 39*:402-411.

HAEFELE, S. M.; HIJMANS, R. J. (2007). In Science, Technology, and Trade for Peace and Prosperity: Proceedings of the 26th International Rice Research Conference, New Delhi, India. (eds Aggarwal P. K., Ladha J. K., Singh R. K., Devakumar C. & Hardy B.) International Rice Research Institute, Indian Council of Agricultural Research, and National Academy of Agricultural Sciences, Los Baños, Philippines, and New Delhi,India, 297–308.

HINSINGER, P. (2001). Bioavailability of soil inorganic P in the rhizosphere as affected by root-induced chemical changes: a review. *Plant Soil* 237:173-195.

HOCHHOLDINGER, F. (2009). The maize root system: morphology, anatomy and genetics. In: BENNETZEN, J.; HAKE, S. (Ed.). Handbook of maize. New York: Springer, 2009. p. 145-160.

HOCHHOLDINGER, F.; PARK, W. J.; SAUER, M.; WOLL, K. (2004) From weeds to crops: genetic analysis of root development in cereals. *Plant Science* 9:42-48.

HOCHHOLDINGER, F.; TUBEROSA, R. (2009). Genetic and genomic dissection of maize root development and architecture. *Current Opinion in Plant Biology* 12:172-177.

HUFNAGEL, B.; DE SOUSA, S. M.; ASSIS, L.; GUIMARAES, C. T.; LEISER, W.; CORRADI, G.; NEGRI, B.; LARSON, B. G.; SHAFF, J. E.; PASTINA, M. M.; BARROS, B. A.; WELTZIEN, E.; RATTUNDE, H. F. W.; VIANA, J. H.; FALCAO, A. GAZAFFI, R.; GARCIA, A. A. F.; SCHARFFERT, R. E.; KOCHIAN, L. V.; MAGALHAES, J. (2014). Duplicate and conquer: multiple homologs of *PHOSPHORUS-STARVATION TOLERANCE1* enhance phosphorus acquisition and sorghum performance on low-phosphorus soils*. Plant Physiol.* 166:659-677.

IMIN, J.; NIZAMIDIN, M.; WU, T.; ROLFE, G. (2007). Factors involved in root formation in *Medicago truncatula. Journal of Experimental Botany* 58:439-451.

INTERNATIONAL SERVICE FOR THE ACQUISITION OF AGRI-BIOTECH APPLICATION – ISAAA (2018). Situação global dos cultivos transgênicos em 2017. Resumo executivo.

ISHIKAWA H.; EVANS M. L. (1995). Specialized zones of development in roots. *Plant Physiol* 109:725-727.

JEONG, K.; MATTES, N.; CATAUSAN, S.; CHIN, J. H.; PASZKOWSKI, U.; HEUER, S. (2015). Genetic diversity for mycorrhizal symbiosis and phosphate transporters in rice. *J Integr Plant Biol* 57:969–79.

JIA, X.; LIU, P.; LYNCH, P. (2018). Greater lateral root branching density in maize improves phosphorus acquisition from low phosphorus soil. Journal of Experimental Botany 69:4961-4970.

JIANG, K.; FELDMAN, L. J. (2005). Regulation of root apical meristem development. *Annual Review of Cell and Developmental Biology* 21:485-509.

KIM, D. W.; LEE, S. H.; CHOI, S.-B.; WON, S.-K.; HEO, Y.-K.; CHO, M.; PARK, Y.-I.; CHO, H.-T. (2006). Functional Conservation of a Root Hair Cell-Specific cis-Element in Angiosperms with Different Root Hair Distribution Patterns. *The Plant Cell* 18:2958–2970.

KIRKBY E. A.; JOHNSTON, A. E. (2008). Soil and fertilizer phosphorus in relation to crop nutrition. In: White P.J., Hammond J.P. (eds) *The Ecophysiology of Plant-Phosphorus Interactions*. Plant Ecophysiology, vol 7. Springer, Dordrecht.

KROFT, D.L., BISGROVE, S.R., HABLE, W.E. (1998). Differing roles of cytoskeleton in intercalary growth and tip growth of plant cells. *Curr. Opin. Cell Biol*. 10:117-122.

LADEJOBI, O.; SALAUDEEN, M.T.; LAVA KUMAR, P.; MENKIR, A.; ADESOYE, A.; ATIRI, G.; GEDIL, M. (2018). Mapping of QTLs associated with recovery resistance to streak virus disease in maize. *Annals of Agricultural Sciences* 63:115-121.

LOPES, A.S.; COX, F.R. (1979). Relação de características físicas, químicas e mineralógicas com fixação de fósforo em solos sob cerrados. *R. Bras. Ci. Solo*, 3:82-88.

LYNCH, J. P. (2007). Roots of the second Green revolution. *Australian Journal of Botany*, 55:493-512.

LYNCH, J.P. (2011). Root Phenes for Enhanced Soil Exploration and Phosphorus Acquisition: Tools for Future Crops. *Plant Physiol*., 156:1041-1049.

LYNCH, J. P.; BROWN, K. M. (2001). Topsoil foraging – an architectural Adaptation of plants to low phosphorus availability. *Plant and Soil* 237: 225-237.

LYNCH, J. P.; BROWN, K. B. (2008). Root strategies for phosphorus acquisition. In: WHITE, P.; HAMMOND, J. (Eds). *The ecophysiology of plant–phosphorus interactions.* Dodrecht: Springer Netherlands, p. 83-116.

LYNCH, J. P.; HO, M. D. (2005). Rhizoeconomics: carbon costs of phosphorus acquisition. *Plant Soil* 269:45-56.

LONDO, J. P.; CHIANG, Y. C.; HUNG, K. H.; CHIANG, T. Y.; SCHAAL, B. A. (2006). Phylogeography of Asian wild rice, *Oryza rufipogon*, reveals multiple independent domestications of cultivated rice, *Oryza sativa*. *Proc. Natl Acad. Sci*. 103:9578–9583.

MAJER, C.; XU, C.; BERENDZEN, K. W.; HOCHHOLDINGER, F. (2012). Molecular interactions of ROOTLESS CONCERNING CROWN AND SEMINAL ROOTS, a LOB domain protein regulating shoot-borne root initiation in maize (*Zea mays* L.). *Philosophical Transactions of the Royal Society of London Series B, Biological Sciences* 367:1542-1551.

MANZANILLA, D. O.; PARIS, T. R.; VERGARA, G. V.; ISMAIL, A. M.; PANDEY, S.; LABIOS, R. V.; TATLINGHARI, G. T.; ACDA, R. D.; CHI, T. T. N.; DUOANGSILA, K.; SILIPHOUTHONE, I.; MANIKMAS, M. O. A.; MACKILL, D. J. (2011). Submergence risks and farmers' preferences: implications for breeding Sub1 rice in Southeast Asia. *Agricultural Systems 104*:335-347.

MALHI, S. S.; VERA, C. L.; BRANDT, S. A. (2015). Seed yield potential of five wheat species/ cultivars without and with phosphorus fertilizer application on a P-deficient soil in northeastern Saskatchewan. *Agric Sci*. 6:224.

MENDES F. F.; GUIMARÃES L. J. M.; SOUZA J. C.; GUIMARÃES P. E. O.; MAGALHAES J. V.; GARCIA A. A. F.; PARENTONI, S.; GUIMARÃES, C. T. (2014). Genetic architecture of phosphorus use efficiency in tropical maize cultivated in a low-P soil. *Crop Sci.* 54:1530-1538.

MILNER, M. J.; HOWELLS, R. M.; CRAZE, M.; BOWDEN, S.; GRAHAM, N.; WALLINGTON, E. J. (2018). A PSTOL-like gene, *TaPSTOL*, controls a number of agronomically important traits in wheat. *BMC plant biology*, *18*:115-129.

MITRA, G. N. (2015). Regulation of nutrient uptake by plants. *India: Springer*.

MOHANTY, S. K.; SWAIN, M. R. (2019). Bioethanol Production From Corn and Wheat: Food, Fuel, and Future. *Bioethanol Production from Food Crops*, 45–59.

MOCKAITIS, K.; ESTELLE, M. (2008). Auxin receptors and plant development: a new signaling paradigm. *Annual Review of Cell and Developmental Biology* 24:55-80.

NI, J. J.; WU, P.; SENADHIRA, D.; HUANG, N. (1998). *Mapping QTLs for phosphorus deficiency tolerance in rice (Oryza sativa L.)*. *Theor. Appl. Genet.* 97:1361-1369.

NILSSON, L.; MUELLER, R.; NIELSEN, T.H. (2007). Increased expression of the MYB-related transcription factor, PHR1, leads to enhanced phosphate uptake in *Arabidopsis thaliana*. *Plant Cell Environ*. 30:1499-1512.

PARENTONI, S.N.; SOUZA-JUNIOR, C.L. DE. (2008). Phosphorus acquisition and internal utilization efficiency in tropical maize genotypes. *Pesq. agropec. bras*., 43: 893-901.

PARENTONI, S. N.; DE SOUZA JR, C. L.; DE CARVALHO ALVES, V. M.; GAMA, E. E. G.; COELHO, A. M.; DE OLIVEIRA, A. C.; GUIMARÃES, C. T.; VASCONCELOS, M. J. V.; PACHECO, C. A. P.; MEIRELLES, W. F.; MAGALHÃES, J. V.; DA SILVA, A. R.; MENDES, F. F.; SCHAFFERT, R. E. (2010). Inheritance and breeding strategies for phosphorous efficiency in tropical maize (Zea mays L). *Maydica*, *55*(1), 1.

PARENTONI, S. N.; MENDES, F. F.; GUIMARÃES, L. J. M. (2011). Melhoramento para eficiência no uso de fósforo. *In*: NETO, R. F.; BORÉM, A. *Melhoramento de plantas para condições de estresses abióticos*. Viçosa: UFV, p.101-126.

PARKER, J. S.; CAVELL, A. C.; DOLAN, L.; ROBERT, K.; GRIERSON, C. S. (2000). Genetic interactions during root hair morphogenesis in *Arabidopsis*. *Plant Cell*, 12:1961-1974.

RAGHOTHAMA, K. G. (2000). Phosphate transport and signaling. *Curr. Opin. Plant Biol*., 3: 182-187.

RAGHOTHAMA K. G. (1999). Phosphate acquisition. *Annual Review of Plant Physiology and Plant Molecular Biology* 50:665-693.

RAIJ, B. VAN. Fertilidade do solo e adubação. Piracicaba*, Ceres*, 1991. 343p.

RAJI, J. A.; FRAME, B.; LITTLE, D.; SANTOSO, T. J.; WANG, K. (2018). *Agrobacterium*- and Biolistic-Mediated Transformation of Maize B104 Inbred. In: Lagrimini L. (eds) Maize. *Methods in Molecular Biology*, vol 1676. Humana Press, New York, NY.

RAMAEKERS, L.; REMANS, R.; RAO, I. M.; BLAIR, M. W.; VANDERLEYDEN, J. (2010). Strategies for improving phosphorus acquisition efficiency of crop plats. *Field Crops Research* 117:169-176.

RAUSCH, C.; BUCHER, M. (2002). Molecular mechanisms of phosphate transport in plants. *Planta*, 216: 23-37.

RHEINHEIMER, D. S.; ANGHIMONI, I.; CONTE, E. (2003). Sorção de fósforo em função do teor inicial e de sistemas de manejo de solos. *Revista Brasileira de Ciências do Solo* 27:41-49.

ROMAY, M. C.; MILLARD, M. J.; GLAUBITZ, J. C.; PEIFFER, J. A.; SWARTS, K. L.; CASSTEVENS, T. M.; ELSHIRE, R. J.; ACHARYA, C. B.; MITCHELL, S. E.; FLINT-GARCIA, S. A.; McMULLEN, M. D.; HOLLAND, J. B.;

BUCKLER, E. S.; GARDNER, C. A. (2013). Comprehensive genotyping of the USA national maize inbred seed bank. *Genome biology* 14:R55.

ROSSI, E. A.; RUIZ, M.; RUEDA CALDERÓN, M. A.; BRUNO, C. I.; BONAMICO, N. C.; BALZARINI, M. G. (2018). Meta-Analysis of QTL Studies for Resistance to Fungi and Viruses in Maize. *Crop Sci*. 59:125-139.

RUBIO, V.; LINHARES, F.; SOLANO, R.; MARTIN, A. C.; IGLESIAS, J.; LEYYA, A.; PAZ-ARES, J. (2001). A conserved MYB transcription factor involved in phosphate starvation signaling both in vascular plants and in unicellular algae. *Genes Dev*. 15:2122-2133.

SANGUINETI, M. C.; GIULIANI, M. M.; GOVI, G.; TUBEROSA, R.; LANDI, P. (1998). Root and shoot traits of maize inbred lines grown in the field and in hydroponic culture and their relationships with root lodging. *Maydica 43*:211-216.

SANO, E. E.; ROSA, R.; BRITO, J. L. S.; FERREIRA, L. G. (2008). Mapeamento semidetalhado do uso da terra do bioma cerrado. *Pesq. Agropec. bras., Brasília*, 43:153-156.

SARININGPURI, J.M.; RIFIN, A.; HASBULLAH, R. (2017). The competitiveness of manual and mechanized corn cultivation Indones. *Jornal Bus Entrep*, 3:24-33.

SASS, J. E. M. In: SPRAGUE, G. F. (Ed.). Corn and corn improvement. Madison: *American Society of Agronomy Publishers*, 1997. p. 89-110.

SATTARI, S.; BOUWMAN, A. F.; MARTINEZ-RODRÍGUEZ, R.; BEUSEN, A. H.; VAN-ITTERSUM, M. K. (2016). Negative global phosphorus budgets challenge sustainable intensification of grasslands. *Nat Commun* 7:10696.

SCHACHTMAN, D. P.; REID, R. J.; AYLING, S. M. (1998). Phosphorus uptake by plants: From soil to cell. *Plant Physiol*., 116:447-453.

SHAH, T.R.; PRASAD, K.; KUMAR, P. (2016). Maize – a potential source of human nutrition and health: a review. *Cogent Food Agr*. 2:1-9.

SMITH, F. W. (2002). The phosphate uptake mechanism. *Plant Soil*, 245:105-114.

SMITH, S.; DE SMET, I. (2012). Root system architecture: insights from Arabidopsis and cereal crops. *Philosophical Transactions of the Royal Society of London. Series B. Biological Sciences*. 367:1441-1452.

SINGH, A.; ANDERSEN, A. P.; JACKSON-ZIEMS, T. A.; LORENZ, A. J. (2016). Mapping Quantitative Trait Loci for Resistance to Goss's Bacterial Wilt and Leaf Blight in North American Maize by Joint Linkage Analysis. *Crop Sci*. 56:2306-2313.

SUN, B.; GAO, Y.; LYNCH, P. (2008). Large crown root number improves topsoil foraging and phosphorus acquisition. *Plant Physiology* 177:90-104.

UNITED STATES DEPARTMENT OF AGRICULTURE - USDA <https://www.usda.gov/oce/commodity/wasde/wasde1218.pdf> Acesso em: 24 fev. 2019.

TARAMINO, G.; SAUER, M.; STAUFFER, J. L.; MULTANI, D.; NIU, X.; SAKAI, H.; HOCHHOLDINGER, F. (2007). The maize (*Zea mays L*.) RTCS gene encodes a LOB domain protein that is a key regulator of embryonic seminal and post-embryonic shoot-borne root initiation. *The Plant Journal* 50:649-659.

TRACHSEL, S.; KAEPPLER, S. M.; BROWN, K. M.; LYNCH, J. P. (2011). Shovelomics: high throughput phenotyping of maize (*Zea mays* L.) root architecture in the field. *Plant and Soil* 314:75-87.

TRACHSEL, S.; KAEPPLER, S. M.; BROWN, K. M.; LYNCH, J. P. (2013). Maize root growth angles become steeper under low N conditions. *Field Crops Research* 140:18-31.

VANCE, C. P.; STONE, C. U.; ALLAN, D. L. (2003). Phosphorus acquisition and use: critical adaptations by plants for securing a nonrenewable resource. *New Phytologist* 157:423-447.

VON BEHRENS, I.; KOMATSU, M.; ZHANG, Y.; BERENDZEN, K. W.; NIU, X.; SAKAI, H.; TARAMINO, G.; HOCHHOLDINGER, F. (2011). Rootless with undetectable meristem 1 encodes a monocotspecific AUX/IAA protein that controls embryonic seminal and postembryonic lateral root initiation in maize. *The Plant Journal* 66:341-353.

WANG, C. X.; QI, C. Y.; LUO, J. H.; LIU, L.; HE, Y.;CHEN, L. Q. (2018). Characterization of LRL 5 as a key regulator of root hair growth in maize. *The Plant Journal*.

WANG, J.; SUN, J. H.; MIAO, J.; GUO, J. K.; SHI, Z. L.; HE, M. Q.; CHEN, Y.; ZHAO, X. Q.; LI, B.; HAN, F. P.; TONG, Y. P.; LI, Z. S. (2013). A phosphate

starvation response regulator Ta-PHR1 is involved in phosphate signalling and increases grain yield in wheat. *Ann Bot-London,* 111:1139-1153.

WEN, T.J.; SCHNABLE, P.S. (1994). Analyses of mutant of three genes that influence root hair development in *Zea mays* (Gramineae) suggest that root hairs are dispensable. *Am. J. Bot*., 81:833-842.

WISSUWA, M.; AE, N. (2001). Genotypic variation for tolerance to phosphorus deficiency in rice and the potential for its exploitation in rice improvement. *Plant Breed.* 120:43-48.

WISSUWA, M.; WEGNER, J.; AE, N.; YANO, M. (2002). Substitution mapping of Pup1: a major QTL increasing phosphorus uptake of rice from a phosphorus-deficient soil. *Theor. Appl. Genet.* 105:890-897.

WISSUWA, M.; YANO, M.; AE, N. (1998). *Mapping of QTLs for phosphorus-deficiency tolerance in rice (Oryza sativa L.)*. *Theor. Appl. Genet.* 97:777-783.

WOLL, K.; BORSUK, L. A.; STRANSKY, H.; NETTLETON, D.; SCHNABLE, P. S.; HOCHHOLDINGER, F. (2005). Isolation, characterization, and pericycle-specific transcriptome analyses of the novel maize lateral and seminal root initiation mutant rum1. *Plant Physiology* 139:1255-1267.

WON, S. K.; LEE, Y. J.; LEE, H. Y.; HEO, Y. K.; CHO, M.; CHO, H.T. (2009) *Cis*-element and transcriptome based screening of root hair specific genes and their functional characterization in Arabidopsis. *Plant Physiol*. 150:1459-1473.

YU, P.; GUTJAHR, C.; LI, C.; HOCHHOLDINGER, F. (2016). Genetic control of lateral root formation in cereals. *Trends in plant science*, *21*:951-961.

XU, C.; TAI, H.; SALEEM, M.; LUDWIG, Y.; MAJER, C.; BERENDZEN, K. W.; NAGEL, K. A.; WOJCIECHOWSKI, T.; MEELEY, R. B.; TARAMINO, G.; HOCHHOLDINGER, F. (2015). Cooperative action of the paralogous maize lateral organ boundaries (LOB) domain proteins RTCS and RTCL in shoot-borne root formation. *New Phytologist*. 207:1123-1133.

XU, K.; XU, X.; FUKAO, T.; CANLAS, P.; MAGHIRANG-RODRIGUEZ, R.; HEUER, S.; ISMAIL, A. M.; BAILEY-SERRES, J.; RONALD, P. C.; MACKILL, D. J. (2006). Sub1A is an ethylene-response-factor-like gene that confers submergence tolerance to rice. *Nature 442*:705-708.

ZHAN, A.; LYNCH, J. P. (2015). Reduced frequency of lateral root branching improves N capture from low-N soils in maize. *Journal of Experimental Botany* 66:2055-2065.

ZHAN, A.; SCHNEIDER, H.; LYNCH, J. P. (2015). Reduced lateral root branching density improves drought tolerance in maize. *Plant Physiology* 168:1603-1615.

ZHANG, Z.; LIAO, H.; LUCAS, W. J. (2014a). Molecular mechanisms underlying phosphate sensing, signaling, and adaptation in plants. *J. Integr Plant Biol.,* 56: 192-220.

ZHANG, Y.; PASCHOLD, A.; MARCON, C.; LIU, S.; TAI, H.; NESTLER, J.; YEH, C. T.; OPITZ, N.; LANZ, C.; SCHNABLE, P. S.; HOCHHOLDINGER, F. (2014b). The Aux/IAA gene *rum1* involved in seminal and lateral root formation controls vascular patterning in maize (*Zea mays L*.) primary roots. *Journal of Experimental Botany* 65:4919-4930.

ZHAO, X.; CAO, Y.; LI, Y.; HU, S.; PAN, G. LIN, H. (2018a). Identification of QTL and candidate genes for Pb accumulation in maize at maturity stage. *Maydica* 61:1-9.

ZHAO, X.; FANG, P.; ZHANG, J.; PENG, Y. (2018b). QTL mapping for six ear leaf architecture traits under water-stressed and well-watered conditions in maize (*Zea mays* L.). *Plant Breed*. 137:60-72.

ZHOU, J.; JIAO, F. C.; WU, Z. C.; LI, Y. Y.; WANG, X. M.; HE, X. W.; ZHONG, W. Q.; WU, P. (2008). OsPHR2 is involved in phosphate-starvation signaling and excessive phosphate accumulation in shoots of plants. *Plant Physiol.* 146:1673-1686.

CAPÍTULO 1

Overexpression of *PSTOL1-like* genes increases root surface area and biomass accumulation for maize cultivated under low P availability

Bárbara F. Negri[a,b,1], Laiane S. Maciel[a,c,1], Antonio Marcos Coelho[a], Beatriz A. Barros[a], Claudia T Guimarães[a,b,c*], Jurandir V. Magalhães [a,b,c*], Sylvia M. de Sousa [a,b*].

[a]Embrapa Milho e Sorgo, 35701-970 Sete Lagoas, MG, Brazil

[b] Universidade Federal de São João Del Rei, 36301-160 São Joao Del Rei, MG, Brazil

[c] Universidade Federal de Minas Gerais, 31270-901 Belo Horizonte, MG, Brazil

[1]B.F.N and L.S.M contributed equally to this work.

*Corresponding author

ABSTRACT

Low phosphorus (P) availability in the soil is one of the major constraints for crop development and grain yield, mainly in tropical regions. In tropical soils, the bioavailability of P is low due to its fixation in the soil clay fraction with iron (Fe) and aluminum (Al) oxides. In order to adapt to this limitation, plants have developed different mechanisms to maximize P acquisition efficiency. These changes include alterations in root morphology and architecture in order to increase the area of the soil explored by the roots. In rice (*Oryza sativa*), the protein kinase *PHOSPHORUS-STARVATION TOLERANCE1* (*OsPSTOL1*) enhances total root length and total root surface area, increasing P acquisition and grain yield under P deficiency. *OsPSTOL1* homologs in sorghum (*Sorghum bicolor*, *SbPSTOL1*) and maize (*Zea mays*, *ZmPSTOL1*) were characterized via QTL and association mapping, and were found to affect root morphology and architecture under P deficiency. In addition, *SbPSTOL1* genes were associated

with increased P acquisition and grain yield under low P availability in the soil. We overexpressed *OsPSTOL1*, *SbPSTOL1* (*Sb07g002840*, *Sb03g031690* and *Sb03g006765*) and *ZmPSTOL1* (*ZmPSTOL1_8.05*, *ZmPSTOL1_3.06* and *ZmPSTOL1_8.02*) in maize B104 in order to functionally characterize the role of these genes. Our data showed a strong negative correlation between root diameter and root length, and moreover, a strong positive correlation between root length with shoot dry weight. These results suggest that *OsPSTOL1* and *SbPSTOL1* genes in maize modulate the root system by increasing proliferation of very fine roots enhancing P uptake and biomass accumulation under low and high P conditions. No significant differences were detected between the *ZmPSTOL1* events and the non-transgenic line, possibly because B104 high endogenous expression of the *ZmPSTOL1* genes. All evidence so far, indicate that *PSTOL1* genes have a more general role in the root system, which resulted in the enhanced P acquisition, which could benefit cereal production worldwide.

Keywords: Phosphorus acquisition, protein Kinase, root system morphology, *PSTOL1-Like* genes

INTRODUCTION

One of the greatest challenges in modern agriculture is to increase food production without expanding agriculture into new areas to preserve the environment and biodiversity. Thus, although food production needs to be increased at a global scale to cope with a continuously growing population (Godfray *et al.*, 2010; Rojas *et al.*, 2016), efficient production systems are equally essential for sustainability. Most of the crop production areas in the world are located on tropical and subtropical regions, where the soils are often acidic (von Uexküll and Mutert, 1995; Lynch, 2011).

The clay fraction of the tropical soils is enriched in Al and Fe oxides, which bind stably to soil P, restricting bioavailability (Marschner, 1996; Heuer *et al.*, 2009). In addition, P shows low mobility in the soil and is more available in the soil superficial layer [0-20 cm (Raghothama, 1999; Rausch and Bucher, 2002;

Vance *et al.*, 2003)]. Soil amendment with P fertilizers is the most common strategy to increase yield on soils with low-P availability. However, phosphate fertilizers are extracted from rock phosphate reserves, a natural non-renewable resource that can be depleted over the next 50 years; in addition, intensive use of P-fertilizers increases production costs (Cordell *et al*., 2009; Sattari *et al.*, 2012). Therefore, the development of cultivars that use P more efficiently becomes an important strategy to improve food security worldwide.

Phosphorus is an essential macronutrient for plant growth and development (Abel *et al.*, 2002; Vance *et al.*, 2003; Niu *et al*., 2013). Plants acquire P from the soil solution in the orthophosphate forms, $H_2PO_4^-$ and HPO_4^{2-}. Throughout evolution, plants have developed mechanisms to overcome low-P availability in the soil, which act to optimize P internal utilization or to enhance P acquisition from the soil (Vance *et al.*, 2003). The mechanisms of internal translocation and acquisition of P are orchestrated by modulation of phosphate transporters, exudation of organic acids, secretion of phosphatases, association with mycorrhizae, chemical modifications of the rhizosphere, root morphology and architecture remodeling (Reviewed by Lopez-Arredondo *et al.*, 2014). Previous studies indicated that P use efficiency in maize and sorghum cultivated on a tropical low-P soils is largely determined by mechanisms that act to enhance P acquisition rather than internal efficiency mechanisms (Parentoni and Souza, 2008; Mendes *et al.*, 2014; Bernardino *et al.*, 2019).

Changes in root morphology and architecture, such as adventitious root proliferation and changes in crown root angle, lead to a broader dispersion of lateral branching that may enhance P uptake (Lynch, 2011; Lambers *et al.*, 2011, 2013). Increase of shallow roots increase topsoil foraging where most of P is available. In maize, increased adventitious root length has been considered as an adaptive response that enable plants to explore more efficiently soil patches enriched in P (Richardson *et al.*, 2011). The density, length and longevity of root hairs are also relevant for P efficiency. In common bean (*Phaseolus vulgaris*), genotypes with both long root hairs and shallow roots had 298% greater biomass accumulation than short-haired, deep-rooted phenotypes under low P-conditions when grown in a low-P soil (Miguel *et al.*, 2015).

Identification of genes that control root morphology and architecture

provide important leads to enhance crop yield under low-P availability (Gamuyao *et al*., 2012; Ma *et al.*, 2013; Li *et al.*, 2016; Lee *et al.*, 2016; Wang *et al.*, 2017; Chen *et al.*, 2018; Zhang *et al.*, 2018). In rice, *PHOSPHORUS-STARVATION TOLERANCE 1* (*OsPSTOL1*) enhances root surface area, P acquisition and grain yield in rice cultivated under low-P conditions. *OsPSTOL1* is a serine/threonine receptor-like kinase of the LRK10L-2 subfamily, involved in the development control of early root growth (Gamuyao *et al*., 2012). Proteins that share more than 55% identity with *OsPSTOL1* were identified in sorghum (*SbPSTOL1*) and maize (*ZmPSTOL1*) (Hufnagel *et al*., 2014; Azevedo *et al.*, 2015). QTL mapping indicated that *SbPSTOL1* genes co-localize with QTLs related to root morphology and increased performance in soils with low P availability (Hufnagel *et al.*, 2014; Bernardino *et al.*, 2019). In addition, single-nucleotide polymorphisms (SNPs) within *SbPSTOL1* genes were associated with grain yield, root morphology, and root system architecture under low P conditions (Hufnagel *et al.*, 2014). In maize, *ZmPSTOL1* genes also co-localized with QTLs related to root morphology and P acquisition efficiency (Azevedo *et al.*, 2015).

OsPSTOL1 as well as maize and sorghum *PSTOL1*-like proteins share a conserved serine/threonine kinase C-terminal domain. The sorghum SbPSTOL1 proteins differed from the rice and maize PSTOL1 proteins by the presence of an extracellular N-terminal portion, composed of a cysteine-rich wall-associated receptor kinase galacturonan-binding (Gub), and an also cysteine-rich wall-associated receptor kinase C-terminal (Wak) domain (Hufnagel et al., 2014). Here, we overexpressed the genes *OsPSTOL1*, *Sb07g002840*, *Sb03g006765*, *Sb03g031690*, *ZmPSTOL1_8.05*, *ZmPSTOL1_3.06*, *ZmPSTOL1_8.03* driven by the ubiquitin promoter in maize to characterize their function in root morphology and biomass accumulation in a low-P soil. Our data demonstrated that the overexpression of *OsPSTOL1* and *SbPSTOL1*, but not of the *ZmPSTOL1* homologs, enhanced total root length and shoot biomass for maize cultivated in low and high-P soils. These results suggest *OsPSTOL1* and S*bPSTOL1* may have a more global effect than simply increasing P uptake, leading to enhanced uptake of other mineral nutrients and possibly water.

MATERIALS AND METHODS

Maize transformation via *Agrobacterium tumefaciens* with rice, maize and sorghum *PSTOL1*

The coding sequence of *Sb07g002840*, *Sb03g006765*, *Sb03g031690* were obtained from the sorghum BR007 line (Hufnagel *et al.*, 2014). *ZmPSTOL1_8.05* and *ZmPSTOL1_8.03* sequences were obtained from the maize line L22, whereas *ZmPSTOL1_3.06* sequence was obtained from L3 (Azevedo *et al.*, 2015). These coding sequences in addition to *OsPSTOL1* (BAK26566) were synthesized by Genscript (Piscataway, NJ). The *PSTOL1* genes were introduced into the pMCG1005 binary vector (McGinnis *et al.*, 2005), where gene expression is driven by the maize ubiquitin promoter (Ubi), and contained the *octopine synthase* gene terminator from *Agrobacterium tumefaciens* (OCs3'). This plasmid contains the *phosphinothricin acetyltransferase* gene (*Bar*) as the plant selection marker, whose expression is driven by the CaMV35S promoter, and contained the *Nopaline synthase* gene terminator from *A. tumefaciens* [NOS (Fig. 2A)].

Maize transformation of the inbred line B104 was mediated by *A. tumefaciens* and carried out at Iowa State University Plant Transformation Center (Iowa State University, Ames, IA), according to Frame *et al*. (2011). The events were named according to the gene used in the transformation (*OsPSTO1, Sb07g002840, Sb03g031690, Sb03g006765, ZmPSTOL1_8.05, ZmPSTOL1_3.06* and *ZmPSTOL1_8.02*) followed by the underline character (_) and the event number (1 to 21).

The maize transgenic progeny T1 was obtained backcrossing the regenerated events T0 with wild -type B104. First, the 204 independent transgenic events for all constructs were grown in a paper pouch system for 14 days in hydroponics with low P (2.5 µM) and sprayed with 0.5% Finale® herbicide [glufosinate ammonium (Bayer CropScience)], to eliminate the non-transgenic plants. A bulk of nine plants was used to evaluate *PSTOL1* expression by quantitative real-time PCR (qRT-PCR), and together with total root length trait was used to select the events for the next generations.

Forty-six independent transgenic events were grown in greenhouse and self-pollinated to obtain T2 progeny. Sixteen seeds from each T2 event, were soaked with 0.2% Finale and incubated at 20 °C for 6 hours, before being planted in soil. DNA from each individual plant was extracted and a semi-quantitative PCR was performed to screen for homozygous plants. T2 events with one copy were self-pollinated to multiply homozygous plants (T3 and T4), that were used for phenotypic characterization under hydroponics and greenhouse conditions. Mendelian segregation based on herbicide resistance was tested for maize transgenic generations T1 and T4 using the chi-square test (χ^2).

Phenotypic assessment of root morphology in hydroponics

Root morphology traits were assessed in nutrient solution as described by de Sousa *et al.* (2012), using a randomized block design with three replicates. Maize seeds were surface-sterilized using 0.5% (w/v) sodium hypochlorite, washed with distilled water and placed in moistened paper rolls. After 4 days, uniform seedlings were transferred to moistened blotting papers and placed into paper pouches (24 × 33 × 0.02 cm) after removing the endosperm (de Sousa *et al.*, 2012).

Each experimental unit consisted of one pouch with three seedlings per pouch, whose bottom 3 cm was immersed in containers filled with 5 L of modified Magnavaca´s nutrient solution (Magnavaca *et al.*, 1987) at pH 5.65 and 2.5 µM P, which was changed every three days. The containers were kept in a growth chamber at 27/20º C day/night temperatures and a 12-h photoperiod under continuous aeration.

After 13 days, root images were acquired using a digital camera Nikon D300S SLR. Images were analyzed using the RootReader2D (http://www.plantmineralnutrition.net/software/rootreader2d/) and WinRhizo (http://www.regent.qc.ca/) softwares. We assessed total root length (cm), average root diameter (mm), total root surface area (cm^2), surface area of very fine roots with diameter between 0 and 1 mm (cm^2), surface area of fine roots with diameter between 1 and 2 mm (cm^2), shoot dry weight (mg) and shoot P content (g).

Root tissues were frozen in liquid nitrogen and stored at -80º C until RNA extraction and shoot tissues were dried at 65ºC in a forced-air oven until constant weight to obtain shoot dry weight. For P concentration analysis, shoot tissues were subjected to a nitric perchloric acid digestion followed by P quantification with an inductively-coupled argon plasma (ICP) emission spectrometry (Silva, 2009). Phosphorus content was calculated by multiplying dry weight and P concentration.

Expression analysis of *PSTOL1* genes under low-P

Total RNA was isolated from a bulk of nine roots grown in nutrient solution with low P, using the SV Total RNA Isolation System kit (Promega, Madison, WI), according to the manufacturer's instructions. Total RNA (1 µg) was used for cDNA synthesis using the High Capacity cDNA Reverse Transcription kit (Applied Biosystems, Foster City, CA). Transcript expression levels were assessed by quantitative real-time PCR (qPCR-RT) using SYBR Green I (for *OsPSTOL1* and *SbPSTOL1* genes) and TaqMan (for *ZmPSTOL1* genes) assays in ABI Prism 7500 Fast System (Applied Biosystems, Foster City, CA), using *18 s rRNA* as an endogenous constitutive control and gene-specific primers (Table S1). Calculation of relative gene expression with three technical replicates was performed using the $2^{-\Delta\Delta Ct}$ method (Schmittgen and Livak, 2008).

Phenotypic assessment of maize biomass accumulation and plant height under low and high P concentrations in the soil

The experiment was conducted in a greenhouse using a randomized complete block design with four replicates. Each experimental unit consisted of a pot with three plants. The soil was a red-latosol with very clayey texture, pH 6.0 and low P (2.8 mg/dm³), supplemented with 2 g/kg of the dolomite lime and 0.5 g/kg of gypsum. For the high P treatment, 0.225 g of super triple phosphate per kg of soil was added.

Seeds of transgenics events were surface-sterilized using sodium

hypochlorite 0.5% for 5 min, washed with distilled water and placed in moistened paper rolls. After seven days, three uniform seedlings of each transgenic event were transferred to pots containing 30 kg of soil. One gram of urea was added to each pot, 15 and 30 days after transplanting. Irrigation was performed daily based on the field capacity.

After 45 days of transplanting, plant height was determined by measuring the distance from the base of the stem to the last fully expanded leaf. Then, the shoots were harvested and dried at 65ºC in a forced-air oven until constant weight. Shoot was ground in a Wiley mill prior determining P content. Chemical analyses were conducted in the Plant Chemical Analysis Laboratory at Embrapa Maize and Sorghum using inductively-coupled argon plasma (ICP-OES) (Nogueira and Souza 2005).

Statistical analyses

Analysis of variance (ANOVA) was performed using the package *Agricole* (Mendiburu, 2019) in R (RCore Team, 2018). Differences between means were assessed by the t-test considering a 5% significance level (α). Scott-Knott clustering analyses were performed considering 5%, 10% and 15% significance level for root morphology , shoot dry weight and plant height, respectively [α (Jelihovschi, 2014)]. Pearson's correlation coefficients were estimated based on trait means for root morphology, shoot dry weight, shoot P content, and *PSTOL1* gene expression (measured by delta Ct) with the R package *Psych* (Revelle, 2018).

RESULTS

Root morphology of non-transgenic lines

In order to phenotypically characterize the non-transgenic background, the root system of B104 was initially compared with L3 and L22, which were previously classified as P-efficient and P-inefficient lines, respectively based on grain yield assessed in low-P soil (Parentoni et al., 2010; de Sousa *et al.*, 2012).

In addition, L3 and L22 were used as parents of the RIL population that previously indicated that the *PSTOL1-like* genes in maize co-localize with QTLs for root morphology, biomass accumulation and P content (Azevedo *et al.*, 2015).

The P-efficient line, L3, showed higher total root length, total root surface area, surface area of very fine roots and fine roots compared to L22 (Fig. 1A-B). Shoot dry weight and shoot P content in a low-P nutrient solution were also higher in L3 compared to L22. These results confirm previous findings indicating that L3 is more efficient than L22, to some extent due to root morphology changes that enhances P acquisition efficiency (de Sousa *et al.*, 2012).Total root length and surface area of fine roots in B104 was found to be higher compared to L3.

B104 showed higher expression of the *ZmPSTOL1* genes, *ZmPSTOL1_8.05, ZmPSTOL1_3.06* and *ZmPSTOL1_8.02* (Fig. 1C) than L3. B104 genome was recently sequenced (www.maizegdb.org) and harbors in its genome one copy of each *ZmPSTOL1*.

Selection of transgenic events

The maize line B104 was transformed with the constructs shown in Fig. 2A. Twenty-one independent T3 transgenic maize events were selected from a total of forty-six independent T1 transgenic maize events. The selection was based on the increase in total root length under low P availability compared to B104. (Table S2). At least one T3 event for each transgenic maize construct (*OsPSTOL1_1, Sb07g002840_5, Sb03g031690_8, Sb03g06765_10, Sb03g06765_11, ZmPSTOL1_8.05_14, ZmPSTOL1_3.06_18* and *ZmPSTOL1_8.02_19*) increased total root length under low availability P (Table S2). Segregation analysis in the T4 generation indicated that the maize events for *OsPSTOL1_1, Sb07g002840_5, ZmPSTOL1_8.05_14* and *ZmPSTOL1_8.02_19* were still segregating (Table S2).

Phenotypic characterization of maize events overexpressing *PSTOL1* for root morphology in nutrient solution with low-P

We performed a correlation analysis with root morphology traits, shoot dry weight, shoot P content and transgene expression (Fig.3). Total root length was highly and positively correlated with root surface area of very fine ($r = 0.96$, $p < 0.01$) and fine roots ($r = 0.68$, $p = 0.064$), whereas increased root length was strongly associated with reduced root diameter ($r = -0.80$, $p = 0.016$). Shoot dry matter accumulation, which reflects maize performance in hydroponics, was highly associated with increased root length, surface area of very fine and fine roots ($r > 0.7$) and negatively correlated with root diameter ($r = -0.84$, $p < 0.01$), which is consistent with the significant negative association between fine root proliferation and root diameter. Shoot P content was neither associated with root length nor root surface area but tended to be negatively correlated with root diameter, which was positively correlated with shoot dry weight. Increased *PSTOL1* expression resulted in higher root surface area via enhanced proliferation of finer roots, which lead to increased shoot dry weight and P content of maize transgenic events cultivated under low-P (Fig. 3).

Events expressing rice (*OsPSTOL1_1*) and sorghum (*Sb07g002840_5, Sb03g031690_8, Sb03g006765_10* and *Sb03g006765_11*) *PSTOL1* genes showed enhanced total root length and surface area when compared to the non-transgenic B104 [$p < 0.05$ (Fig. 4A-B)]. Root length, root surface area of very fine and fine roots of *Sb07g002840_5* were increased by 35%, 46% and 20% respectively, compared to B104 ($p < 0.05$). Root length and root surface of very fine roots were also increased by 10% and 19% in *OsPSTOL1_1*, 16% and 25% in *Sb03g3g31690_8* and 24%-12% and 18%-20% for the maize events overexpressing *Sb03g006765* (*Sb03g006765_10* and *Sb03g006765_11*) ($p > 0.05$). Transgenic *OsPSTOL1* and *SbPSTOL1* events showed a reduction in root diameter from 5.4% (*Sb03g006765_10*) to 8.3% (*Sb03g031690_8*) in comparison with the wild type B104 ($p < 0.1$). However, the events for *ZmPSTOL1* presented no significant differences for root traits compared to wild-type B104.

A linear regression model fitted to B104 and the *PSTOL1* transgenic

events suggested that, in general, overexpression of *PSTOL1* genes led to an increase in root length specifically of finer roots (Fig. 4C). These root traits were negatively correlated ($r = -0.8$ and $p < 0.05$), suggesting that the increased total root length tended to reduce its diameter.

Overexpression of *PSTOL1* genes increases shoot dry matter accumulation in a low P soil

We assessed dry matter accumulation of selected transgenic and wild type B104 lines in pots containing soil supplemented with 0 or 200 kg P ha^{-1}. B104 line flowers late, the kernels do not always mature before the end of the growing season, hampering routine seed yield evaluations of biotech traits introduced in B104 at many geographical locations (Feys *et al.*, 2018), thus we evaluated the plant performance before flowering. The ANOVA analysis for shoot dry weight and plant height showed significant effects of P and genotype but non-significant P x genotype (Table 1).

Shoot biomass for *OsPSTOL1_1, Sb03g031690_8, Sb03g006765_10,* and *Sb03g006765_11* was significantly increased by 22% (*OsPSTOL1_1*) and 11% (*Sb03g006765_10*) compared to B104 [$p < 0.10$ (Fig. 5A)]. There was no significant different for root dry weight (Fig. 5C). Plant height of transgenic maize was also enhanced compared with B104 (Fig. 5B). The differences found were ~10% for *OsPSTOL1_1*, ~13% for *Sb03g006765_10*, ~6% for *Sb03g006765_11,* and ~9% for *ZmPSTOL1_3.06_18* ($p < 0.15$). No significant difference was detected on shoot biomass accumulation between transgenic maize lines expressing maize *PSTOL1* genes and B104.

A correlation analysis among total root length assessed in hydroponics and shoot dry matter accumulation in a low P soil revealed a significant and positive correlation [$r = 0.6$, $p > 0.01$ (Fig. 5C)]. Differences in the development of transgenic maize grown with low P availability were also visually detected (Fig. 5D).

DISCUSSION

The knowledge of the molecular mechanisms involved in the regulation of phenotypic plasticity in roots can assist plant breeders to develop strategies to select cultivars more adapted to abiotic stresses (Villordon *et al.*, 2014; Topp, 2016). Studies conducted with important crops, such as maize and rice, confirmed the association between genes and root system modulation, which increased grain yield in soils with nutrient or water deprivation (Saengwilai *et al.*, 2014; Lee *et al.*, 2016; Wang *et al.*, 2017). Unravelling adaptive mechanisms associated to root morphology and architecture is crucial for crops cultivated in regions with marginal soil fertility and in low-input agricultural systems, where low P availability is a major constraint can significantly improve food security worldwide.

We showed that the overexpression in maize of rice *PSTOL1* (*OsPSTOL1)* and its sorghum homologs (*Sb07g002840*, *Sb03g006765* and *Sb03g031690*) increased total root length and surface area of very fine and fine roots in maize seedlings grown in nutrient solution with low-P. In addition, these transgenic lines improved shoot dry weight in high and low-P soil in greenhouse low P soil. In rice, overexpression of *OsPSTOL1* increased total root length and surface area of transgenic seedlings and led to an enhancement of more than 60% of grain yield (Gamuyao *et al*., 2012). In maize, the presence of *OsPSTOL1* increased the biomass accumulation by 22%, suggesting that this gene has potential to be used in different species to improve P acquisition efficiency and yield.

Total root length in nutrient solution was positively correlated with shoot biomass accumulation in soil, being the highest for transgenic maize overexpressing *OsPSTOL1*, *Sb03g031690* and *Sb03g006765* (Fig. 5B). Although, *Sb07g002840* presented higher root surface area of fine roots in nutrient solution (Fig. 4), its shoot biomass accumulation and height on soil were similar to the wild type B104 (Fig. 5). These results suggested that overexpression of the *Sb07g002840* gene could interfere with plant development, as lethality was observed in some events overexpressing *Sb07g002840*. The lethal phenotype has been described for other genes that were overexpressed, such as the more root transcription factor (TaMOR-D) in wheat (Li *et al.*, 2016),

and auxin-responsive genes in petunia and rice (Tobeña-Santamaria *et al.*, 2002; Yamamoto *et al.*, 2007).

Although, *ZmPSTOL1* genes co-localize with QTLs for root and P-acquisition traits in hydroponics (Azevedo *et al*., 2015) and were coincident with QTLs for grain yield (Mendes *et al.*, 2014), the transgenic events for *ZmPSTOL1_8.05*, *ZmPSTOL1_3.06* and *ZmPSTOL1_8.03* presented the same performance as the wild type B104. Unlike the *Pup1* QTL that explains 80% of the phenotypic variance for P-efficiency in rice (Wissuwa *et al.*, 2002), maize QTLs explain from 6.87% to 15.17% (Azevedo *et al.*, 2015), having a much minor effect than *OsPSTOL1*. *ZmPSTOL1* genes co-localized with QTLs for root morphology, biomass accumulation and/or P content are preferentially expressed in roots of the parental lines that contributed the alleles enhancing the respective phenotypes (Azevedo *et al*., 2015). One possible explanation for the absence of phenotypic differences of the expression of *ZmPSTOL1* genes could be the high expression of such genes in the B104 inbred line, which was higher than in L3 and L22, the parental lines of our QTL mapping study (Azevedo *et al*., 2015). The high endogenous expression levels of such transcripts could mask their phenotypic effect of the *ZmPSTOL1* transgenes.

Increased root surface area, especially of finer roots in transgenic maize overexpressing *SbPSTOL1* genes is consistent with the results obtained in an association mapping undertaken in two sorghum panels and in a biparental QTL mapping phenotyped for P uptake, root system morphology in hydroponics (Hufnagel *et al*., 2014; Bernardino *et al*., 2019). *SbPSTOL1* alleles reducing root diameter enhanced P uptake under low P in hydroponics, whereas *Sb03g006765* and *Sb03g0031680* alleles increase root surface area and grain yield in a low-P soil. Tightly linked or pleiotropic QTL underlying the surface area of fine roots and grain yield co-located with *Sb03g006765* and *Sb03g031690*. *Sb07g02840* appears to enhance grain yield via small increases in root diameter. In sorghum, root surface area was positively associated with grain yield (Hufnagel *et al*., 2014; Bernardino *et al*., 2019) and maize overexpressing *SbPSTOL1* genes presented a significant correlation between root length and shoot biomass. There was no interaction between the transgenic events and P treatment in a greenhouse. However, *PSTOL1*-like genes were under the control of the constitutive promoter

Ubiquitin and most *PSTOL1* genes do not respond strongly to low P (Gamuyao *et al*., 2012; Azevedo *et al.*, 2015). Sorghum homologs of *OsPSTOL1* seemed to be linked with enhanced early root growth and grain yield under low-P availability.

The significant negative correlation of root diameter and surface area of very fine roots and total root length indicate that overexpression of *OsPSTOL1* and *SbPSTOL1* increased root surface area via enhanced proliferation of very fine roots, but not root dry weight, leading to an increasing of absorption surface with a minimal metabolic cost (Wu *et al.*, 2016). Proliferation of fine roots allows greater soils exploration and nutrient uptake, especially for nutrients with low mobility such as P. For cylindrical roots, root diameter determines the ratio of root length to root volume, which can be directly compared to the root length/root dry mass ratio (i.e. specific root length, SRL, [Eissenstat, 1991]). Zhu and Lynch (2004) found a negative correlation between SRL and average root diameter of both lateral and non-lateral roots in maize RILs. These authors implicated the elongation ability of lateral roots to their smaller diameter and greater SRL than non-lateral roots in most maize genotypes, which is related to the P investment for lateral root growth. All evidences so far, indicate that *PSTOL1* genes have a more general role in the root system, which results in the enhancement of P acquisition, benefiting cereal production worldwide.

SUPPLEMENTARY DATA

Supplemental Table S1: Primers used for PCR and RT-qPCR assays

Supplemental Table S2: Description of maize transgenic events overexpressing *OsPSTOL1*, *SbPSTOL1* and *ZmPSTOL1* genes

ACKNOWLEDGEMENTS

The authors would like to acknowledge funding from Embrapa Macroprogram grant (02.14.10.003.00.01) and Generation Challenge Programme. PhD fellowship for BFN was granted by Coordenação de Aperfeiçoamento de Pessoal de Nível Superior (CAPES) and for LSM was granted by Conselho Nacional de

Desenvolvimento Científico e Tecnológico (CNPq). We thank all staff and trainees of Embrapa and Sorghum that indirectly collaborated in the execution of this work.

REFERENCE

Abel S, Ticconi CA, Delatorre CA. 2002. Minireview Phosphdaate sensing in higher plants. Physiologia Plantarum **115**, 1–8.

Azevedo GC, Cheavegatti-Gianotto A, Negri BF, Hufnagel B, e Silva L da C, Magalhaes J V, Garcia AAF, Lana UGP, de Sousa SM, Guimaraes CT. 2015. Multiple interval QTL mapping and searching for PSTOL1 homologs associated with root morphology, biomass accumulation and phosphorus content in maize seedlings under low-P. BMC Plant Biology **15**, 172.

Bernardino KC, Pastina MM, Menezes CB, *et al.* 2019. The genetic architecture of phosphorus efficiency in sorghum involves pleiotropic QTL for root morphology and grain yield under low phosphorus availability in the soil. BMC Plant Biology **19**, 87.

Chen Y, Wu P, Zhao Q, Tang Y, Chen Y, Li M, Jiang H, Wu G. 2018. Overexpression of a Phosphate Starvation Response AP2/ERF Gene From Physic Nut in Arabidopsis Alters Root Morphological Traits and Phosphate Starvation-Induced Anthocyanin Accumulation . Frontiers in Plant Science **9**, 1186.

Cordell D, Drangert J-. O, White S. 2009. The story of phosphorus. Global food security and food for thought. Global Environmental Change **19**, 292–305.

de Sousa SM, Clark RT, Mendes FF, Carlos de Oliveira A, Vilaça de Vasconcelos MJ, Parentoni SN, Kochian L V, Guimarães CT, Magalhães JV. 2012. A role for root morphology and related candidate genes in P acquisition efficiency in maize. Functional Plant Biology **39**, 925–935.

Eissenstat DM. 1991. On the relationship between specific root length and the rate of root proliferation: a field study using citrus rootstocks. New Phytologist **118**, 63–68.

Feys K, Demuynck K, De Block J, Bisht A, De Vliegher A, Inzé D, Nelissen H. 2018. Growth rate rather than growth duration drives growth heterosis in maize B104 hybrids. Plant, Cell & Environment **41**, 374–382.

Frame B, Main M, Schick R, Wang K. 2011. Genetic Transformation Using Maize Immature Zygotic Embryos BT - Plant Embryo Culture: Methods and Protocols. In: Thorpe TA,, In: Yeung EC, eds. Totowa, NJ: Humana Press, 327–341.

Gamuyao R, Chin JH, Pariasca-Tanaka J, Pesaresi P, Catausan S, Dalid C, Slamet-Loedin I, Tecson-Mendoza EM, Wissuwa M, Heuer S. 2012. The protein kinase Pstol1 from traditional rice confers tolerance of phosphorus deficiency. Nature **488**, 535–539.

Godfray HCJ, Beddington JR, Crute IR, Haddad L, Lawrence D, Muir JF,

Pretty J, Robinson S, Thomas SM, Toulmin C. 2010. Food Security: The Challenge of Feeding 9 Billion People. Science **327**, 812–818.

Hallauer AR, Lamkey KR, White PR. 1997. Registration of Five Inbred Lines of Maize: B102, B103, B104, B105, and B106. Crop Science **37**, 1405–1406.

Heuer S, Lu X, Chin JH, *et al.* 2009. Comparative sequence analyses of the major quantitative trait locus phosphorus uptake 1 (Pup1) reveal a complex genetic structure. Plant Biotechnology Journal **7**, 456–471.

Hufnagel B, de Sousa SM, Assis L, *et al.* 2014. Duplicate and conquer: multiple homologs of PHOSPHORUS-STARVATION TOLERANCE1 enhance phosphorus acquisition and sorghum performance on low-phosphorus soils. Plant Physiology **166**, 659–77.

Hund A, Trachsel S, Stamp P. 2009. Growth of axile and lateral roots of maize. I. Devolopment of a phenotying platform. Plant Soil **325**,335-349.

Jelihovschi EG. FJC and AIB. 2014. ScottKnott: A Package for Performing the Scott-Knott Clustering Algorithm in R. Trends in Applied and Computational Mathematics **15**, 3–17.

Lambers H, Clements JC, Nelson MN. 2013. How a phosphorus-acquisition strategy based on carboxylate exudation powers the success and agronomic potential of lupines (Lupinus, Fabaceae). American Journal of Botany **100**, 263–288.

Lambers H, Finnegan PM, Laliberté E, Pearse SJ, Ryan MH, Shane MW, Veneklaas EJ. 2011. Phosphorus Nutrition of Proteaceae in Severely Phosphorus-Impoverished Soils: Are There Lessons To Be Learned for Future Crops? Plant Physiology **156**, 1058 LP-1066.

Lee D-K, Jung H, Jang G, Jeong JS, Kim YS, Ha S-H, Do Choi Y, Kim J-K. 2016. Overexpression of the OsERF71 Transcription Factor Alters Rice Root Structure and Drought Resistance. Plant physiology **172**, 575–588.

Li B, Liu D, Wang J, Li Q, Chang X, Mao X, Jing R. 2016. Overexpression of wheat gene TaMOR improves root system architecture and grain yield in Oryza sativa. Journal of Experimental Botany **67**, 4155–4167.

Lopez-Arredondo LD, Leyva-González MA, González-Morales SI, Opez-Bucio J, Herrera-Estrella L. 2014. Phosphate Nutrition: Improving Low-Phosphate Tolerance in Crops. Annual Review of Plant Biology **65**, 95–123.

Lynch JP. 2011. Root phenes for enhanced soil exploration and phosphorus acquisition: tools for future crops. Plant Physiology **156**, 1041–1049.

Ma N, Wang Y, Qiu S, Kang Z, Che S, Wang G, Huang J. 2013. Overexpression of OsEXPA8, a Root-Specific Gene, Improves Rice Growth and Root System

Architecture by Facilitating Cell Extension. PLOS ONE **8**, e75997.

Magnavaca R, Gardner CO, Clark RB. 1987. Evaluation of inbred maize lines for aluminium tolerance in nutrient solution. Genetic aspects of Plant mineral nutrition, 255–265.

Marschner H. 1996. *Mineral nutrition of higher plants*. Academic Press, London.

McGinnis K, Chandler V, Cone K, *et al.* 2005. Transgene-Induced RNA Interference as a Tool for Plant Functional Genomics. RNA Interference. Academic Press, 1–24.

Mendes FF, Guimarães LJM, Souza JC, Guimarães PEO, Magalhaes J V, Garcia AAF. 2014. Genetic architecture of phosphorus use efficiency in tropical maize cultivated in a low-P soil. Crop Science **54**, 1–9.

Mendiburu FD. 2019. agricolae: Statistical Procedures for Agricultural Research. R Package Version 1.2-3.

Miguel MA, Postma JA, Lynch JP. 2015. Phene synergism between root hair length and basal root growth angle for phosphorus acquisition. Plant physiology **167**, 1430–9.

Niu YF, Chai RS, Jin GL, Wang H, Tang CX, Zhang YS. 2013. Responses of root architecture development to low phosphorus availability: A review. Annals of Botany **112**, 391–408.

Parentoni SN, Souza CL. 2008. Phosphorus acquisition and internal utilization efficiency in tropical maize genotypes. Pesquisa Agropecuaria Brasileira **43**, 893–901.

Parentoni SN, Souza Jr CL, Carvalho Alves VMC, Gama EEG, Coelho AM, Oliveira AC. 2010. Inheritance and breeding strategies for phosphorus efficiency in tropical maize (Zea mays L.). Maydica **55**, 1–15.

Raghothama KG. 1999. Phosphate acquisition. Annual Review of Plant Physiology and Plant Molecular Biology **50**, 665–693.

Rausch C, Bucher M. 2002. Molecular mechanisms of phosphate transport in plants. Planta **216**, 23–37.

Revelle W. 2018. psych: Procedures for Psychological, Psychometric, and Personality Research.

Richardson AE, Lynch JP, Ryan PR, *et al.* 2011. Plant and microbial strategies to improve the phosphorus efficiency of agriculture. Plant and Soil **349**, 121–156.

Rojas RV, Achouri M, Maroulis J, Caon L. 2016. Healthy soils: a prerequisite

for sustainable food security. Environmental Earth Sciences **75**, 180.

Saengwilai P, Tian X, Lynch JP. 2014. Low Crown Root Number Enhances Nitrogen Acquisition from Low-Nitrogen Soils in Maize. Plant Physiology **166**, 581 LP-589.

Saghai-Maroof MA, Soliman KM, Jorgensen RA, Allard RW. 1984. Ribosomal DNA spacer length polymorphisms in barley: Mendelian inheritance, chromosomal location, and population dynamics. Proceedings of the National Academy of Sciences of the USA **81**, 8014–8018.

Sattari SZ, Bouwman AF, Giller KE, van Ittersum MK. 2012. Residual soil phosphorus as the missing piece in the global phosphorus crisis puzzle. Proceedings of the National Academy of Sciences of the USA **109**, 6348–6353.

Schmittgen TD, Livak KJ. 2008. Analyzing real-time PCR data by the comparative CT method. Nature protocols **3**, 1101–1108.

Silva FC da. 2009. *Manual de análises químicas de solos, plantas e fertilizantes*. Brasília.

Team RC al C. 2018. R: A Language and Environment for Statistical Computing.

Tobeña-Santamaria R, Bliek M, Ljung K, Sandberg G, Mol JNM, Souer E, Koes R. 2002. FLOOZY of petunia is a flavin mono-oxygenase-like protein required for the specification of leaf and flower architecture. Genes & Development **16**, 753–763.

Topp CN. 2016. Hope in Change: The Role of Root Plasticity in Crop Yield Stability. Plant Physiology **172**, 5 LP-6.

Vance CP, Uhde-Stone C, Allan DL. 2003. Phosphorus aquisition and use: critical adaptations by plants for securing a nonrewable resource. New Phytologist **157**, 423–447.

Villordon AQ, Ginzberg I, Firon N. 2014. Root architecture and root and tuber crop productivity. Trends in Plant Science **19**, 419–425.

von Uexküll HR, Mutert E. 1995. Global extent, development and economic impact of acid soils. Plant and Soil **171**, 1–15.

Wang J, Pei L, Jin Z, Zhang K, Zhang J. 2017. Overexpression of the protein phosphatase 2A regulatory subunit a gene ZmPP2AA1 improves low phosphate tolerance by remodeling the root system architecture of maize. PLOS ONE **12**, e0176538.

Wissuwa M, Wegner J, Ae N, Yano M. 2002. Substitution mapping of Pup1: a major QTL increasing phosphorus uptake of rice from a phosphorus-deficient soil. Theoretical and Applied Genetics **105**, 890–897.

Wu Q, Pagès L, Wu J. 2016. Relationships between root diameter, root length and root branching along lateral roots in adult, field-grown maize. Annals of Botany **117**, 379–390.

Yamamoto Y, Kamiya N, Morinaka Y, Matsuoka M, Sazuka T. 2007. Auxin Biosynthesis by the YUCCA Genes in Rice. Plant Physiology **143**, 1362 LP-1371.

Zhang C, Simpson RJ, Kim CM, Warthmann N, Delhaize E, Dolan L, Byrne ME, Wu Y, Ryan PR. 2018. Do longer root hairs improve phosphorus uptake? Testing the hypothesis with transgenic Brachypodium distachyon lines overexpressing endogenous RSL genes. New Phytologist **217**, 1654–1666.

Zhu J, Lynch JP. 2004. The contribution of lateral rooting to phosphorus acquisition efficiency in maize (*Zea mays*) seedlings. Functional Plant Biology **31**, 949–958.

TABLES

Table 1: Analysis of variance for three quantitative traits of transgenic maize grown in greenhouse conditions with low and high P.

	Df	Mean Square		
		Shoot dry weight	Plant height	Root dry weight
Block	3	239.1*	546.4***	14.55
Genotype	8	118.6	114.9	7.67
Phosphorus	1	31224.6***	28751.4***	1175.24***
Phosphorus X Genotype	8	66.2	49.2	2.08
Residuals	51	79.2	68.9	10.51

Df: degree of freedom (n-1). Values are significant at p-value <0.05 (*), <0.01 (**) and <0.01 (***).

Supplemental Table S1: Primers used for PCR and RT-qPCR assays

Gene ID	Assays	Primer sequence 5' - 3'	Product length (bp)
Bar	PCR	Bar F: AGAAACCCACGTCATGC Bar R: GTGGTTGACGATGGTGCA	427
OsPSTOL1	PCR	Ubi_F: GTGTTTAGCAAGGGCGAAAA sp_R: TCAGATGGCACAGTTTGCTC	707
	RT-qPCR SYBR Green	F: GTTTGTGGTGCATACAACTCGT R: GGTTCCTCAAAAACAGAAGATG	165
Sb07g002840	PCR	Ubi_F: GTGTTTAGCAAGGGCGAAAA sp_R CAGCGGGTAGGTAAGCAAGA	667
	RT-qPCR SYBR Green	F: CACCAGCCTCGATTTCATACAA R: AGCCGCACCGGAAGTAGAC	59
Sb03g03190	PCR	Ubi_F: GTGTTTAGCAAGGGCGAAAA sp_R TTGGTAGGGCACCTCTGAAG	721
	RT-qPCR SYBR Green	F: CGCTCCTCCTTGCTGTCTTG R: TGTAATCGTCGTCGGAAGGAT	60
Sb03g006765	PCR	Ubi_F: GTGTTTAGCAAGGGCGAAAA sp_R CACTCCACGAGAAACCCATT	738
	RT-qPCR SYBR Green	F: CGCCGACGATGAACATCTC R: TGGCTCTGCTGAAGACGAA	57
18 S rRNA	RT-qPCR SYBR Green	F: CGTCCTAGTCTCAACCATAAACG R: CCCCGGAACCCAAAGACT	82
ZmPSTOL1_8.05	PCR	Ubi_F: GTGTTTAGCAAGGGCGAAAA sp_R: TAGGTATTCGAGCCCTCTGG	733
	RT-qPCR Taqman	F: ATCAAAAAGAAAAGAAGCAGCA R: AAGGATGTGAGAATGACTAGACAC	78

		Probe: AACGGCAACAGCACCAACAATAGG	
ZmPSTOL1_3.06	PCR	Ubi_F: GTGTTTAGCAAGGGCGAAAA sp_R: GGCCAATCCAAAGTCAGAGA	670
	RT-qPCR Taqman	F: AGTATCAGCAGGACTTGTCATG R: CGCCCTCTTGGATCCTTG Probe: CAAGCAGAACCCCGTCAGTGTCA	97
ZmPSTOL1_8.02	PCR	Ubi_F: GTGTTTAGCAAGGGCGAAAA sp_R: CCATCCTAAAACTGCCTTCG	736
	qRT-PCR Taqman	F: TGGTTTTCAAGGGAAGGCTAG R: CCGTCACCTTTGGAGTCATG Probe: CAGGAATTTCACTGCAACTAGACGACCA	73

Ubi= Ubiquitin gene. sp = specific gene. F= forward. R =reverse. Taqman assay: 18S rRNA is a primer pair re-designed from the TaqMan ® Eukaryotic 18S rRNA (Applied Biosystems, Foster City, CA) and used as endogenous control.

Supplemental Table S2: Description of maize transgenic events overexpressing *OsPSTOL1*, *SbPSTOL1* and *ZmPSTOL1* genes

Event	Selection of transgenics events maize				
	T1		T3		T4
	χ^2 value	Relative expression	Total Root Length (cm)	Relative expression	χ^2 value
OsPSTOL1_1+	0.529*	937	467	1.15	0.01**
OsPSTOL1_2	0.250*	593	319	2.47	
OsPSTOL1_3	0.067*	393	355	2.3	
Sb07g002840_4	0.429*	1	325	2.24	
Sb07g002840_5+	0.800*	6	575	1.89	0.05**
Sb07g002840_6	1.190*	12	264	3.86	
Sb03g031690_7	6	1	400	1.08	
Sb03g031690_8+	0.200*	4308	493	414.1	-
Sb03g031690_9	0.200*	1764	331	70.2	
Sb03g006765_10+	0.474*	709	525	1.65	-
Sb03g006765_11+	0.474*	1124	474	7.79	-
Sb03g006765_12	0.182*	1253	402	6.69	
ZmPSTOL1_8.05_13	0.154*	25	295	58.44	
ZmPSTOL1_8.05_14+	5	4180	418	1649.51	2.97**
ZmPSTOL1_8.05_15	2.33*	2828	375	2935.19	
ZmPSTOL1_3.06_16	3.20*	6	254	19.46	
ZmPSTOL1_3.06_17	0.200*	20	295	51.76	
ZmPSTOL1_3.06_18+	6	19	375	9.43	-
ZmPSTOL1_8.02_19+	0.474*	38	387	49.29	4.76
ZmPSTOL1_8.02_20	0.250*	64	340	11.03	
ZmPSTOL1_8.02_21	0.474*	3	395	3.29	
B104			424		

+ selected maize transgenic events. χ^2 =chi-square test. *χ^2 <3.841, follows the 1:1 segregation ($p < 0.05$). ** χ^2 <3.841, follows the 3:1 segregation ($p < 0.05$).

FIGURE LEGENDS

Figure 1: Phenotypic characterization of non-transgenic maize lines in low P conditions. (A) Images of the B104, L3 and L22 root systems. (B) Phenotypic means for total root length (cm); root diameter (mm); total root surface area (cm^2); root surface area 1 (very fine roots, diameter between 0 and 1 mm) (cm^2); root surface area 2 (fine roots, diameter between 1 and 2 mm) (cm^2); shoot dry weight (mg) and shoot P content (g). (C) Expression profile of *ZmPSTOL1* genes in B104, L3 and L22. Root image, root morphology traits and expression profile were assessed after 13 days in nutrient solution with low-P. Error bars are shown. Different letters indicated statistical differences by the t-test (p-values $\leq$ 0.5).

Figure 2: Schematic structure of pMCG1005-*PSTOL1* cassette. (A) LB: left border T-DNA. RB: right border T-DNA. *Ubi*: ubiquitin promoter. Adn1-intron: enhancer of the ubiquitin promoter. *OCs3'* terminator (*octopine synthase* gene *A. tumefaciens*). 4x35S: *Cauliflower mosaic virus* (CaMV) 35S promoter tetramer. *Bar*: *phosphinothricin acetyltransferase* gene. *NOS*: terminator (*nopaline synthase* gene in *A. tumefaciens*). (B) Protein domain prediction of *OsPSTOL1, Sb07g002840, Sb03g006765, Sb03g031690, ZmPSTOL1_8.05, ZmPSTOL1_3.06, ZmPSTOL1_8.02.* Predicted domains are in color. Wall-associated receptor kinase galacturonan-binding (GUB_WAK). Wall-associated receptor kinase C-terminal (Wak). Serine/threonine kinase C-terminal (Kinase).

Figure 3: Correlation analysis of root morphology traits, shoot dry weight and shoot P content traits and *PSTOL1* expression (ΔCt). All traits were assessed after 13 days of treatment in nutrient solution with low-P. The root morphology traits assessed were root length (cm), root diameter (mm), root surface area 1 (very fine roots, diameter between 0 and 1 mm) (cm^2) root surface area 2 (fine roots, diameter between 1 and 2 mm) (cm^2). Pearson correlation coefficients (r) and p values (p).

Figure 4: Phenotypic characterization of wild type B104 and transgenic lines *PSTOL1* (*OsPSTOL1, SbPSTOL1* and *ZmPSTOL1*) in nutrient solution with low-P. (A) Images of the B104, *OsPSTOL1 (OsPSTOL1_1), SbPSTOL1 (Sb07g002840_5, Sb03g031690_8, Sb03g006765_10* and *Sb03g006765_11)* and *ZmPSTOL1 (ZmPSTOL1_8.05_14, ZmPSTOL1_3.06_18, ZmPSTOL1_8.02_19*) events root systems. (B) Phenotypic means

for total root length (cm); root diameter (mm); root surface area 1 (very fine roots, diameter between 0 and 1 mm) (cm^2) and root surface area 2 (fine roots, diameter between 1 and 2 mm) (cm^2). Significance level of Scott-Knott test, p-value ≤ 0.05 for total root length, root surface area 1 and root surface area 2; p-value ≤ 0.10 for root diameter. (C) Linear regression between total root length and root diameter. Pearson correlation coefficients (r) and p-values (p) are shown. B104, *ZmPSTOL1- OsPSTOL1- SbPSTOL1*-expressing lines are depicted by black, red and blue circles, respectively.

Figure 5: Phenotypic characterization of wild type B104 and transgenic lines PSTOL1 (*OsPSTOL1, SbPSTOL1* and *ZmPSTOL1*) grown in a low P soil. (A) Shoot dry weight (g). (B) Plant height (cm). (C) Root dry weight (g) were assessed after 45 days in soil with low and high-P. Error bars are shown. Different letters indicated statistical differences by the Scott-Knott test (p-values≤0.15). (D) Linear regression between total root length (cm) of plants grown in nutrient solution under low-P and shoot dry weigh (g) of the plants grown in soil with low-P in the greenhouse. Pearson correlation coefficients (r) and p-values (p) are shown. B104, *ZmPSTOL1, OsPSTOL1, SbPSTOL1* expressing lines are depicted by black, red and blue circles, respectively. (E) Images comparing the wild type B104, *OsPSTOL1_1, Sb03g006765_10* and *Sb03g006765_11* events after 45 days in low soil.

FIGURES

Figure 1

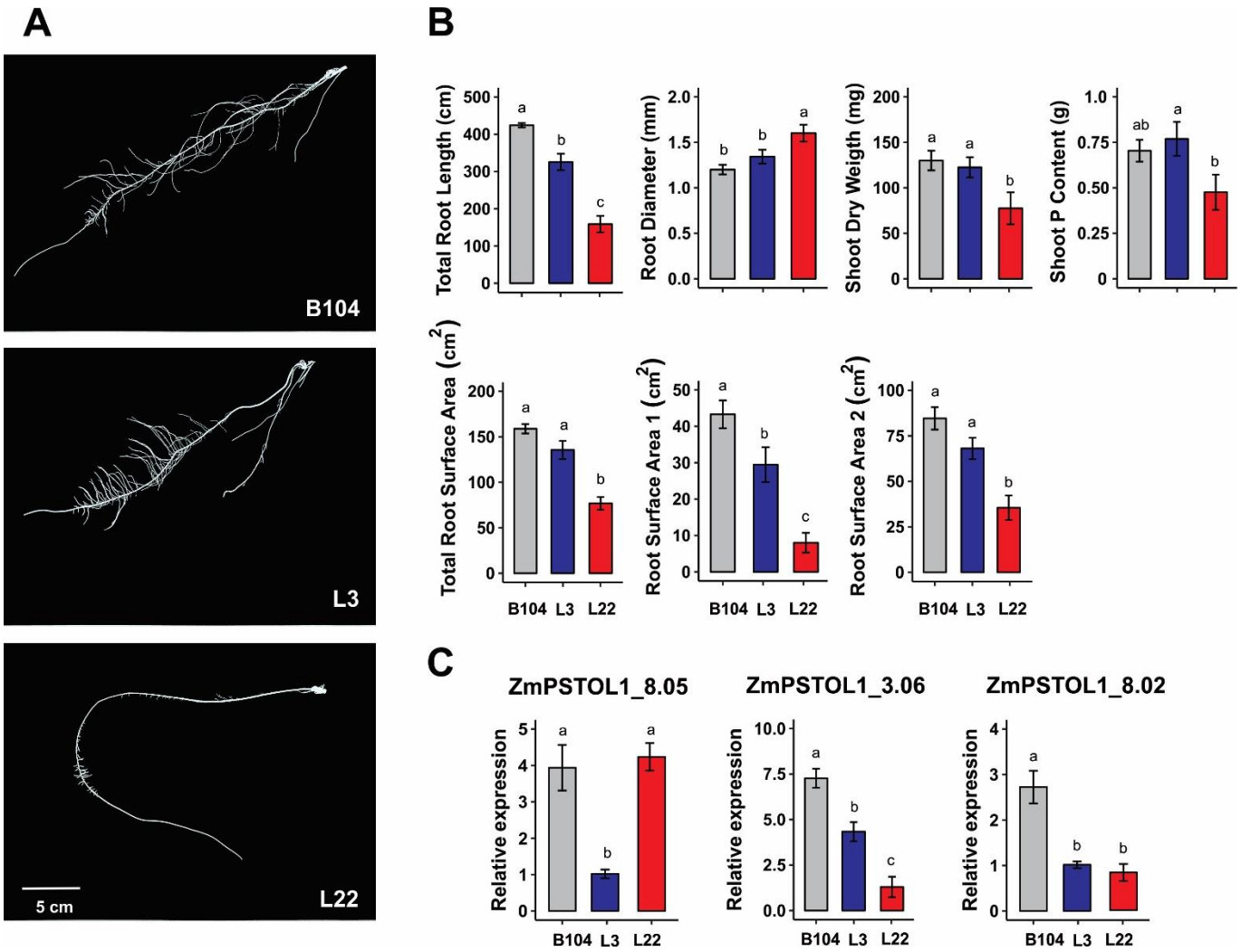

Figure 2

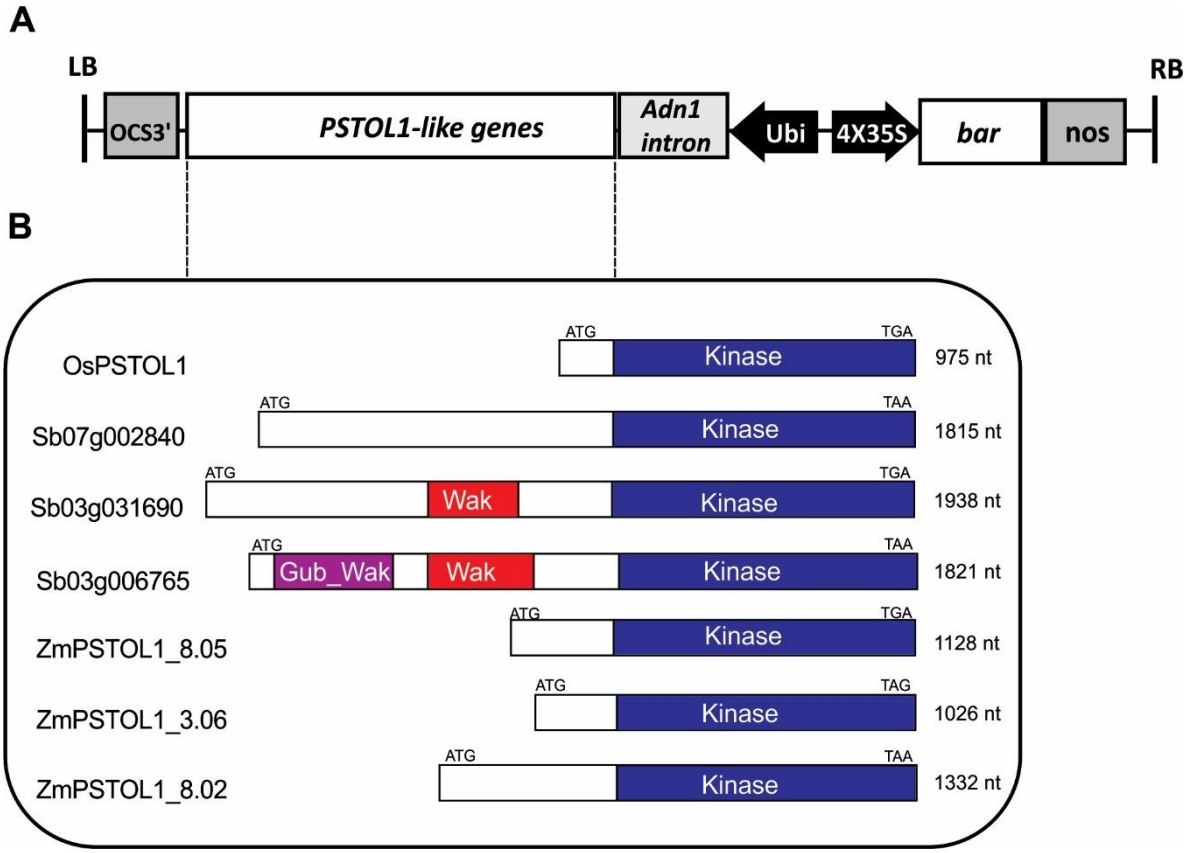
A
LB
RB
OCS3'
PSTOL1-like genes
Adn1 intron
Ubi
4X35S
bar
nos
B
OsPSTOL1
ATG
TGA
Kinase
975 nt
Sb07g002840
ATG
TAA
Kinase
1815 nt
Sb03g031690
ATG
TGA
Wak
Kinase
1938 nt
Sb03g006765
ATG
TAA
Gub_Wak
Wak
Kinase
1821 nt
ZmPSTOL1_8.05
ATG
TGA
Kinase
1128 nt
ZmPSTOL1_3.06
ATG
TAG
Kinase
1026 nt
ZmPSTOL1_8.02
ATG
TAA
Kinase
1332 nt

Figure 3

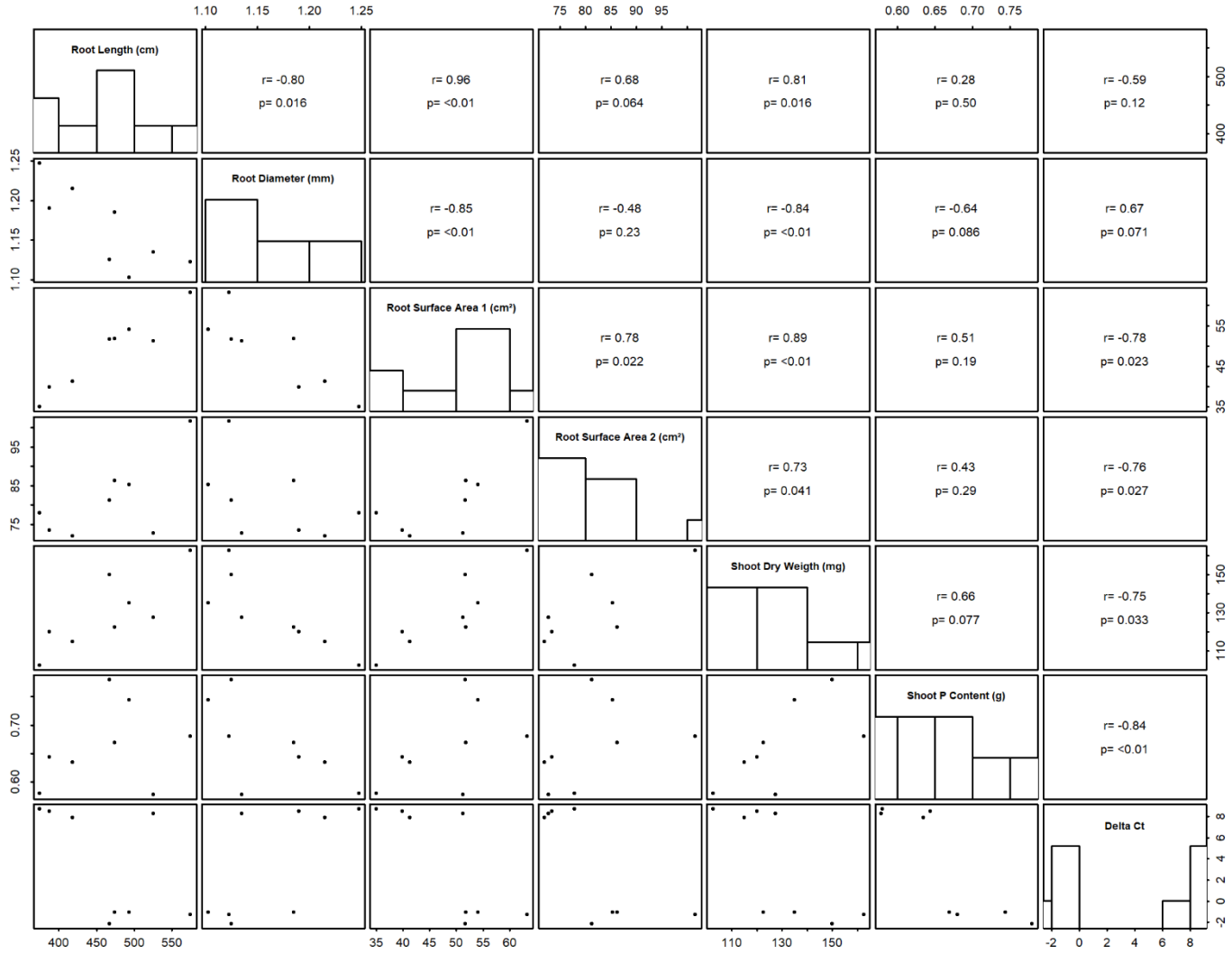
Root Length (cm)
Root Diameter (mm)
Root Surface Area 1 (cm²)
Root Surface Area 2 (cm²)
Shoot Dry Weigth (mg)
Shoot P Content (g)
Delta Ct
r= -0.80
p= 0.016
r= 0.96
p= <0.01
r= 0.68
p= 0.064
r= 0.81
p= 0.016
r= 0.28
p= 0.50
r= -0.59
p= 0.12
r= -0.85
p= <0.01
r= -0.48
p= 0.23
r= -0.84
p= <0.01
r= -0.64
p= 0.086
r= 0.67
p= 0.071
r= 0.78
p= 0.022
r= 0.89
p= <0.01
r= 0.51
p= 0.19
r= -0.78
p= 0.023
r= 0.73
p= 0.041
r= 0.43
p= 0.29
r= -0.76
p= 0.027
r= 0.66
p= 0.077
r= -0.75
p= 0.033
r= -0.84
p= <0.01
1.10 1.15 1.20 1.25
75 80 85 90 95
0.60 0.65 0.70 0.75
400 450 500 550
35 40 45 50 55 60
110 130 150
-2 0 2 4 6 8

Figure 4

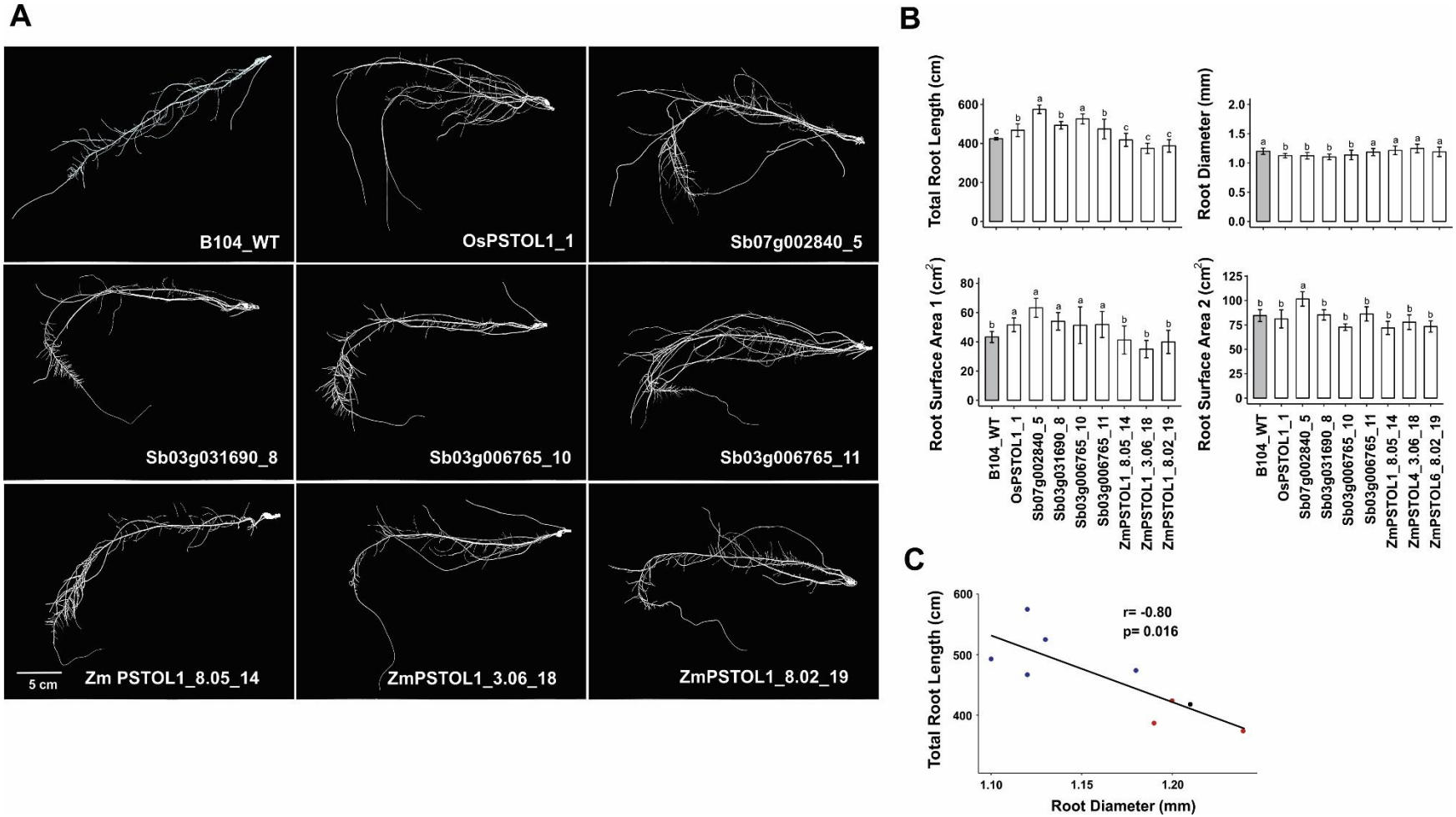
A
B104_WT
OsPSTOL1_1
Sb07g002840_5
Sb03g031690_8
Sb03g006765_10
Sb03g006765_11
5 cm
Zm PSTOL1_8.05_14
ZmPSTOL1_3.06_18
ZmPSTOL1_8.02_19
B
Total Root Length (cm)
Root Diameter (mm)
Root Surface Area 1 (cm2)
Root Surface Area 2 (cm2)
B104_WT
OsPSTOL1_1
Sb07g002840_5
Sb03g031690_8
Sb03g006765_10
Sb03g006765_11
ZmPSTOL1_8.05_14
ZmPSTOL1_3.06_18
ZmPSTOL1_8.02_19
ZmPSTOL4_3.06_18
ZmPSTOL6_8.02_19
C
r= -0.80
p= 0.016
Total Root Length (cm)
Root Diameter (mm)

Figure 5

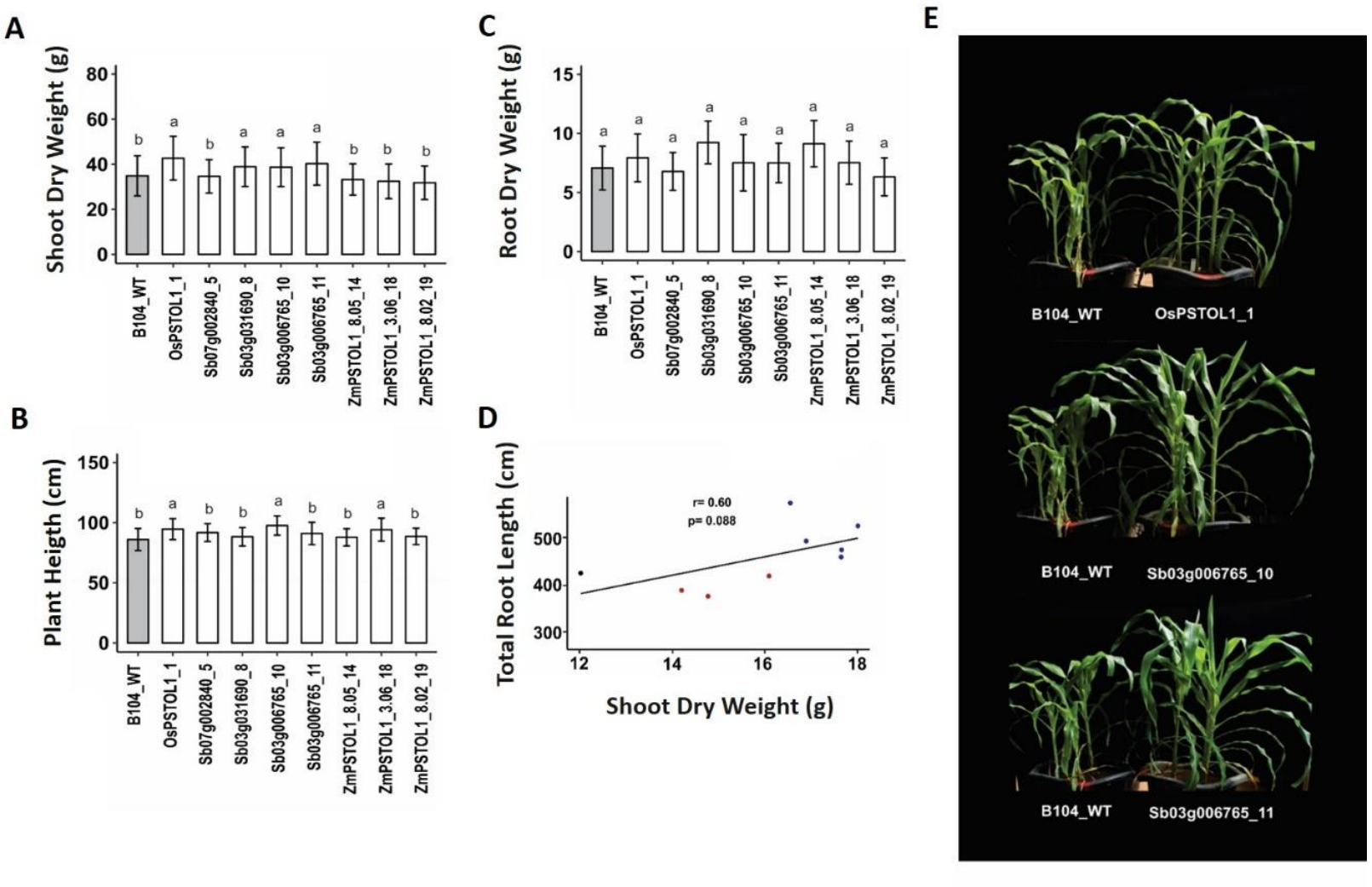
A
Shoot Dry Weight (g)
B
Plant Heigth (cm)
C
Root Dry Weight (g)
D
Total Root Length (cm)
r= 0.60
p= 0.088
Shoot Dry Weight (g)
E
B104_WT
OsPSTOL1_1
B104_WT
Sb03g006765_10
B104_WT
Sb03g006765_11
B104_WT
OsPSTOL1_1
Sb07g002840_5
Sb03g031690_8
Sb03g006765_10
Sb03g006765_11
ZmPSTOL1_8.05_14
ZmPSTOL1_3.06_18
ZmPSTOL1_8.02_19

CAPÍTULO 2

PHOPHORUS-STARVATION TOLERANCE 1 (ZmPSTOL1_3.06) ESTÁ ASSOCIADO A FORMAÇÃO DO PELO RADICULAR E EFICIÊNCIA DE FÓSFORO EM MILHO

Negri, BF[1]; Ferreira, NF[2]; Ribeiro, CAG[3]; Lopes, SS[1]; Lana, UGP[3]; Alves, MC[3]; Magalhães, JV[3]; Guimarães, CT[3]; Carneiro, AA[3]; de Sousa, SM[1,2,3]

[1]Universidade Federal de São João Del Rei (UFSJ), Sete Lagoas, MG, Brasil
[2]Centro Universitário de Sete Lagoas (UNIFEMM), Sete Lagoas, MG, Brasil
[3]Embrapa Milho e Sorgo, Sete Lagoas, MG, Brasil

ABSTRACT

Phosphorus (P) is an essential macronutrient, however tropical soils are deficient in readily available forms of P, which limits cereal production. A multiple interval QTL mapping in a maize recombinant inbred line population derived from a bi-parental cross between contrasting lines for P-efficiency revealed maize homologs to *Phosphorus-Starvation Tolerance 1* (*OsPstol1*) that enhances root surface area, P acquisition and grain yield under P deficiency in rice. Of these candidate genes, *ZmPSTOL1_3.06* co-localized with QTLs for root morphology, biomass accumulation and/or P content on chromosome 3 and is highly expressed in the root of L3 maize line, the donor line of the favorable QTL allele. To gain insights on the role of *Phosphorus-Starvation Tolerance 1* in maize roots we cloned and characterized the transcriptional control of the *ZmPSTOL1_3.06* gene. *ZmPSTOL1_3.06* was more expressed in L3 primary root, especially at the differentiation zone. We verified the expression of *ZmPSTOL1_3.06* in 77 genotypes from a maize diversity panel genotyped with over 300,000 GBS based-SNPs and in order to detect possible genomic regions related to *ZmPSTOL1_3.06* expression we performed an eGWAS analysis. We found an extend gene expression variation within the genotypes. The most significant SNP (Single Nucleotide Polymorphism) associated with *ZmPSTOL1_3.06* expression in the GWAS (Genome Wide Association Studies) was the closest to the target

gene, indicating that the variation in this gene expression was mainly controlled by cis elements. Furthermore, sequencing around 2 Kb of L3 and L22 promoter region revealed an insertion of a MITE transposon (*PIF/Harbinger*) in the promoter of L22 line around -800 bp, which probably disrupted the *ZmPSTOL1_3.06* expression in the inefficient genotype. Cis-regulatory elements (CREs) related to phosphorus deficiency and root hairs were found in this region using Genomatix MatInspector software. To confirm the region responsible for transcriptional regulation of *ZmPSTOL1_3.06*, 2,282 Kb upstream of ATG from L3 line was isolated and cloned on pTF102 vector with *Gus* as a reporter gene for permanent expression assays. *GUS* activity driven by the *ZmPSTOL1_3.06* promoter was higher under low P, corroborating with expression analysis. *Histochemical* staining of the transgenic plants showed that GUS was specifically expressed in maize root hairs. It is interesting to notice that L3 presented longer and denser root hairs than L22. The overexpression of *ZmPSTOL1_3.06* affects the expression of genes reported with the hair root development of maize, *Rth1* and *Rth3* and increases the length of the root hair. We speculate that *ZmPSTOL1_3.06* is related to root hair formation and adaptation to the low-P environment.

Key words: Root, Nutrient solution, Gene expression, Cis-regulatory elements

INTRODUÇÃO

Baixa disponibilidade de P representa um dos principais entraves à produtividade das culturas agrícolas. Mais de 70% da biomassa terrestre ocorre em solos com baixo conteúdo de fósforo, incluindo mais da metade das terras agricultáveis do planeta (Lynch, 2011). Comparado com outros macronutrientes, a concentração de P inorgânico (Pi) na solução de solo é sub-ótima para a produção de grãos, fazendo do P um dos macronutrientes menos disponíveis no solo (Vance *et al.,* 2003). Além disso, é um dos nutrientes com difusão mais lenta, criando uma zona de deficiência ao redor da rizosfera. O problema ainda é agravado pelo fato de que o P pode se fixar ao Ca em solos calcários e ao Fe e Al em solos ácidos, reduzindo sua solubilidade e disponibilidade para as

plantas (Marschner, 1995). Assim, a disponibilidade de P nos solos, em geral, é muito baixa, apesar do conteúdo total de P ser muito maior que a quantidade disponível para uso pelas plantas. Nesse sentido, nos diversos sistemas de produção agrícola, principalmente nos solos tropicais, são necessárias aplicações de grandes quantidades de P no solo para garantir a produtividade, uma vez que a eficiência de absorção do fosfato adicionado pode ser inferior a 20% (Zhu *et al.,* 2006). Outro grande problema relacionado ao P é que ele constitui um recurso natural não renovável, e, seu uso indiscriminado, pode levar ao esgotamento das jazidas em até 60 anos (Vance & Chiou, 2011).

A eficiência de uso de um nutriente (EFUSO) pode ser definida como gramas de grãos produzidos por grama de nutriente suprido à cultura. Este índice é dividido em dois componentes principais: eficiência de aquisição (EAQ) e eficiência de utilização interna (EUTIL) (Moll *et al.,* 1982). Para milho tropical, foi verificado que a EAQ foi duas e três vezes mais importante que a EUTIL em solos com baixa e alta disponibilidade de P, respectivamente. Além disso, tais características não foram correlacionadas significativamente entre si, indicando um possível envolvimento de mecanismos e genes distintos no controle de cada uma delas (Parentoni & Souza Júnior, 2008). Os principais mecanismos ligados à eficiência de aquisição de P podem ser agrupados em: modificações de atributos morfológicos da raiz, modificações químicas na rizosfera, alterações fisiológicas na cinética de absorção e interações com microrganismos, principalmente fungos micorrízicos (Lynch & Brown, 2012).

Modificações na configuração espacial do sistema radicular são importantes para a eficiência na aquisição de P em plantas devido à baixa mobilidade do fósforo no solo (Zhu *et al.,* 2005). Como estratégia para aumentar a aquisição de P, as plantas eficientes tendem a ter maior relação de massa seca da raiz e da parte aérea e maior comprimento de raiz, além de raízes mais finas, pelos radiculares mais longos e densos, obtendo assim uma maior área superficial do sistema radicular (Marschner, 1995; Zhu *et al.,* 2006, Zhu *et al*., 2010). Como resposta adaptativa, a arquitetura do sistema radicular alterada aumenta a aquisição de P com um custo metabólico mínimo (Lynch & Brown 2001; Lynch & Ho, 2005).

A complexidade da eficiência na aquisição de fósforo em plantas tem sido explorada por meio de estratégias de mapeamento de QTLs (*Quantitative Trait Loci*) relacionados com a arquitetura do sistema radicular, formação de pelos radiculares (Lynch & Brown 2001; Zhu *et al*., 2005; Zhu *et al.,* 2006; Miguel *et al*., 2015), associação com fungos micorrízicos e produção de matéria seca (Kaeppler *et al.,* 2000). Apesar de alguns QTLs já terem sido descritos (revisado por Magalhães *et al.,* 2017), eles ainda são pouco utilizados como critério de seleção nos programas de melhoramento. O *Pup1* é um QTL de efeito maior na absorção de fósforo (P), que afeta a morfologia radicular de plantas de arroz (Ni *et al.,* 1998; Wissuwa & Ae, 2001; Wissuwa *et al.,* 1998). Trabalhos utilizando uma população de mapeamento derivada de Kasalath (eficiente na aquisição de P) e Nipponbare (ineficiente) indicaram que *Pup1* responde por cerca de 80% da variabilidade fenotípica para características correlacionadas com absorção de P em arroz (Wissuwa *et al.,* 2002). O gene responsável pelo loco *Pup1* foi isolado e chamado *Phosphorus-starvation tolerance 1* (*Pstol1*). Este gene codifica uma serina/treonina quinase que quando superexpressa em arroz aumenta o crescimento radicular e a aquisição de P e, consequentemente, a produtividade de grãos (Gamuyao *et al.,* 2012). Em sorgo foram identificados homólogos do *OsPSTOL1* que possuem um papel mais geral no sistema radicular, alterando não somente a morfologia radicular, como também a arquitetura da raiz, contribuindo assim para o ganho de rendimento de grãos em solos com baixa disponibilidade de P (Hufnagel *et al.,* 2014; Bernardino *et al.,* 2019).

Em milho foram identificadas seis proteínas com identidade superior a 55% com o OsPSTOL1 (BAK26566). Dos seis genes homólogos ao *OsPSTOL1* em milho, quatro candidatos co-localizam com *clusters* de QTLs relacionados à morfologia radicular, peso seco total e eficiência na aquisição de P e três deles tiveram maior expressão gênica no sistema radicular do que na parte aérea (*ZmPSTOL1_8.05*, *ZmPSTOL1_3.06* e *ZmPSTOL1_8.02*) (Azevedo *et al.,* 2015). As proteínas codificadas por esses genes apresentam um domínio quinase receptora serina/treonina citoplasmática (RLCKs) semelhante com do *OsPSTOL1*, além de possuírem um domínio conservado de ligação de ATP (Gamuyao *et al.,* 2012; Azevedo *et al.,* 2015).

Apesar dos recentes avanços no entendimento das redes de sinalização, poucas proteínas quinases foram diretamente relacionadas com o sistema radicular e a eficiência na aquisição de fósforo (Gamuyao *et al.,* 2012; Haruta *et al.,* 2014; Hufnagel *et al.,* 2014; Azevedo *et al.,* 2015; Boisson-Dernier *et al.,* 2015; Liao *et al.,* 2016). O trabalho descrito nesse capítulo visou a caracterização do gene *ZmPSTOL1_3.06* e o mecanismo de regulação transcricional implicado na sua expressão em raízes de milho.

MATERIAL E MÉTODOS

Análise da expressão gênica em genótipos contrastantes para eficiência no uso de P

Genótipos contrastantes para eficiência no uso de P, L3 (eficiente) e L22 (ineficiente) (de Sousa *et al.,* 2012) foram crescidos em casa de vegetação por 100 dias em condições ideais de fertilização e irrigação, sendo coletados inflorescência masculina, caule, sementes, folhas e raiz.

Em câmara de crescimento, as sementes dos genótipos de milho (L3 e L22) foram desinfestadas com hipoclorito de sódio à 0,5% por 5 minutos, lavadas com água deionizada e germinadas em papel de germinação. Após quatro dias, foram selecionadas plântulas uniformes e para garantir o estresse de P foi retirado o endosperma. As plantas foram crescidas em solução nutritiva de Magnavaca modificada (pH 5,65) (Magnavaca *et al.,* 1987) com 2,5 µM de P em um sistema composto de pastas de arquivo forradas com papel de germinação (Hund *et al.,* 2009) por 13 dias em câmara de crescimento com temperatura diurna média de 27 ± 3 °C, noturna de 20 ± 3 °C e fotoperíodo de 12 horas, sob aeração contínua. A solução nutritiva, em contato com aproximadamente 3 cm das pastas, foi trocada a cada três dias (de Sousa *et al.,* 2012). As raízes foram posteriormente separadas em raiz primária, nodal, seminal e lateral, sendo a raiz primária dividida em zona de divisão celular (o primeiro centímetro a partir do ápice apical), zona de alongamento celular (os três centímentos após o ápice radicular) e zona de diferenciação celular (restante da raiz primária). Nos experimentos de expressão temporal as linhagens L3 e L22 foram coletadas 4

dias após a germinação e então submetidas ao estresse com baixo P (definido como tempo zero), três, seis, nove, treze e vinte dias após o início do tratamento.

O RNA total foi extraído utilizando o kit Plant RNeasy (Qiagen), seguindo as orientações do fabricante. A síntese do cDNA foi realizada utilizando-se 1 ug de RNA total, previamente tratados com DNase I, utilizando o kit “High Capacity cDNA Reverse Transcription” (Applied Biossystems, CA). As análises de qPCR quantitativo foram realizadas no equipamento ABI Prism 7500 Sequence Detection System (Applied Biosystems) utilizando a técnica de Taqman para o *ZmPSTOL1_3.06* (Direto: 5’-AGTATCAGCAGGACTTGTCATG-3’, Reverso: 5’-CGCCCTCTTGGATCCTTG-3’ e sonda: 5’-CAAGCAGAACCCCGTCAGTGTCA-3’) (Azevedo *et al.,* 2015) e SYBRGreen® para o gene *Gus* (Direto: 5’-CGTGGCAAAGGATTCGATAA-3’ e reverso: 5’-CTCTTCAGCGTAAGGGTAATG-3’), *Rth1* (direto: 5'-CAACCGGAAAGTTGACGAAT-3' e reverso: 3'-ACAACTCGTCGGAGGTCAGT-5') (Wen *et al.,* 2005) e *Rth3* (direto: 5'-TGGGTCCGACTACCTTGTTC-3' e reverso: 3'-AAGCCATCTCCAGCAACAAC-5') (Hochholdinger *et al.,* 2008), segundo as recomendações do fabricante. Foi utilizado um par de primers 18S ribossomal TaqMan® (Life Technologies^{TM}) e 18S ribossomal SYBR como controle endógeno (direto: 5'-CGTCCTAGTCTCAACCATAAACG-3' e reverso: 3'-CCCCGGAACCCAAAGACT-5'). A expressão gênica relativa foi cálculada conforme o método $2^{-\Delta\Delta CT}$ (Livak & Schmittgen, 2001).

Análise de *expression Genome*-W*ide* Association *Study* (*eGWAS*)

Os dados de expressão gênica (Ct) dos 73 genótipos, pertencentes ao Banco de Germoplasma e Programa de Melhoramento da Embrapa Milho e Sorgo (Tabela 1), e das linhagens L3 e L22 foram utilizados para as análises de eGWAS. Os acessos foram genotipados com mais de 300.000 SNPs por GBS (*Genotyping-by-Sequencing*) (Ribeiro, 2015). Brevemente, o DNA genômico das linhagens foram extraídos usando o método CTAB (Saghai-Marrof *et al*., 1984) e submetido a GBS utilizando a enzima de restrição *ApeK1* para preparação da biblioteca (Elshire *et al.,* 2011). As sequências brutas produzidas foram processadas de acordo com Glaubitz e colaboradores (2014). O processo de

filtragem foi realizado no software TASSEL 5 (Bradbury *et al*., 2007). O perfil do QQ-plot foi considerado para a seleção do modelo do GWAS. A estrutura foi corrigida através dos cinco primeiros componentes principais, que foram gerados a partir dos dados genotípicos com no máximo 10% de dados perdidos. Um conjunto aleatório desses SNPs foram selecionados (24722 SNPs).

Tabela 1 – Lista dos genótipos de milho pertencentes ao Banco de Germoplasma e Programa de Melhoramento da Embrapa Milho e Sorgo utilizados nos experimentos de expressão gênica.

Nº do genótipo	**Pedigree**	**Nº do genótipo**	**Pedigree**
1	L57500_07	41	DTMA-52
2	L57500_08	43	DTMA-56
3	L521274	44	DTMA-60
4	L521280	45	DTMA-70
6	L521462	46	DTMA-71
7	L521529	47	DTMA-73
8	L(228_3x876518)_4_1_1_1_1	48	DTMA-79
9	L724	50	DTMA-99
10	L726	51	DTMA-117
11	L845	52	DTMA-126
12	L1113_01	53	DTMA-138
13	CatAl237/67	54	DTMA-155
14	L2_3_2_1	55	DTMA-156
15	L4	62	DTMA-204
16	LPF963173	64	DTMA-219
17	CMS61L10	65	DTMA-222
18	L540404_11	66	DTMA-242
19	L5780121	67	DTMA-243
20	CMS28_17_2	68	DTMA-275
21	L578073	69	DTMA-296
22	CML343	70	DTMA-297
23	CML348	71	DTMA-298
24	L56_3_228_9560_58	72	L(L3xL37)_5_6_1_1_1
25	L(5046xL3)xL3)_3_7)xL3)_1)xL3	73	L(5046x228_3)_2_1_1
26	L371056_1	76	L512388
27	L371060_1	77	L520992
28	L3L31113_01_1_1_1_1S2	78	L530837
29	L5702816	80	L83_3/28
30	L3810227_1	81	L951021_2_2
31	L482041_30	82	LPiracicaba14_04B

Continua

Continuação

Nº do genótipo	Pedigree	Nº do genótipo	Pedigree
32	L3910994_1	83	L(228_3x1612841_102_2)_1_4
33	L590449_1	84	L19
34	L2110764_3	85	L513330_01
35	L3100243_1	86	L5133302016_08
36	L3100182_7	87	L(504611_01xL3_17)
38	DTMA-11	88	L5320708
39	DTMA-27		

Sequenciamento da região promotora de *ZmPSTOL1_3.06* e obtenção de eventos *ZmPSTOL1_3.06*::*Gus*

A região promotora do gene *ZmPSTOL1_3.06* foi amplificada a partir das linhagens L3 e L22. O DNA foi extraído de acordo com Saghai-Maroof e colaboradores (1984) e oligonucleotídeos foram desenhados a partir da sequência *ZmPSTOL1_3.06* da linhagem Mo17 (http://www.phytozome.net/maize.php) com o software livre *Primer3Plus* (Untergasser *et al*., 2007). Para a linhagem L3 foram amplificados 2282 pb (Direto: 5'- GGATCCAAACCTCTTAGTTTCCAGTAGCA-3 e Reverso: 5'-GGATCCCCCGTATTTGTAAGCAGAGAAGAAT-3') e L22, 2039 pb (Direto: 5'-CCCGGGACAAACCATTTGGGGTTGAACCAT-3' e Reverso: 5'-CCCGGG CCCGTATTTGTAAGCAGAGAAGAAT-3') *upstream* ao códon de início da transcrição. O fragmento referente à região promotora do gene na linhagem L3 foi subclonado no pGEM®-T Easy com *BamHI* e inserido no vetor binário pTF102 (Paz *et al*., 2004), que possui o gene repórter *Gus* e o marcador de seleção *Bar*. O cassete de expressão foi inserido na *Agrobacterium tumefaciens* EHA101, via eletroporação (Sambrook *et al.,* 1989) e a transformação de milho Hi II foi realizada utilizando o protocolo desenvolvido por Frame e colaboradores (2011). As plantas T0 foram plantadas em vaso em casa de vegetação e polinizadas com L3 para obtenção de plantas transgênicas T1.

Análise *in silico* da região promotora

Para a identificação de possíveis elementos cis-regulatórios na região promotora, foi considerado 2.282 pb acima do códon de início da transcrição do gene para L3 e de 2.613 pb para L22. As sequências foram analisadas com o software *Genomatix MaTinspector* (Cartharius *et al*., 2005) considerando apenas motivos com o score de similaridade com o banco de dados maior que 0.8. Para a análise de elementos transponíveis, a sequência da região promotora foi contraposta no banco de dados de elementos transponíveis de plantas (P-MITE disponível em http://pmite.hzau.edu.cn/).

Ensaios fluorimétrico e histoquímico

Sementes de milho *ZmPSTOL1_3.06*::*Gus* T1 foram submersas em herbicida Glufosinato (Finale®) 0,2% (v/v) por seis horais, para eliminar as sementes não transgênicas, e depois colocadas em rolos de papel de germinação por quatro dias. Após esse período, o endosperma foi retirado com o auxílio de um bisturi, retirando as reservas nutricionais e garantindo o estresse de P. As plântulas foram mantidas em rolos de papel de germinação contendo solução nutritiva de Magnavaca modificada (Magnavaca *et al.,* 1987) com baixo P (2,5 µM) e alto P (250 µM). Após 7 dias as plântulas foram coletadas para realização da análise fluorimétrica, de acordo com o protocolo descrito por Francis e Spiker (2005), histoquímicas conforme Jefferson e colaboradores (1987) e de expressão gênica, conforme descrito acima. A atividade de GUS foi fotografada com o auxílio do com o esteroscópio Axio Zoom V16 (Zeiss). Plantas de milho contendo a construção gênica CaMV35S::*Gus* foram utilizadas como controle positivo e como controle negativo foi utilizada a linhagem selvagem L3.

O delineamento experimental foi inteiramente casualizado com três repetições biológicas com três plantas cada e triplicata técnica. Foi realizado uma Anova seguido do teste de média de Tukey, com o $P< 0,05$, usando o pacote *emmeans* do software livre R Core Team versão 3.5.2.

Obtenção das plantas transgênicas superexpressando *ZmPSTOL1_3.06*

A região codificante do gene *ZmPSTOL1_3.06* (1026 pb) da linhagem L3 foi sintetizada e clonada nos sítios *AvrII* e *SpeI* no vetor binário pMCG1005 (Iowa State University Plant Transformation Facility) pela empresa GenScript USA Inc. (http://www.genscript.com). O vetor pMCG1005 tem o promotor ubiquitina, marcados de seleção *Bar* sob promotor 4x35S. As plantas de milho da linhagem B104 foram transformadas via *A. tumefaciens* pela "Plant Transformation Facility" da Iowa State University. As plantas foram plantadas em casa de vegetação e autofecundadas até a geração T3. Para a seleção das plantas transgênicas foi utilizado o herbicida Glufosinato (Finale®) 0,2% (v/v).

Comprimento dos pelos radiculares

As raízes foram coradas com solução de corante azul de tripano (m/v) em lactoglicerol (1:1:1 ácido láctico, glicerol e água) por 24 horas e posteriormente lavadas progressivamente em etanol 70%. Os pelos radiculares foram fotografados, cerca de três centímetros a partir da base da raiz, com o esteroscópio Axio Zoom V16 (Zeiss). O comprimento foi medido com o auxílio do software livre IMAGEJ (http://rsbweb.nih.gov/ij/). O comprimento dos pelos foi estimado pela média de dez pelos de cada uma das dez imagens da raiz de cada plântula (Miguel, 2004). Foi realizado uma Anova seguido do teste de média de Tukey, com o $P< 0,05$, usando o pacote *emmeans* do software livre R Core Team versão 3.5.2.

RESULTADOS

***ZmPSTOL1_3.06* é mais expresso na zona de diferenciação celular da raiz primária do genótipo eficiente ao uso de P**

A análise de expressão tecidual nas plantas adultas de L3 (eficiente) e L22 (ineficiente) crescidas em casa de vegetação mostrou uma maior expressão na raiz, seguida da inflorescência, caule e folhas, enquanto não foi detectado

expressão nas sementes (Figura 1A). A linhagem eficiente para aquisição de P teve maior expressão em todos os tecidos em comparação com a linhagem ineficiente (L22).

Buscando uma melhor compreensão da fase do desenvolvimento radicular que esses genes são expressos sob condição limitante de P, foi realizada uma análise de expressão gênica durante o desenvolvimento. Os resultados obtidos revelaram que a expressão do *ZmPSTOL1_3.06* aumentou no início do crescimento da raiz da linhagem L3 e manteve-se superior a linhagem L22 durante os 20 dias de estresse (Figura 1B).

A análise de expressão relativa nos diferentes tipos radiculares de plântulas de milho crescidas sob deficiência de P mostrou maiores níveis do transcrito *ZmPSTOL1_3.06* na raiz primária e menores níveis na raiz lateral (Figura 1C). A expressão de *ZmPSTOL1_3.06* foi maior em L3 em todos os tipos radiculares (Figura 1C). Com o gene apresentou maior expressão na raiz primária, foi feito um detalhamento sobre a localização dos transcritos neste tipo radicular. *ZmPSTOL1_3.06* apresentou maiores níveis de expressão na zona de diferenciação celular na linhagem L3 (Figura 1D). Este gene foi expresso 5 e 45 vezes mais na zona de elongação e diferenciação celular do que na zona de divisão celular na linhagem L3, com baixos níveis de expressão em todas as regiões da raiz primária na L22.

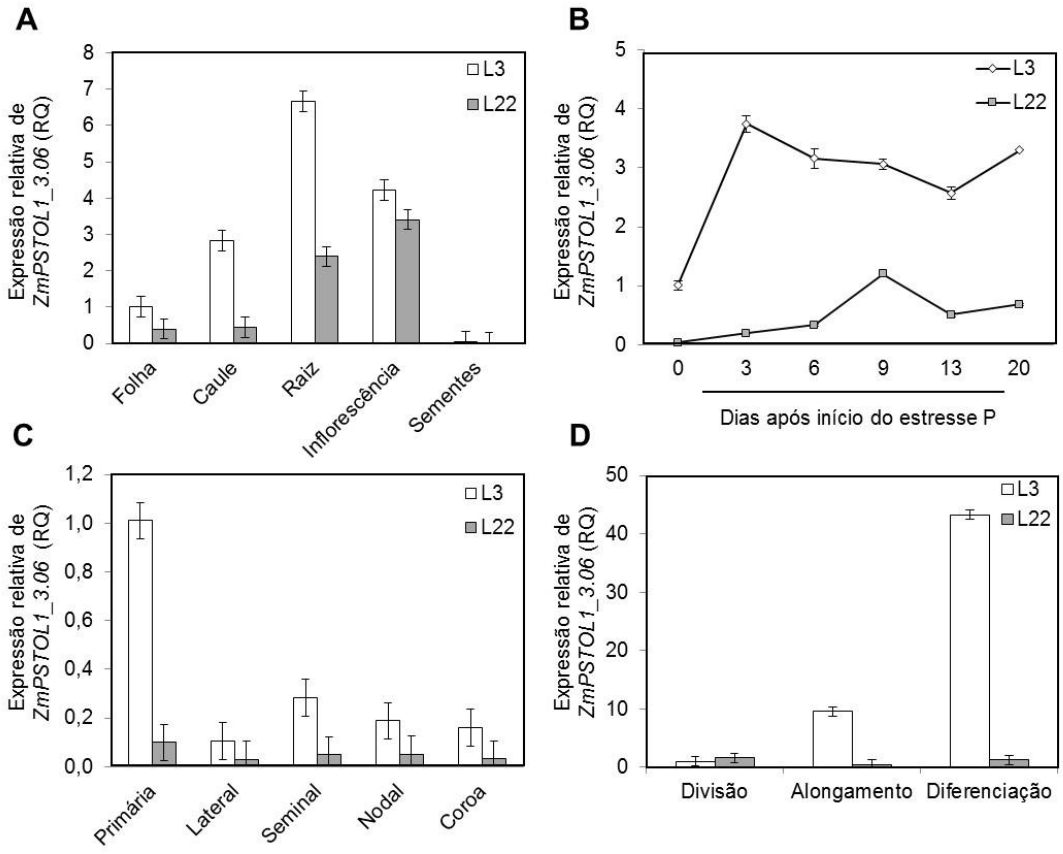

Figura 1 – Perfil de expressão do gene *ZmPSTOL1_3.06* nas linhagens L3 e L22 crescidas em solução nutritiva com baixo P (2,5 µM). **A** – Diferentes tecidos da planta adulta de milho crescida em casa de vegetação por 100 dias (folha, caule, raiz, inflorescência e sementes). **B** – Diferentes tempos de coleta (0, 3, 6, 9, 13 e 20 dias) após o início do estresse com baixo P. **C** - Diferentes tipos de raízes (primária, lateral, seminal, nodal e coroa). **D** - Diferentes regiões da raiz primária (divisão, alongamento e diferenciação). Cada amostra é composta por triplicata biológica com três plantas cada. A expressão gênica relativa foi calculada utilizando o método $2^{-\Delta\Delta CT}$ com três repetições técnicas.

Análise de eGWAS com linhagens de milho contrastantes para morfologia radicular

Foi verificada grande variabilidade de expressão do gene *ZmPSTOL1_3.06* entre as linhagens do Banco de Germoplasma e do Programa de Melhoramento da Embrapa Milho e Sorgo (Figura 2). As linhagens 8, 15, 32, 34 e 87 mostraram maior expressão do que a linhagem eficiente (L3) para

aquisição de P, sendo que na linhagem 34 o *ZmPSTOL1_3.06* foi quatro vezes mais expresso do que na linhagem eficiente L3. Os dados obtidos na análise de expressão gênica das linhagens do painel de milho contrastantes para comprimento total da raiz revelaram que não há correlação significativa entre as características de morfologia radicular e a expressão desses genes.

A análise de *eGWAS* utilizando os dados de expressão de *ZmPSTOL1_3.06 e* os dados genotípicos, mostraram a presença de SNPs (*Single Nucleotide Polymorphism*) significativos associados com a expressão do gene *ZmPSTOL1_3.06* (Tabela 2). Dois dos sete SNPs mais significativos estão localizados no cromossomo 3 a cerca de 23 Kb, sendo o mais significativo de todos ($p=9,99E^{-09}$), e 10.000 Kb de distância do gene *ZmPSTOL1_3.06* (Tabela 1).

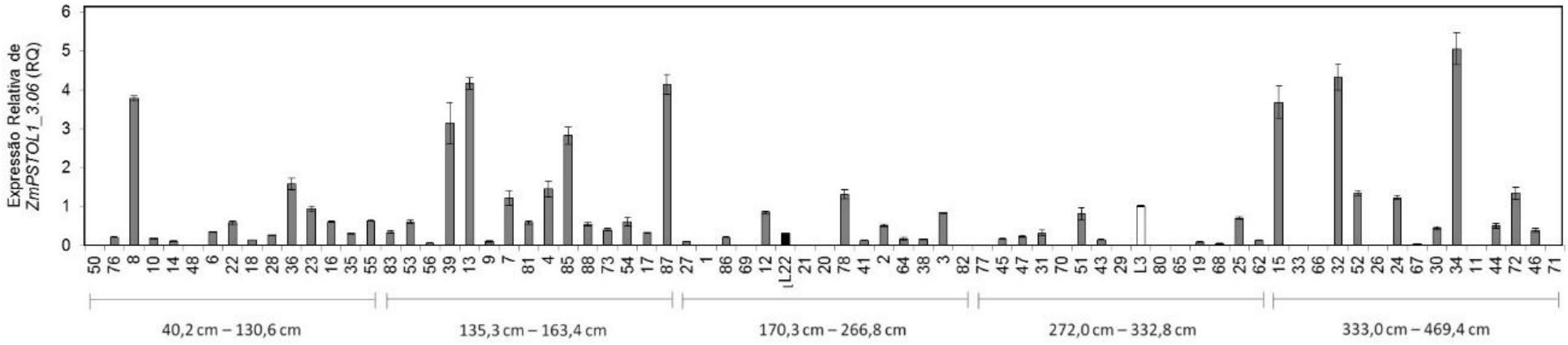

Figura 2 - Expressão dos genes candidatos no sistema radicular de linhagens de milho contrastantes quanto ao comprimento total de raízes. As linhagens do painel estão em cinza, a linhagem L22 em preto e L3 em branco. As plântulas foram germinadas por 4 dias e crescidas em solução nutritiva com baixo P (2,5 µM) por 13 dias. Cada amostra foi composta por nove plântulas por genótipo. A expressão gênica relativa foi calculada utilizando o método $2^{-\Delta\Delta CT}$ com três repetições técnicas e a amostra L3 usada como calibrador. As barras de erro são referentes ao desvio padrão das médias das repetições técnicas.

Tabela 2 – Posição, distância e p-valor dos marcadores significativos na análise de eGWAS.

Marcador	Cromossomo	Posição física	p-valor	Distância de *ZmPSTOL1_3.06*
S3_206944073	3	206944073	$9{,}99E^{-09}$	23 Kb
S2_230865775	2	230865775	$3{,}44E^{-08}$	-
S10_122268788	10	122268788	$2{,}90E^{-07}$	-
S2_202635930	2	202635930	$3{,}60E^{-07}$	-
S1_117161946	1	117161946	$4{,}47E^{-07}$	-
S3_216948516	3	216948516	$9{,}59E^{-07}$	10.000Kb
S6_124855634	6	124855634	$9{,}64E^{-07}$	-

Caracterização da região promotora de *ZmPSTOL1_3.06*

Por meio da comparação da região promotora do gene *ZmPSTOL1_3.06* das linhagens contrastantes para uso de P, foi detectada uma inserção de 352 pb entre as posições -790 e -1142 pb na linhagem L22, que corresponde a posição -827 da linhagem L3 (Figura 3). Essa sequência de 352 pb tem identidade de 93% com o transposon DTH_Zem11, pertencente à família MITE (*Miniature inverted-repeat transposable element*) e superfamília PIF (*P instability fator*)/Harbinger.

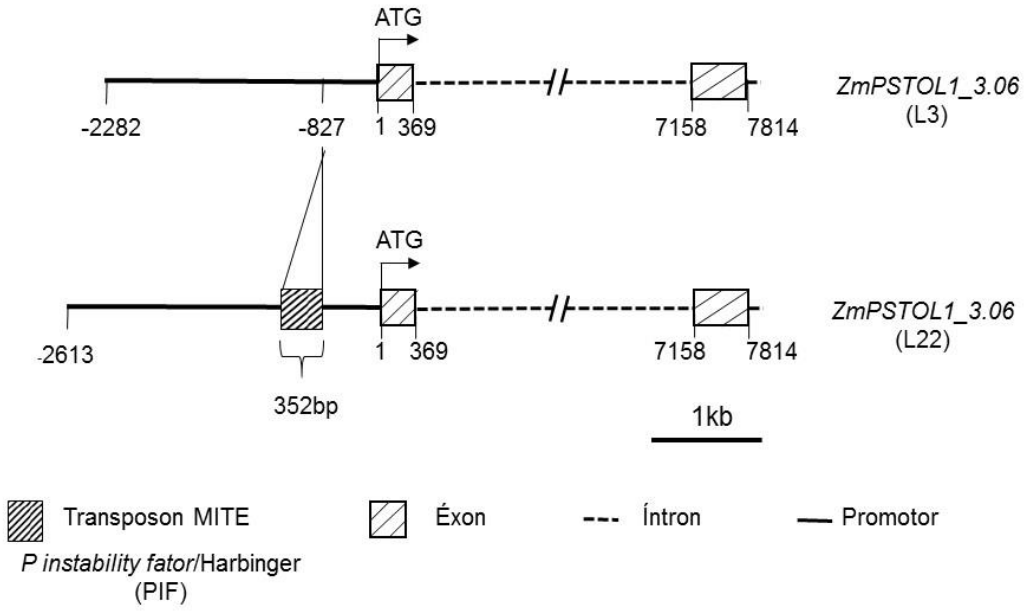

Figura 3 – Esquema da sequência do gene *ZmPSTOL1_3.06* das linhagens L3 e L22. A figura ilustra a região promotora, éxons, íntrons e inserção do elemento transponível da família DTHZm11, da superfamília PIF/Harbinger na região regulatória do *ZmPstol1_3.06* na linhagem L22.

A análise de elementos cis-regulatórios da região promotora do gene *ZmPSTOL1_3.06* nas linhagens L3 e L22 revelou a presença de três sítios do motivo P1BS (sequência GNATATNC), que é o sítio de ligação do fator de transcrição relacionado ao estresse de P, *Phosphate Starvation Response 1* (PHR1) na posição -705, -818 e -2268 da linhagem L3, e na posição -378, -668 e -781 da linhagem L22 (Tabela 3). Essas sequências apresentaram similaridade de 1 a 0,8, sendo o máximo 1, com as sequências dispostas no banco de dados do software MatInspector para motivos de ligação de fatores de transcrição de plantas. Além do motivo de ligação do fator de transcrição da família MYB, PHR1, foi verificado a presença de um motivo de ligação específico de pelos radiculares na posição -81 com similaridade de 0,9 em ambas as linhagens (Tabela 3).

Tabela 3 – Elementos cis regulatórios localizados na região promotora do gene *ZmPSTOL1_3.06* (L3) (-2282 pb) e *ZmPSTOL1_3.06* (L22) (-2613 pb) envolvidos na formação de raiz e estresse de P.

Elemento	**Posição**		**Sequência**		**Similaridade**	
Cis	**L3**	**L22**	**L3**	**L22**	**L3**	**L22**
Phosphate starvation response 1 (PHR1)	-2268	-781	acaagaATTTgctactgga	ggcagaATATaccaaaaat	0,9	1,0
Phosphate starvation response 1 (PHR1)	-818	-668	ggcagaATATaccaaaaat	tcctgtATATgccaacaaa	1,0	1,0
Phosphate starvation response 1 (PHR1)	-705	-378	tcctgtATATgccaacaaa	gtttgaATATgggtattgg	1,0	0,8
Root hair-specific element	-81	-81	aggtattcttgcaggCACGctgtcg	ttttattcttgcaggCACGctgtcg	0,9	0,9

A análise de expressão gênica e fluorimétrica do *GUS* sob a regulação do promotor *ZmPSTOL1_3.06*(L3) (Figura 4 A) mostraram indução da expressão sob baixo P nas raízes das plântulas de milho (Figura 4B e C). Apesar dos eventos apresentarem maior atividade e expressão do *GUS* em relação a planta selvagem L3 (controle negativo), os eventos transgênicos apresentaram valores baixos em relação ao promotor constitutivo CaMV35S (controle positivo), sendo a diferença entre o *CaMV35S:Gus* e o *ZmPSTOL1:Gus*_EV2 de 15 a 120 vezes no ensaio fluorimétrico e de expressão, respectivamente. A análise histoquímica mostrou coloração azul em toda a planta no evento transgênico *CaMV35S:Gus* (controle constitutivo) (Figura 4D) e nos eventos *ZmPSTOL1:Gus* a coloração azul referente ao *GUS* foi observada apenas na raiz e mais precisamente nos pelos radiculares das plantas crescidas sob baixo P (Figura 4E e F).

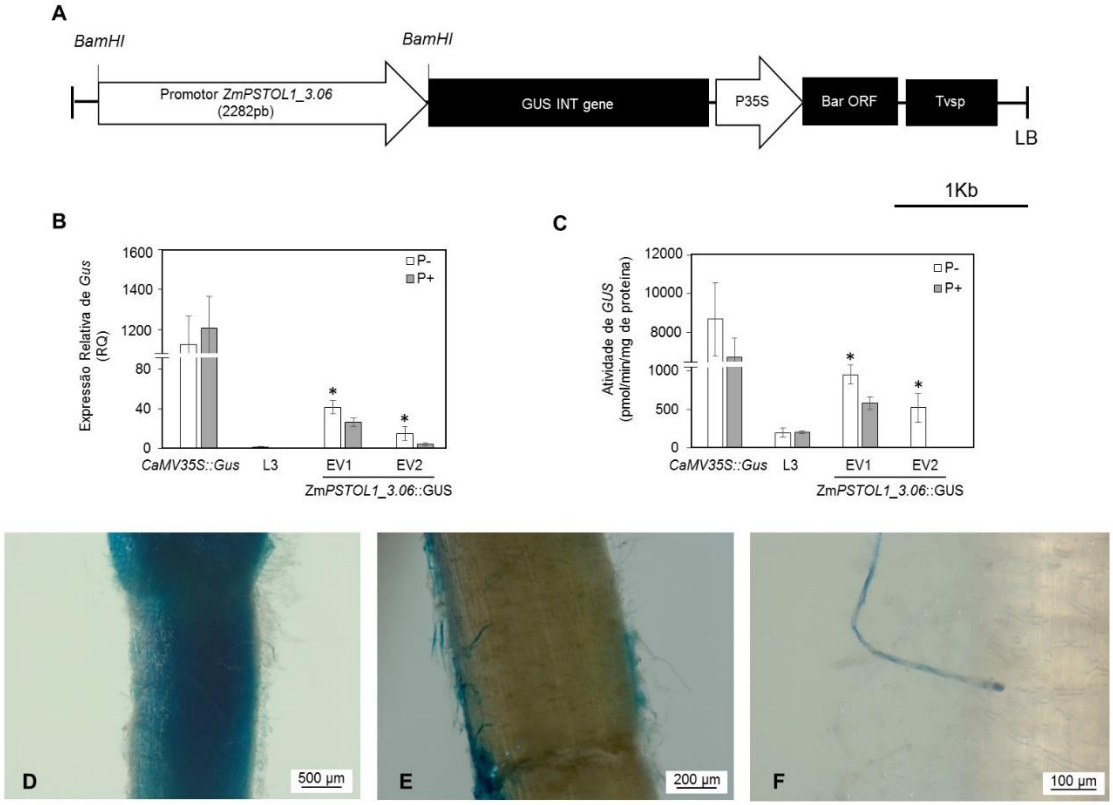

Figura 4 – Perfil da atividade de GUS sob regulação do promotor *ZmPSTOL1_3.06*(L3). (**A**) Esquema do cassete de transformação inserido no vetor pTF102. (**B**) Ensaio de expressão gênica, (**C**) ensaio fluorimétrico e histoquímico de plantas transgênicas *CaMV35S::Gus* (**D**) (Controle positivo), *ZmPSTOL1_3.06::GUS* (**E, F**) e selvagem L3 (controle negativo) *Médias com diferença significativa entre o tratamento de baixo e alto P pelo teste de Tukey (p<0,05).

Caracterização de eventos superexpressando *ZmPSTOL1_3.06*

O evento *UBI::ZmPSTOL1_3.06*_EV2 apresentou a maior expressão de *ZmPSTOL1_3.06* entre os eventos transgênicos analisados, tendo uma diferença de quase seis vezes em relação ao selvagem (B104) (Figura 5A). Além da expressão do gene *ZmPSTOL1_3.06* foi analisada a expressão dos genes relacionados com o desenvolvimento de pelos radiculares em milho, o *Rth1* (*Roothairless 1*) (Wen *et al*., 2005) e *Rth3* (*Roothairless 3*) (Hochholdinger *et al.,* 2008) (Figura 5B e C). Foi observado que o evento 2 de *UBI::ZmPSTOL1_3.06*, que teve o maio nível de expressão do gene *ZmPSTOL1_3.06,* apresentou os níveis mais baixos de expressão dos genes *Rth1* e *Rth3,* enquanto o evento 1

apresentou os maiores níveis de expressão de *Rth1* e *Rth3*, porém não diferiu de forma significativa do controle negativo quanto a expressão de *ZmPSTOL1_3.06*.

O comprimento dos pelos radiculares de todos eventos transgênicos *ZmPSTOL1_3.06* foi superior ao comprimento de pelos radiculares das plantas não transgênica (B104) (Figura 5D, E e F). Uma análise mais detalhada do sistema radicular mostrou que a linhagem L3, que possui maior expressão do gene *ZmPSTOL1_3.06,* também possui pelos radiculares mais longos em relação à linhagem L22, que possui baixa expressão desse gene. A diferença de expressão sob baixo P entre L3 e L22 chega a quase 2,5 vezes, podendo ser notada visualmente (Figura 6).

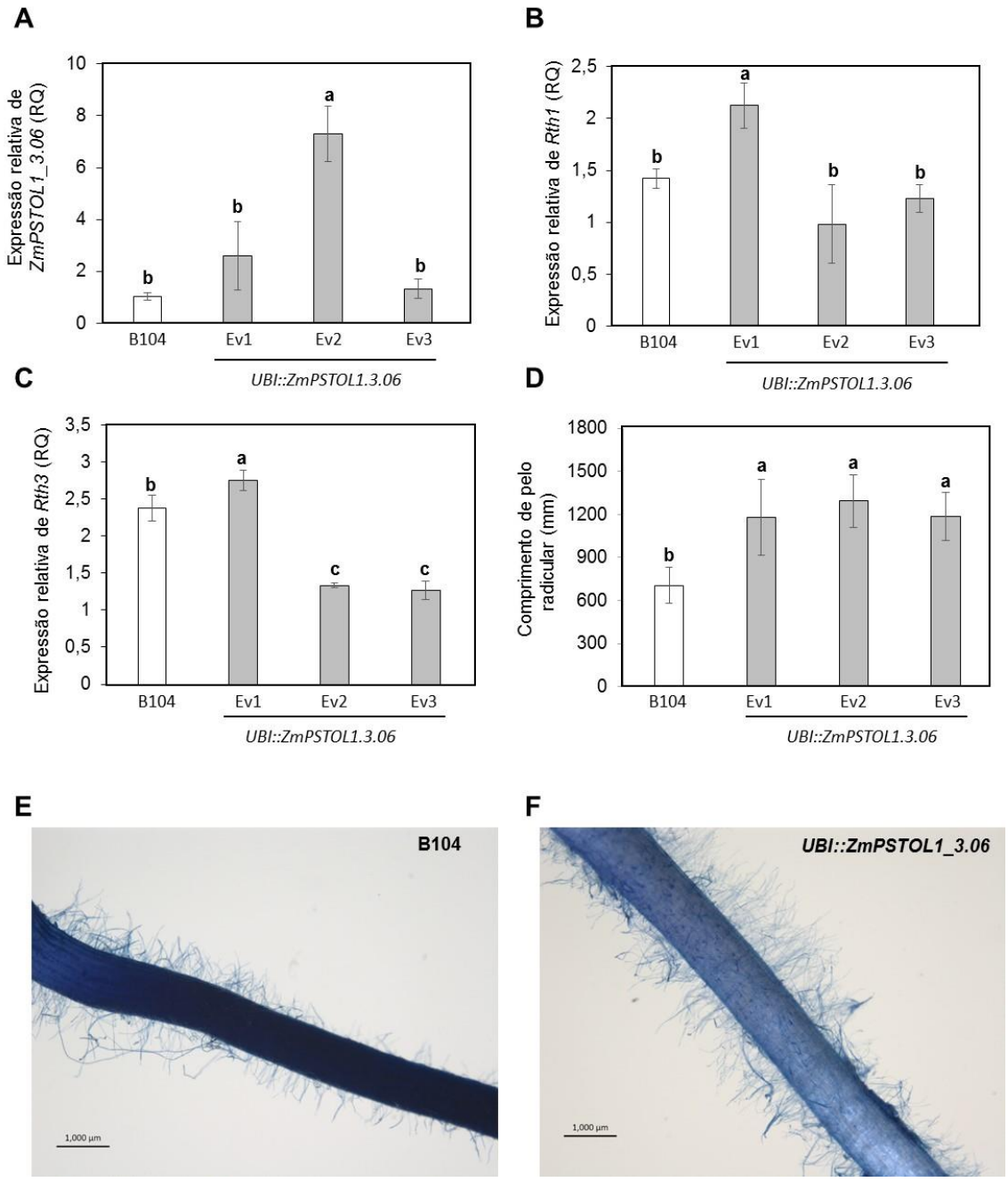

Figura 5 – Análise de expressão gênica dos genes (**A**) *ZmPSTOL1_3.06*, (**B**) *Rth1,* (**C**) *Rth3* e imagem de raiz selvagem – B104 (**E**) e de eventos *UBI::ZmPSTOL1_3.06* (**F**). As médias foram significativas a 5% de probabilidade pelo teste de Tukey.

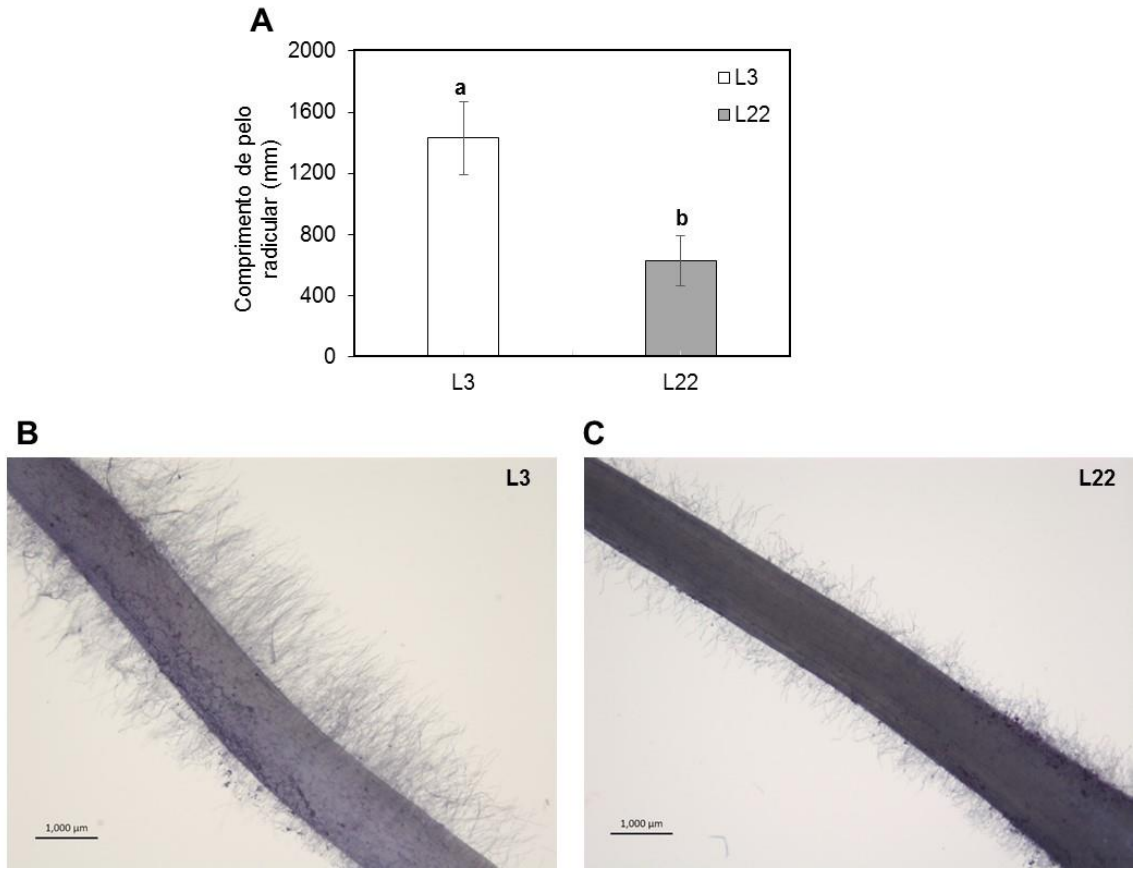

Figura 6 – Quantificação dos pelos radiculares (mm) das linhagens L3 e L22. As médias foram significativas a 5% de probabilidade pelo teste Tukey.

DISCUSSÃO

ZmPSTOL1_3.06 é uma quinase expressa preferencialmente na raiz em diferentes estágios da planta

As quinases do tipo receptoras em plantas são conhecidas por regular uma ampla gama de processos, entre eles, a simbiose entre plantas e fungos micorrízicos arbusculares (Roth *et al.,* 2018), resistência a doenças (Hurni *et al.,* 2015; Miranda *et al.,* 2017), regulação do crescimento celular (Hématy & Hofte, 2008), resposta a estresses abióticos, como hídrico (Ramegowda *et al.,* 2014), privação de P (Gamuyao *et al.,* 2012; Hufnagel *et al.,* 2014; Azevedo *et al.,* 2015; Milner *et al.,* 2018; Bernadino *et al*., 2019) e salino (Yu & Assmann, 2018). No

entanto, muito sobre os mecanismos genéticos e moleculares das vias de sinalização envolvendo essas quinases de milho ainda precisa ser compreendido.

Neste trabalho verificamos o perfil de expressão detalhado do gene *ZmPSTOL1_3.06,* que codifica uma quinase do tipo receptora citoplasmática serina/treonina, relacionada com características morfológicas radiculares, peso seco raiz:parte aérea, biomassa e conteúdo de P em plântulas crescidas sob condições de baixo P (Azevedo *et al.,* 2015). A expressão de *ZmPSTOL1_3.06* nos parentais (L3 e L22) das linhagens endogâmicas recombinantes (RILs) de milho utilizadas no mapeamento de QTL para eficiência no uso de P é maior na raiz das plantas crescidas sob baixo P, por essa razão as análises foram realizadas apenas nessa condição (Azevedo *et al*., 2015). Apesar da expressão de *ZmPSTOL1_3.06* ser cerca de cinco vezes superior na linhagem L3 (eficiente) em comparação com L22 (ineficiente) (Azevedo *et al.,* 2015), foi feito um detalhamento da expressão gênica em diferentes tempos e tecidos em ambas as linhagens.

Na fase vegetativa foram detectados transcritos não apenas no sistema radicular, mas também na inflorescência masculina, caule e folhas. Recentemente, foi mostrado que *ZmPSTOL1_3.06* é induzido na inflorescência feminina de plantas inoculadas com *Colletotrichum graminicola,* um fungo que afeta o desenvolvimento normal da planta causando redução do rendimento de grãos em milho (Miranda *et al.,* 2017). Já foi mostrado, que algumas quinases podem participar de diversos processos na planta, como é o caso da FERONIA (FER), uma quinase do tipo receptora que contém os domínios extra e intracelular, importante para a fertilidade feminina (Escobar-Restrepo *et al.,* 2006; Huck *et al.,* 2003), crescimento de pelos radiculares (Duan *et al.,* 2010), modulação da sinalização do sistema imunológico (Stegman *et al.,* 2017) crescimento celular, integridade da parede celular e tolerância ao estresse salino em *Arabidopsis* (Hofte, 2015; Yu & Assmann, 2018). Outro gene é a MARIS (MIR), uma quinase citoplasmática que é preferencialmente expressa no tubo polínico e nos pelos radiculares e está relacionada com o seu desenvolvimento (Boisson-Dernier *et al.,* 2015). Os dados de expressão gênica sugerem que apesar do *ZmPSTOL1_3.06* ter sido mapeado para eficiência de aquisição de P

(Azevedo *et al.,* 2015), ele pode atuar em diferentes vias de fosforilação e estar relacionado com a formação e desenvolvimento do pólen, e na sinalização em resposta à patógenos, como descrito para outras quinases.

A expressão *ZmPSTOL1_3.06* foi maior na linhagem L3 crescida em solução nutritiva do que na linhagem L22 desde o início do desenvolvimento, onde há presença apenas da radícula, tendo seu pico aos três dias após o início do estresse de P e indo até o final do tratamento, quando há presença de raiz primária, seminal e lateral. A maior expressão de *ZmPSTOL1_3.06* acontece na zona de diferenciação celular da raiz primária.

A região promotora de *ZmPSTOL1_3.06* possui elementos cis-regulatórios relacionados com P e formação de pelos radiculares

A análise de eGWAs sugeriu que a regulação da expressão do gene *ZmPSTOL1_3.06* pode estar próxima à região promotora do gene. O sequenciamento da região promotora desse gene revelou que na linhagem ineficiente L22, na qual o gene é menos expresso, existe uma inserção de um transposon do tipo DTH_Zem11, pertencente à família MITE (*Miniature inverted-repeat transposable element*) e da superfamília PIF (*P instability fator*)/Harbinger, que pode estar reduzindo a transcrição do *ZmPSTOL1_3.06* nesta linhagem. A família MITE é composta de cinco superfamílias, sendo a DTH, que é a nomeação dada a superfamília PIF/Harbinger, composta por cerca de 108 diferentes elementos transponíveis (www.pmite.hzau.edu.cn). Os elementos transponíveis do tipo MITE são distribuídos principalmente nos braços cromossômicos e estão em grande parte associados a genes (Wessler, 1998; Feng *et al*., 2002; Santiago *et al*., 2002; Oki *et al*., 2008). Esses elementos transponíveis podem conter sequências regulatórias (Oki *et al*., 2008; Kuang *et al*., 2009) e reduzir a expressão de genes por meio de pequenos RNAs (Kuang *et al*., 2009). Além disso, os MITEs podem transpor para diferentes locais em diferentes genótipos, formando polimorfismo de presença/ausência (Casa *et al.,* 2000; Lyons *et al*., 2008), e se inseridos em regiões que contenham motivos de regulação gênica, podem alterar sua expressão.

Elementos cis-regulatórios relacionado a resposta a privação de P, como o P1BS, foram encontrados tanto na região promotora do gene em L3 quanto em L22. O P1BS é um elemento cis presente em vários promotores de genes responsivos ao P que são cruciais para o estabelecimento da homeostase em situações de privação de P (Rubio *et al.,* 2001; Schünmann *et al.,* 2004a; Bustos *et al.,* 2010; Nilsson *et al.,* 2010; Oropeza-Aburto *et al.,* 2012). O *ZmPHR1* é expresso na raiz, colmo e folhas quando plantas de milho são submetidas a baixo P e sua superexpressão aumenta o conteúdo de P na parte área e regula genes relacionados à resposta a privação de P em Arabidopsis (Wang *et al.,* 2012).

Além do motivo P1BS, foi encontrado um elemento cis específico de pelo radicular. Esse motivo conservado de sequência composta por 'GWACGW' (onde W = C/T) é descrito em 765 promotores dos 1063 genes específicos de pelo radicular de milho (Wang *et al.,* 2018). Além disso, esse elemento cis está presente na região promotora de dois genes específicos (*AtEXPA7* e *AtEXPA18)* de pelo radicular de Arabidopsis (Kim *et al.,* 2006; Won *et al.,* 2009). Em milho, esse motivo foi relatado como possível local de ligação do fator de transcrição com o domínio bHLH (Helix-Loop-Helix Basic), ZmLRL5 (Wang *et al.,* 2018). *ZmLRL5* é mais expresso em pelos radiculares e uma mutação única em *ZmLRL5* resulta em uma redução no alongamento do pelo radicular (Wang *et al.,* 2018). Outros fatores de transcrição bHLH de outras espécies tem um papel crítico no controle do desenvolvimento de pelos radiculares (Jang *et al.,* 2011; Bruex *et al.,* 2012; Pires *et al.,* 2013; Tam *et al.,* 2015; Breuninger *et al.,* 2016; Kim & Dolan, 2016; Proust *et al.,* 2016; Kim *et al.,* 2017).

A superexpressão de *ZmPSTOL1_3.06* aumenta o comprimento dos pelos radiculares em milho

A superexpressão do gene *ZmPSTOL1_3.06* aumenta significativamente o comprimento dos pelos radiculares, além disso a linhagem L3, eficiente na aquisição de P e com maior expressão de *ZmPSTOL1_3.06* apresenta maior comprimento dos pelos radiculares do que a linhagem ineficiente L22. Os pelos radiculares aumentam a superfícies da raiz para ajudar na absorção de água e nutrientes e interação com a rizosfera biótica e abiótica. Os pelos radiculares são

unicelulares e sua forma é dada pelo crescimento polarizado das suas pontas, um processo que é mediado pela fusão de vesículas das membranas e exocitose da parede celular. A formação do pelo radicular pode ser dividida em duas fases distintas: a iniciação da protuberância ou iniciação do pelo radicular e transformação da protuberância na ponta crescente do pelo radicular emergente (Ciamporova *et al.*, 2003). No milho, a última divisão das células de superfície produz duas células filhas do mesmo tamanho e ambas podem produzir pelos radiculares (Row & Reeder, 1957).

Apenas três mutantes que apresentam fenótipos de alongamento de pelo radicular foram identificados no milho. O *Rth1*, que codifica uma proteína do tipo SEC-3, que é um membro do complexo exocisto (Wen *et al*., 2005). O *Rth2*, ainda não foi clonado (Wen & Schnable, 1994) e o *Rth*3, que codifica uma proteína do tipo COBRA, é necessário para a elongação dos pelos radiculares e produtividade normal dos grãos (Hochholdinger *et al*., 2008). A expressão do gene *Rth1* e *Rth3* foi maior no Ev1 *UBI::ZmPSTOL1_3.06*, que não apresentou a maior expressão de *ZmPSTOL1_3.06,* no entanto todos os eventos *UBI::ZmPSTOL1_3.06* apresentaram comprimento radicular maior do que o controle selvagem B104. Os resultados sugerem que cada gene desempenhe um papel específico na rede altamente coordenada de genes responsáveis pelo alongamento dos pelos radiculares na epiderme.

O gene *Rth3* é mais expresso no genótipo eficiente L3 (de Sousa *et al*., 2012), que tem pelos radiculares mais longos e mais abundantes. Além disso, o *Rth3* tem a expressão mais elevada em raízes primárias jovens (Hochholdinger & Zimmermann, 2008), assim como o *ZmPSTOL1_3.06.* A ausência ou redução de pelos radiculares leva a redução do crescimento, ausência de espigas e pouca produção de pendão, provavelmente causado pela deficiência de nutrientes (Wen & Schnable, 1994; Hochholdinger *et al*., 2008). Genótipos de feijão com pelos radiculares mais longos e com raízes mais superficiais acumulam 298% mais biomassa que genótipos com raiz mais profunda e pelos radiculares mais curtos, demonstrando que o sinergismo entre esses fenótipos tem importância substancial para o aumento na aquisição de P (Miguel *et al*., 2015).

A plasticidade fenotípica dos pelos radiculares a adaptação em condições com baixa disponibilidade de fósforo foi avaliada em seis RILs de milho indicando que genótipos com pelos radiculares mais longos em condições de baixo P apresentam maior crescimento, aquisição de P, taxas metabólicas com custo-benefício melhores do que genótipos de pelo radicular curto (Zhu *et al*., 2010). A linhagem L3 (eficiente) apresenta maior área de superfície radicular e produção de grãos em campo (de Sousa *et al*., 2012), além de pelos radiculares mais longos do que a linhagem L22 (ineficiente). A plasticidade dos pelos radiculares pode ser um componente de um conjunto mais amplo de características, incluindo a plasticidade na respiração radicular, que permite maior crescimento da raiz e aquisição de fósforo em solos pobres em P (Zhu *et al*., 2010).

Concluindo, nossos resultados mostraram que a expressão de *ZmPSTOL1_3.06* ocorre preferencialmente na zona de diferenciação da raiz primária, mais precisamente nos pelos radiculares, do genótipo eficiente na aquisição de P e foi modulada pela disponibilidade de P. A presença dos motivos de ligação relacionados a aquisição de P (*ZmPHR1)* e formação de pelos radiculares (*ZmLRL5)* na região promotora de *ZmPSTOL1_3.06*, junto ao fato das plantas transgênicas sob seu promotor apresentarem maior atividade de GUS sob baixo P e nos pelos radiculares indicaram uma potencial relação entre esses fatores de transcrição e *ZmPSTOL1_3.06.* Além disso, plantas transgênicas superexpressando *ZmPSTOL1_3.06* alteraram o alongamento dos pelos radiculares e a expressão de genes relacionados a sua formação. Esta é a primeira vez que uma quinase foi relacionada com o processo de desenvolvimento de pelo radicular de milho. Estudos mais aprofundados sobre os complexos mecanismos de sinalização são necessários para melhor compreensão da regulação do gene *ZmPSTOL1_3.06* em milho.

REFERÊNCIAS

AZEVEDO, G. C.; CHEAVEGATTI-GIANOTTO, A.; NEGRI, B. F.; HUFNAGEL, B.; SILVA, L DA C.; MAGALHAES, J. V.; GARCIA, A.; LANA, U. G. P.; DE SOUSA, S. M.; GUIMARÃES, C. T. (2015). Multiple interval QTL mapping and searching for PSTOL1 homologs associated with root morphology, biomass accumulation and phosphorus content in maize seedlings under low-P. *BMC Plant Biol*. 15:172.

BERNARDINO, K. C.; PASTINA, M. M.; MENEZES, C. B.; DE SOUSA, S. M.; MACIEL, L. S.; CARVALHO JR, G.; GUIMARÃES, C. T.; BARROS, B. A.; COSTA e SLVA, L.; CARNEIRO, P. C. S.; SCHAFFERT, R. E.; KOCHIAN, L. V.; MAGALHÃES, J. V. (2019). The genetic architecture of phosphorus efficiency in sorghum involves pleiotropic QTL for root morphology and grain yield under low phosphorus availability in the soil. *BMC plant biology*, *19*(1), 87.

BOISSON-DERNIER, A.; FRANCK, C. M.; LITUIEV, D. S.; GROSSNIKLAUS, U. (2015). Receptor-like cytoplasmic kinase MARIS functions downstream of CrRLK1L-dependent signaling during tip growth. *PNAS* 112:12211-16.

BRADBURY, P. J.; ZHANG, Z.; KROON, D. E.; CASSTEVENS, T. M.; RAMDOSS, Y.; BUCKLER, E. S. (2007). TASSEL: software for association mapping of complex traits in diverse samples. *Bioinformatics* 23:2633-2635.

BREUNINGER, H.; THAMM, A.; STREUBEL, S.; SAKAYAMA, H.; NISHIYAMA, T.; DOLAN, L. (2016). Diversification of a transcription factor family led to the evolution of antagonistically acting genetic regulators of root hair growth. *Curr. Biol*. 26:1622–1628.

BRUEX, A.; KAINKARYAM, R. M.; WIECKOWSKI, Y.; KANG, Y. H.; BERNHARDT, C.; XIA, Y.; ZHENG, X.; WANG, J. Y.; LEE, M. M.; BENFEY, P.; WOOLF, P. J.; SCHIEFELBEIN, J. (2012). A gene regulatory network for root epidermis cell differentiation in Arabidopsis. *PLoS genetics*, *8*(1), e1002446.

BUSTOS, R.; CASTRILLO, G.; LINHARES, F.; PUGA, M. I.; RUBIO, V.; PÉREZ-PÉREZ, J.; SOLANO, R.; LEYVA, A.; PAZ-ARES, J. (2010). A central regulatory system largely controls transcriptional activation and repression responses to phosphate starvation in *Arabidopsis*. *PLoS Genet.* 6, e1001102.

CARTHARIUS, K.; FRECH, K.; GROTE, K.; KLOCKE, B.; HALTMEIER, M.; KLINGENHOFF, A.; FRISCH, M.; BAYERLEIN, M.; WERNER, T. (2005). MatInspector and beyond: Promoter analysis based on transcription factor binding sites. *Bioinformatics* v: 2933-2942.

CASA, A. M.; BROUWER, C.; NAGEL, A.; WANG, L.; ZHANG, Q.; KRESOVICH, S.; WESSLER, S. R. (2000). Inaugural article: the MITE family heartbreaker (Hbr): molecular markers in maize. *Proc Natl Acad Sci USA* 97:10083-10089.

ČIAMPOROVÁ, M., DEKÁNKOVÁ, K., HANÁČKOVÁ, Z., PETERS, P., OVEČKA, M., & BALUŠKA, F. (2003). Structural aspects of bulge formation during root hair initiation. In *Roots: The Dynamic Interface between Plants and the Earth* (pp. 1-7). Springer, Dordrecht.

DE SOUSA, S. M.; CLARK, R. T.; MENDES, F. F.; DE OLIVEIRA, A. C.; VASCONCELOS, M. J. V.; PARENTONI, S. N.; KOCHIAN, L. V.; GUIMARÃES, C. T.; MAGALHÃES, J. V. (2012) A role root morphology candidates genes in P acquisition efficiency in maize. *Functional Plant Biology* 39:925-935.

DUAN, Q.; KITA, D.; LI, C.; CHEUNG, A. Y.; WU, H. M. (2010). FERONIA receptor-like kinase regulates RHO GTPase signaling of root hair development. *PNAS* 107:17821-26.

ELSHIRE, R. J.; GLAUBTIZ, J. C.; SUN, Q.; POLAND, J. A.; KAWAMOTO, K.; BUCKLER, E. S.; MITCHELL, S. E. (2011). A Robust, Simple Genotyping-by-Sequencing (GBS) Approach for High Diversity Species. *Plos One*.

ESCOBAR-RESTREPO J. M.; HUCK, N.; KESSLER, S.; GAGLIARDINI, V.; GHEYSELINCK, J.; YANG, W. C.; GROSSNIKLAUS, U. (2007). The FERONIA receptor-like kinase mediates male-female interactions during pollen tube reception. Science 317:656–60.

FENG, Q.; ZHANG Y, H. A. O. P. *et al*. (74 co-autores). (2002). Sequence and analysis of rice chromosome 4. *Nature* 420:316-320.

FRANCIS, K. E.; SPIKER, S. (2005). Identification of Arabidopsis thaliana transformants without selection reveals a high occurrence of silenced T-DNA integrations. *The Plant Journal* 41:464-477.

FRAME, B. R.; MAIN, M.; SCHICK, R.; WANG, K. Genetic Transformation Using Maize Immature Zygotic Embryos. In: TREVOR, A.; YEUNG, E. (eds.). *Plant Embryo Culture Methods and Protocols: Methods in Molecular Biology*. Springer Science and Business Media, LLC, 2011, p.327-341.

GAMUYAO, R.; CHIN, J. H.; TANAKA, J. P. PESARESI, P.; CATAUSAN, S.; DALID, C. LOEDIN, I. S.; MENDOZA, E. M. T.; WISSUWA, M.; HEUER, S. (2012). The protein kinase Pstol1 from traditional rice confers tolerance of phosphorus deficiency. *Nature* 488: 535-539.

GLAUBITZ, J. C.; CASSTEVENS, T. M.; LU, F.; HARRIMAN, J.; ELSHIRE, R. J.; SUN, Q.; BUCKLER, E. S. (2014). TASSEL-GBS: A High Capacity Genotyping by Sequencing Analysis Pipeline. *Plos One*.

HARUTA, M.; SABA, T M.; STECKER, K.; MINKOFF, B. B.; SUSSMAN, M. R. (2014). A peptide hormone and its receptor protein kinase regulate plant cell expansion. *Science* 343:408–11.

HÉMATY, K.; HÖFTE, H. (2008). Novel receptor kinases involved in growth regulation. *Cuhrrent opinion in plant biology 11*:321-328.

HOCHHOLDINGER, F.; WEN, T. J.; ZIMMERMANN, R.; CHIMOT-MAROLLE, P.; DA COSTA E SILVA, O.; BRUCE, W.; LAMKEY, K. R.; WIENAND, U.; SCHNABLE, P. S. (2008) The maize (Zea mays L.) roothairless3 gene encodes a putative GPI-anchored, monocot-specific, COBRA-like protein that significantly affects grain yield. *The Plant Journal,* 54:888-898.

HOCHHOLDINGER, F.; ZIMMERMANN, R. (2008). Conserved and diverse mechanisms in root development. *Curr Opin Plant Biol* 11:70-74.

HÖFTE, H. (2015). The yin and yang of cell wall integrity control: brassinosteroid and FERONIA signaling. *Plant and Cell Physiology 56*: 224-231.

HUCK, N.; MOORE, M, J.; FEDERER, M.; GROSSNIKLAUS, U. (2003). The Arabidopsis mutant feronia disrupts the female gametophytic control of pollen tube reception. *Development 130*:2149-2159.

HUFNAGEL, B.; DE SOUSA, S. M.; ASSIS, L.; GUIMARAES, C. T.; LEISER, W.; CORRADI, G.; NEGRI, B.; LARSON, B. G.; SHAFF, J. E.; PASTINA, M. M.; BARROS, B. A.; WELTZIEN, E.; RATTUNDE, H. F. W.; VIANA, J. H.; FALCAO, A. GAZAFFI, R.; GARCIA, A. A. F.; SCHARFFERT, R. E.; KOCHIAN, L. V.; MAGALHAES, J. (2014). Duplicate and conquer: multiple homologs of *PHOSPHORUS-STARVATION TOLERANCE1* enhance phosphorus acquisition and sorghum performance on low-phosphorus soils*. Plant Physiol.* 166:659-677.

HUND, A.; TRACHSEL, S.; STAMP, P. (2009). Growth of axile and lateral roots of maize: I development of a phenotying platform. *Plant Soil*, 325:335-349.

HURNI, S.; SCHEUERMANN, D.; KRATTINGER, S. G.; KESSEL, B.; WICKER, T.; HERREN, G.; FITZE, M. N.; BREEN, J.; PRESTERL, T.; OUZUNOVA, M.; KELLER, B. (2015). The maize disease resistance gene *Htn1* against northern corn leaf blight encodes a wall-associated receptor-like kinase. *Proceedings of the National Academy of Sciences 112*:8780-8785.

JANG, G.; YI, K.; PIRES, N. D.; MENAND, B.; DOLAN, L. (2011) RSL genes are sufficient for rhizoid system development in early diverging land plants. *Development* 138:2273–2281.

JEFFERSON, R.A.; KAVANAGH, T.A.; BEVAN, M.W. (1987). Gus fusion: beta-glucuronidase as a sensitive and versatile gene fusion marker in higher plants. *EMBO J*. 6:3901-3907.

KAEPPLER, S. M.; PARKE, J. L.; MUELLER, S. M.; SENIOR, J.; STUBER, C.; TRACY, W. F. (2000). Variation among maize inbred lines ans detection of quantitative trait loci for growth at low phosphorus and responsiveness to arbuscular mycorrhizal fungi. *Crop Sci* 40:358:364.

KIM, D.W.; LEE, S.H.; CHOI, S. B.; WON, S. K.; HEO, Y. K.; CHO, M.; PARK, Y. I.; CHO, H.T. (2006) Functional conservation of a root hair cell-specific cis-element in angiosperms with different root hair distribution patterns. *Plant Cell* 18:2958–2970.

KIM, C. M.; DOLAN, L. (2016) Root hair defective six-like class I genes promote root hair development in the grass *Brachypodium distachyon*. *PLoS Genet*. 12, e1006211.

KIM, C. M.; HAN, C. D.; DOLAN, L. (2017) RSL class I genes positively regulate root hair development in Oryza sativa. *New Phytol*. 213:314–323.

KIM, D. W.; LEE, S. H.; CHOI, S. B.; WON, S. K.; HEO, Y. K.; CHO, M.; PARK, Y. I.; CHO, H. T. (2006). Functional conservation of a root hair cell-specific cis-element in angiosperms with different root hair distribution patterns. *Plant Cell* 18:2958–2970.

KUANG, H.; PADMANABHAN, C.; LI, F.; KAMEI, A.; BHASKAR, P. B.; OUYANG, S.; JIANG, J.; BUELL, C. R.; BAKER, B. (2009). Identification of miniature inverted-repeat transposable elements (MITEs) and biogenesis of their siRNAs in the Solanaceae: new functional implications for MITEs. *Genome Res* 19:42-56.

LIAO, H.; ZHU, M. M.; CUI, H. H.; DU, X. Y.; TANG, Y; CHEN, L. Q.; YE, D.; ZHANG, X. Q. (2016). MARIS plays important roles in Arabidopsis pollen tube and root hair growth. *J. Integr. Plant Biol.* 58:927-940.

LIVAK, K. J.; SCHMITTGEN, T. D. (2001). Analysis of relative gene expression data using real-time quantitative PCR and the 2-DDCt method*. Methods,* 25:402-408.

LYNCH, J.P. (2011). Root Phenes for Enhanced Soil Exploration and Phosphorus Acquisition: Tools for Future Crops. *Plant Physiol*. 156:1041-1049.

LYNCH, J. P.; BROWN, K. M. (2012). New roots for agriculture: exploiting the root phenome. *Philosophical Transaction* 367:1598-1604.

LYNCH, J. P.; BROWN, K. M. (2001). Topsoil foraging – an architectural Adaptation of plants to low phosphorus availability. *Plant and Soil* 237: 225-237.

LYNCH, J. P.; HO, M. D. (2005). Rhizoeconomics: carbon costs of phosphorus acquisition. *Plant Soil* 269:45-56.

LYONS, M.; CARDLE, L.; ROSTOKS, N.; WAUGH, R.; FLAVELL, A. J. (2008). Isolation,analysis and marker utility of novel miniature inverted repeat transposable elements from the barley genome. *Mol Genet Genomics* 280:275-285.

MAGALHAES, J. V.; DE SOUSA, S. M.; GUIMARAES, C. T.; & KOCHIAN, L. V. (2017). The role of root morphology and architecture in phosphorus acquisition: physiological, genetic, and molecular basis. *Plant Macronutrient Use Efficiency*, 123–147.

MAGNAVACA, R.; GARDNER, C. O; CLARK, R. B. Evaluation of maize inbred lines for aluminum tolerance in nutrient solution. In: GABELMAN, H. W.; LONGHMAN, B. C. (Eds.) (1987). *Genetic aspects of plant mineral nutrition*. Martinus Nijhoff Publishers, Dordrecht/Boston/Lancaster, p. 255-265.

MARSCHENER, H. Mineral nutritional of higher plants. Boston: *Academic Press*, 2ed. 1995.

MARZEC, M.; MELZER, M.; SZAREIKO, I. (2015). Root hair development in the grasses: what we already know and what we still need to know. *Plant Physiol* 168:407-414.

MIGUEL, M.A. Genotypic variation in root hairs and phosphorus efficiency in common bean (Phaseolus vulgaris L.). 2004. 106p. Thesis (M.Sc.) - Penn State University, University Park.

MIGUEL, M. A.; POSTMA, J. A.; LYNCH, J. P. (2015). Phene synergism between root hair length and basal root growth angle for phosphorus acquisition. *Plant Physiology 167*:1430-1439.

MILNER, M. J.; HOWELLS, R. M.; CRAZE, M.; BOWDEN, S.; GRAHAM, N.; WALLINGTON, E. J. (2018). A PSTOL-like gene, *TaPSTOL*, controls a number of agronomically important traits in wheat. *BMC plant biology 18*:115-129.

MIRANDA, V.; PORTO, W. F.; DA ROCHA FERNANDES, G.; POGUE, R.; NOLASCO, D. O.; ARAUJO, A. C. G.; COTA, L. V.; DE FREITAS, C. G.; DIAS, S. C.; FRANCO, O. L. (2017). Comparative transcriptomic analysis indicates genes associated with local and systemic resistance to Colletotrichum graminicola in maize. *Scientific reports 7*:2483.

MOLL, R. H.; KAMPRATH, E. J.; JACKSON, W. A. (1982). Analysis and interpretation of factors which contribute to efficiency of nitrogen utilization 1. *Agronomy Journal 74*:562-564.

NI, J. J.; WU, P.; SENADHIRA, D.; HUANG, N. (1998). *Mapping QTLs for phosphorus deficiency tolerance in rice (Oryza sativa L.)*. *Theor. Appl. Genet.* 97:1361-1369.

NILSSON, L.; MÜLLER, R.; NIELSEN, T. H. (2010). Dissecting the plant transcriptome and the regulatory responses to phosphate deprivation. *Physiol. Plant.* 139:129-143.

OKI, N.; YANO, K.; OKUMOTO, Y.; TSUKIYAMA, T.; TERAISHI, M.; TANISAKA, T. (2008). A geome-wide view of miniature inverted-repeat transposable elements (MITEs) in rice, *Oryza sativa ssp*. japonica. *Genes Genet Syst* 83:321-329.

OROPEZA-ABURTO, A.; CRUZ-RAMÍREZ, A.; ACEVEDO-HERNÁNDEZ, G. J.; PÉREZ-TORRES, C. A.; CABALLERO-PÉREZ, J.; HERRERA-ESTRELLA, L. (2012). Functional analysis of the *Arabidopsis* PLDZ2 promoter reveals an evolutionarily conserved low-Pi-responsive transcriptional enhancer element. *J. Exp. Bot.* 63:2189-2202.

PARENTONI, S. N.; SOUZA JR., C. L. (2008). Phosphorus acquisition and internal utilization efficiency in tropical maize genotypes. *Pesquisa Agropecuaria Brasileira* 43:893-901.

PAZ, M.; SHOU, H.; GUO, Z.; ZHANG, Z.; BANERJEE, A.; WANG, K. (2004). Assessment of conditions affecting Agrobacterium-mediated soybean transformation using the cotyledonary node explant. *Euphytica* 136:167-179.

PIRES, N. D.; YI, K.; BREUNINGER, H.; CATARINO, B.; MENAND, B.; DOLAN, L. (2013). Recruitment and remodeling of an gene regulatory network during land plant evolution. *Proc. Natl Acad. Sci. USA* 110:9571–9576.

PROUST, H.; HONKANEN, S.; JONES, V. A.; MORIERI, G.; PRESCOTT, H.; KELLY, S.; ISHIZAKI, K.; KOHCHI, T.; DOLAN, L. (2016). RSL class I genes controlled the development of epidermal structures in the common ancestor of land plants. *Curr. Biol*. 26:93–99.

RAMEGOWDA, V.; BASU, S.; KRISHNAN, A.; PEREIRA, A. (2014). Rice GROWTH UNDER DROUGHT KINASE is required for drought tolerance and grain yield under normal and drought stress conditions. *Plant Physiology 166*: 1634-1645.

RIBEIRO, C. A. G. Identificação de regiões geômicas relacionadas à seca e deficiência de fósforo via análise de ligação e mapeamento associativo em milho tropical. 2015. 89 p. Tese (Doutorado em Genética e Melhoramento) – Universidade Federal de Viçosa, Viçosa.

ROTH, R.; CHIAPELLO, M.; MONTERO, H.; GEHRIG, P.; GROSSMANN, J.; O'HOLLERAN, K.; HARTKEN, K.; YANG, S.Y.; HILMER, S.; SCHUMACHER, K.; BOWDEN, S.; CRAZE, M.; WALLINGTON, E. J.; MIYAO, A.; SAWERS, R.; MARTINOIA, E.; PASZKPWSKI, U. 2018). A rice Serine/Threonine receptor-like kinase regulates arbuscular mycorrhizal symbiosis at the peri-arbuscular membrane. *Nature communications 9*: 4677.

ROW, H. C.; REEDER, J. R. (1957). Root-hair development as evidence of relationships among genera of Gramineae. *American Journal of Botany 44*:596-601.

RUBIO, V.; LINHARES, F.; SOLANO, R.; MARTIN, A. C.; IGLESIAS, J.; LEYYA, A.; PAZ-ARES, J. (2001). A conserved MYB transcription factor involved in phosphate starvation signaling both in vascular plants and in unicellular algae. *Genes Dev*. 15:2122-2133.

SAGHAI-MAROOF, M. A.; SOLIMAN, K. A.; JORGENSEN, R. A.; ALLARD, R. W. Ribossomal DNA spacer length polymorphism in barley: Mendelian inheritance, chromosomal location and population dynamics. *Proc. Natl. Acad. Sci. USA*, v.81, p.8014-8018, 1984.

SAMBROOK, J.; FRITSCH, E. F.; MANIATIS, T. Molecular cloning: a laboratory edition, 2nd ed. New York: Cold Spring Harbour Laboratory Press, 1989.

SANTIAGO, N.; HERRAIZ, C.; GONI, J. R.; MESSEGUER, X.; CASACUBERTA, J. M. (2002). Genome-wide analysis of the Emigrant family of MITEs of *Arabidopsis thaliana*. *Mol Biol Evol* 19:2285-2293.

SCHÜNMANN, P. H. D.; RICHARDSON, A. E.; SMITH, F. W.; DELHAIZE, E. (2004a). Characterization of promoter expression patterns derived from the Pht1 phosphate transporter genes of barley (*Hordeum vulgare* L.). *J. Exp. Bot*. 55:855-865.

STEGMANN, M.; MONAGHAN, J.; SMAKOWSKA-LUZAN, E.; ROVENICH, H.; LEHNER, A.; HOLTON, A.; BELKHADIR, Y.; ZIPFEL, C. (2017). The receptor kinase FER is a RALF-regulated scaffold controlling plant immune signaling. *Science* 355:287-289.

TAM, T. H.; CATARINO, B.; DOLAN, L. (2015). Conserved regulatory mechanism controls the development of cells with rooting functions in land plants. *Proc. Natl Acad. Sci. USA* 112:3959–3968.

VANCE, C. P.; CHIOU, T. J. (2011). Phosphorus focus editorial. *Plant Physiology* 155:987-988.

VANCE, C. P.; STONE, C. U.; ALLAN, D. L. (2003). Phosphorus acquisition and use: critical adaptations by plants for securing a nonrenewable resource. *New Phytologist* 157:423-447.

WANG, C.; QI, C.; LUO, J.; LIU, L.; HE, Y.; CHEN, L. (2018), Characterization of LRL5 as a key regulator of root hair growth in maize. Plant J. doi: 10.1111/tpj.14200.

WANG, X.; BAI, J.; LIU, H.; SUN, Y.; SHI, X.; & REN, Z. (2012). Overexpression of a Maize Transcription Factor ZmPHR1 Improves Shoot Inorganic Phosphate Content and Growth of Arabidopsis under Low-Phosphate Conditions. *Plant Molecular Biology Reporter* 31:665–677.

WEN, T. J.; HOCHHOLDINGER, F.; SAUER, M.; BRUCE, W.; SCHNABLE, P. S. (2005). The roothairless1 gene of maize encodes a homolog of sec3, which is involved in polar exocytosis. *Plant Physiology* 138:1637-1643.

WESSLER, S. R. (1998). Transposable elements and the evolution of gene expression. *Symp Soc Exp Biol*. 51:115-122.

WISSUWA, M.; AE, N. (2001). Genotypic variation for tolerance to phosphorus deficiency in rice and the potential for its exploitation in rice improvement. Plant Breed. 120:43-48.

WISSUWA, M.; WEGNER, J.; AE, N.; YANO, M. (2002). Substitution mapping of Pup1: a major QTL increasing phosphorus uptake of rice from a phosphorus-deficient soil. *Theor. Appl. Genet.* 105:890-897.

WISSUWA, M.; YANO, M.; AE, N. (1998). *Mapping of QTLs for phosphorus-deficiency tolerance in rice (Oryza sativa L.)*. *Theor. Appl. Genet.* 97:777-783.

WON, S. K.; LEE, Y. J.; LEE, H. Y.; HEO, Y. K.; CHO, M.; CHO, H. T. (2009) Cis-element- and transcriptome-based screening of root hair specific genes and their functional characterization in Arabidopsis. *Plant Physiol*. 150:1459-1473.

YU, Y., & ASSMANN, S. M. (2018). Inter-relationships between the heterotrimeric Gβ subunit AGB1, the receptor-like kinase FERONIA, and RALF1 in salinity response. *Plant, cell & environment 41*: 2475-2489.

YU, Y.; CHAKRAVORTY, D.; ASSMANN, S. M. (2018). The G protein β-subunit, AGB1, interacts with FERONIA in RALF1-regulated stomatal movement. *Plant physiology 176*:2426-2440.

ZHU, J.; KAEPPLER, S. M.; LYNCH, J. P. (2005). Mapping of QTL controlling root hair length in maize (*Zea mays* L.) under phosphorus deficiency. *Plant and Soil 270*:299-310.

ZHU, J.; MICKELSON, S. M.; KAEPPLER, S. M.; LYNCH, J. P. (2006). Detection of quantitative trait loci for seminal root traits in maize (Zea mays L.) seedlings grown under differential phosphorus levels. *Theor Appl Genet* 113:1-10.

ZHU, J.; ZHANG, C.; LYNCH, J. P. (2010). The utility of phenotypic plasticity of root hair length for phosphorus acquisition. *Functional Plant Biology 37*:313-322.

4 CONCLUSÃO GERAL

Os eventos superexpressando os genes *OsPSTOL1* e *SbPSTOL1* tiveram um incremento de raízes superfinas, o que levou a um aumento da área de superfície radicular e de biomassa vegetal, tanto em câmara de crescimento quanto em casa de vegetação. Os eventos superexpressando os genes *ZmPSTOL1* não apresentaram diferenças significativas em relação à linhagem selvagem B104.

A expressão do gene de milho *ZmPSTOL1_3.06* ocorreu preferencialmente na zona de diferenciação da raiz primária, mais precisamente nos pelos radiculares, do genótipo eficiente na aquisição de P - L3 e foi modulada pela disponibilidade de P.

A presença dos motivos de ligação relacionados a aquisição de P (*ZmPHR1)* e formação de pelos radiculares (*ZmLRL5)* na região promotora de *ZmPSTOL1_3.06*, juntamente com o fato das plantas transgênicas sob seu promotor apresentarem maior atividade de GUS sob baixo P e nos pelos radiculares indicaram uma potencial relação entre esses fatores de transcrição e *ZmPSTOL1_3.06.*

Plantas transgênicas superexpressando o gene *ZmPSTOL1_3.06* alteraram o alongamento dos pelos radiculares e a expressão de genes relacionados com a sua formação.

Os resultados sugerem até o momento, que os genes *PSTOL1* tem um papel mais geral no desenvolvimento do sistema radicular, o que resulta no aumento da eficiência de P, que pode beneficiar a produção de cereais.

5 ANEXO

Este anexo contém o artigo científico intitulado: “Multiple interval QTL mapping and searching for PSTOL1 homologs associated with root morphology, biomass accumulation and phosphorus contente in maize seedlings under low-P, publicado na revista BMC Plant Biology (2015), com co-autoria de Bárbara França Negri.

Azevedo *et al. BMC Plant Biology*
DOI 10.1186/s12870-015-0561-y

BMC Plant Biology

RESEARCH ARTICLE Open Access

Multiple interval QTL mapping and searching for *PSTOL1* homologs associated with root morphology, biomass accumulation and phosphorus content in maize seedlings under low-P

Gabriel C Azevedo[1], Adriana Cheavegatti-Gianotto[2], Bárbara F Negri[3], Bárbara Hufnagel[1], Luciano da Costa e Silva[2], Jurandir V Magalhaes[4], Antonio Augusto F Garcia[2], Ubiraci GP Lana[4], Sylvia M de Sousa[4] and Claudia T Guimaraes[4*]

Abstract

Background: Modifications in root morphology are important strategies to maximize soil exploitation under phosphorus starvation in plants. Here, we used two multiple interval models to map QTLs related to root traits, biomass accumulation and P content in a maize RIL population cultivated in nutrient solution. In addition, we searched for putative maize homologs to *PSTOL1*, a gene responsible to enhance early root growth, P uptake and grain yield in rice and sorghum.

Results: Based on path analysis, root surface area was the root morphology component that most strongly contributed to total dry weight and to P content in maize seedling under low-P availability. Multiple interval mapping models for single (MIM) and multiple traits (MT-MIM) were combined and revealed 13 genomic regions significantly associated with the target traits in a complementary way. The phenotypic variances explained by all QTLs and their epistatic interactions using MT-MIM (23.4 to 35.5 %) were higher than in previous studies, and presented superior statistical power. Some of these QTLs were coincident with QTLs for root morphology traits and grain yield previously mapped, whereas others harbored *ZmPSTOL* candidate genes, which shared more than 55 % of amino acid sequence identity and a conserved serine/threonine kinase domain with *OsPSTOL1*. Additionally, four *ZmPSTOL* candidate genes co-localized with QTLs for root morphology, biomass accumulation and/or P content were preferentially expressed in roots of the parental lines that contributed the alleles enhancing the respective phenotypes.

Conclusions: QTL mapping strategies adopted in this study revealed complementary results for single and multiple traits with high accuracy. Some QTLs, mainly the ones that were also associated with yield performance in other studies, can be good targets for marker-assisted selection to improve P-use efficiency in maize. Based on the co-localization with QTLs, the protein domain conservation and the coincidence of gene expression, we selected novel maize genes as putative homologs to *PSTOL1* that will require further validation studies.

Keywords: Phosphorus acquisition, Protein kinase, SNP marker, OsPSTOL1, *Zea mays*

* Correspondence: claudia.guimaraes@embrapa.br
[4]Núcleo de Biologia Aplicada, Embrapa Milho e Sorgo, Rodovia MG 424, km 65, Caixa Postal 151, Sete Lagoas, MG 35701-970, Brazil
Full list of author information is available at the end of the article

Background

The increasing demand for agricultural production poses a global challenge to improve the phosphorus (P) use efficiency in plants due to its low availability in a large proportion of arable lands [1, 2]. Plants uptake phosphorus from the soil in the orthophosphate forms (P_i), which are available at low concentration in the soil solution [3]. In a large fraction of soils, P is tightly fixed to the clay's surface, which requires high amounts of phosphate fertilizers for high-yielding farming systems, increasing production costs and hampering soil fertility management [3–5]. However, low-input farmers have limited access to phosphate fertilizer, which is the second most used fertilizer for plant growth [6]. Maize is the most common grain produced worldwide and a major staple food in Africa and Latin America [7], where soils often show limited P availability. Thus, improving maize P-use efficiency is expected to increase yield stability and, consequently, food security [1, 4, 8].

Plants have evolved two major strategies to overcome P limitation in the soil, which are P internal utilization and P uptake [3]. P internal utilization mechanisms involve transport, partitioning and remobilization of P within the plant, whereas the mechanisms that increase P uptake are associated with alterations in the root system, interactions with microorganisms, and chemical modifications of the rhizosphere [3]. Indeed, P acquisition efficiency has been considered from two to three times more important than P internal utilization to explain the variability for P-use efficiency in tropical maize genotypes evaluated in low- and high-P soils [9]. Considering the limited mobility and low P concentration in the soil, mechanisms related to P acquisition are greatly dependent of the proximity of this nutrient to the root system [3, 10]. Thus, a well-developed root system should be an important adaptation mechanism to maximize soil exploitation, enabling plants to improve P acquisition efficiency [11–13]. Studies have shown that plants that are more efficient in P acquisition presented higher root:shoot dry weight ratios [14, 15], reduced root diameters [16], longer and denser root hairs [17], increased lateral roots [18], greater lateral branching and shallower basal roots [17, 19]. These changes in root morphology are key strategies used by plants to improve soil exploitation at a minimal metabolic cost [5, 20].

Root morphology is controlled by multiple genes in maize [13, 21], but only a few of them such as *roothairless* (*Rth1*) [22], *brittle stalk-2-like protein 3* (*Bk2l3*) [23], and *rootless concerning crown and seminal roots* (*Rtcs*) [24] have been cloned and characterized. However, an appropriate strategy to dissect these traits is through quantitative trait loci (QTL) mapping. Indeed, several QTLs were mapped for root traits under contrasting conditions of P availability in nutrient solution [25–27], in glasshouse [28] and in the field [29–32]. These QTLs individually explained from 1 to 14 % of the phenotypic variation, confirming the genetic complexity of root traits. These studies were carried out using composite interval mapping (CIM) strategy, however, multiple interval mapping (MIM) [33] offers a significant improvement on both statistical power and precision for detecting main and epistatic QTLs over CIM. This happens because MIM utilizes the estimated positions of QTLs as cofactors in the multiple regression model, whereas CIM utilizes the nearest markers to the estimated QTL as cofactors [34]. Besides all statistical advantages achieved by MIM, it still cannot capture the genetic correlation that might exist between traits. The multiple-trait multiple interval mapping (MT-MIM) method [35], which is an extension of MIM, applies multiple regression on a multiple dimensional (traits) space context, which enables it to capture information that might be available from the existing genetic correlation between traits, therefore, boosting the precision and power to detect QTLs [35]. To the best of our knowledge, this method has never been applied to map QTLs with effects on root morphology traits in maize.

In rice, a major QTL controlling phosphorus uptake (*Pup1*) was mapped to chromosome 12, explaining approximately 80 % of the phenotypic variance of this trait [36]. Rice near isogenic lines (NILs) carrying the *Pup1* QTL showed a three-fold increase in P uptake and enhanced root surface area when grown in P-deficient soil [36, 37]. Additionally, irrigated and upland rice varieties introgressed with *Pup1* showed a significant improvement in grain yield in different low-P soils compared to their parents [38, 39]. The gene underlying the *Pup1* locus was identified and named *Phosphorus-starvation tolerance 1* (*PSTOL1*), which encodes a serine/threonine kinase of the LRK10L-2 subfamily [40]. The overexpression of *PSTOL1* in two transgenic rice varieties enhanced the grain yield over 60 % under low-P conditions due to larger root system (i.e., root length, and total root surface area), which also improved the uptake of P and other nutrients [40]. Furthermore, Hufnagel *et al.* [41] showed that sorghum homologs to *OsPSTOL1* were associated with enhanced P uptake and grain yield in sorghum grown in a low-P soil due modifications on root system morphology and architecture. A remarkable conservation of protein-encoding genes among maize, sorghum and rice has been confirmed *in silico* based on genome sequencing comparison, once approximately 89 % of the 11,892 maize gene families predicted in the B73 genome were shared with rice and sorghum [42]. Of these, genes encoding important adaptive traits are expected to be conserved among these grass species.

In order to better understand the genetic basis of root morphology and P acquisition related traits, as well as the relationship between these traits, a path analysis and

a QTL mapping study were carried out in a maize RILs in nutrient solution cultivated under low P. We also integrated the QTL mapping, sequence comparison and expression analysis to identify putative homologs to *PSTOL1* in maize.

Results

Transgressive segregation of phenotypic traits in RILs

Significant genetic variation in root morphology traits, biomass accumulation and phosphorus content in the seedlings were observed for the RIL population with high broad sense heritability estimates, which ranged from 0.65 for root:shoot dry weight ratio to 0.82 for root length (Additional file 1: Table S1). The P-efficient line, L3, tended to present superior phenotypic measurements for all traits compared with the P-inefficient line L22, with the exception of root diameter and root:shoot ratio (Fig. 1a). The range of the phenotypic variation in the RILs was larger than both parents, suggesting transgressive segregation for all phenotypic traits (Fig. 1a). The RILs showing extreme root systems in comparison with their parental lines were highlighted in the Fig. 1b. The parental lines belonged to distinct heterotic groups (L3, flint and L22, dent) [43], were genetically divergent based on SNP

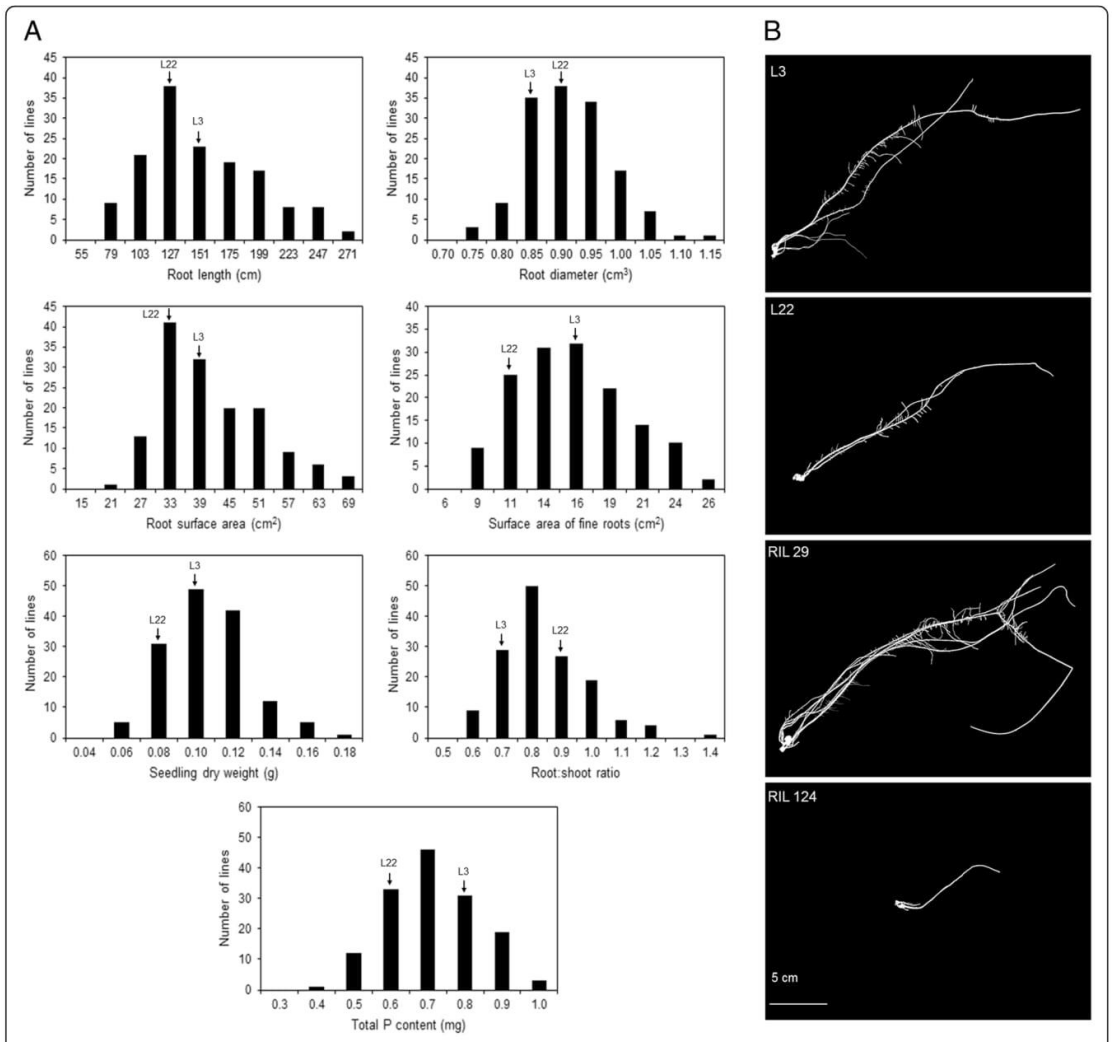

Fig. 1 a Frequency distribution of traits evaluated in 145 maize RILs grown in low-P (2.5 μM). The P-efficient (L3) and the P-inefficient (L22) parental lines are indicated by arrows. **b** Root system of the parental lines (L3 and L22) and two extreme RILs (RIL 66 and 113) after 13 days cultivated in nutrient solution under low-P

markers [44] and contrasted for grain yield in low-P soil [45] and for root morphology traits in nutrient solution [46].

Surface area is an important root trait contributing to seedling dry weight and P content

Root length, root surface area and surface area of fine roots were high and positively correlated with each other (Table 1). The correlation coefficients among these traits exhibited comparable magnitudes to those observed in a sorghum diversity panel composed of 287 accessions [41] and in a group of 30 maize lines [46]. These root traits also showed strong correlation coefficients with total seedling dry weight (0.77 to 0.86), moderate correlations with total P content in the seedling (0.31 to 0.48), and negative correlations with root:shoot ratio (−0.29 to −0.38) (Table 1). In contrast, root diameter was negatively correlated with root length, root surface area and total seedling dry weight, but no significant correlation was found with total P content. The negative correlation between root length and root diameter (−0.62) was similar to the coefficients obtained for root diameter with lateral (−0.65) and non-lateral (−0.68) roots in temperate maize RILs [18].

To further investigate the relative importance of root traits on seedling dry weight and P content, we performed a path analysis, using the root traits as explanatory variables and the total seedling dry weight and P content as dependent variables. As P content was the product of total seedling dry weight and P concentration as previously proposed [30, 31], both dependent variables were significantly correlated (0.58) and were evaluated separately. The partitioning of the correlation coefficients revealed that root length had the lowest direct effect on total seedling dry weight (−4.831) and P content (−0.997), but had a strong indirect effect through root surface area (5.816 and 1.565, respectively) (Table 2). Thus, the negative direct effect of root length was counterbalanced by the indirect effect via root surface area, probably due to the high positive correlation between these traits ($r = 0.98$). A similar pattern was observed for surface area of fine roots, which was also positively correlated with root surface area ($r = 0.8$). This trait exerted a minor negative direct influence on total seedling dry weight (−0.681) and P content (−0.117), which were mitigated by the positive indirect effect via root surface area (4.748 and 1.277, respectively). Root diameter also played a more important effect indirectly via root surface area on both variables, masking its direct contribution, which corroborates with the negative correlation between these root traits ($r = -0.48$). Therefore, root surface area contributed the highest direct effect on total seedling dry weight (5.935) and P content (1.597) and mediated an important proportion of the indirect effects of the other root traits on the dependent variables.

Thus, the path analysis clarified the direct and indirect importance of a greater root surface area, which is a combination of longer roots with smaller diameters, to improve total dry weight and P content in the seedlings under P deficiency. This root morphology also promoted an additional advantage for shoot over root development, confirming that the investment in root growth was beneficial to P acquisition as discussed by Zhu and Lynch [18].

Table 1 Phenotypic correlation coefficients (*r*) among traits evaluated in the RILs under low-P condition in nutrient solution

Traits	RL	SA2	RD	R:S	TDW	Pcont
SA	0.98**	0.80**	−0.48**	−0.38**	0.86**	0.39**
RL		0.69**	−0.62**	−0.38**	0.79**	0.31**
SA2			0.03	−0.29**	0.77**	0.48**
RD				0.26**	−0.25**	0.14
R:S					−0.43**	−0.02
TDW						0.58**

Traits: root surface area (SA), root length (RL), surface area of fine roots (SA2), root diameter (RD), root:shoot dry weight ratio (R:S), total seedling dry weight (TDW), and total P content (Pcont)
Correlation coefficients followed by ** are significant at $p < 0.01$

Two distinct QTL mapping strategies reveal complementary results

A linkage map was constructed using 292 markers that covered 1787.5 cM of the maize genome, with an average interval of 6.1 cM between adjacent markers (Additional file 2: Figure S1). In addition to SSR and SNP markers, six *ZmPSTOL* candidate genes and three genes previously associated with root morphology (*Rth1*, *Bk2l3,* and *Rtcs*) were mapped to their predicted physical positions. Multiple interval mapping models for single (MIM) and multiple traits (MT-MIM) provided statistical evidence for 13 genomic regions harboring QTLs on all maize chromosomes, with the exception of chromosome 5 (Tables 3 and 4). The QTL regions were named using the trait initials if they were detected through single trait analysis or as "multi" if they were detected by multiple trait analysis, followed by their genetic position in bin (Fig. 2). A bin is the interval of approximately 20 cM between two core markers previously defined and mapped in maize [47], which are designated with the chromosome number followed by a two-digit decimal.

MIM models for individual traits detected seven QTLs controlling root length, root diameter, surface area of fine roots, and root:shoot ratio. The proportion of the phenotypic variance explained by each QTL (R^2) ranged from 6.84 % (*qRD4.05*) to 15.12 % (*qSA2_10.03*). The magnitude of QTL effects ranged from 0.270 standard deviations from the progeny mean (sd) to −0.393 sd (Table 3).

The MT-MIM analysis revealed the presence of ten QTLs with R^2 ranging from 2.04 % (*qMulti8.02* for R:S)

Table 2 Path analysis showing the partitioning of the phenotypic correlations into direct and indirect effects of root traits on total seedling dry weight and P content

Independent variables		Dependent variables	
		Total dry weight	Total P content
Root surface area	Direct effect	5.935	1.597
	Indirect effect via root length	−4.734	−0.977
	Indirect effect via surface area of fine roots	−0.544	−0.094
	Indirect effect via root diameter	0.203	−0.135
	Phenotypic correlation (*r*)	0.86	0.39
Root length	Direct effect	−4.831	−0.997
	Indirect effect via surface area	5.816	1.565
	Indirect effect via surface area of fine roots	−0.462	−0.081
	Indirect effect via root diameter	0.267	−0.177
	Phenotypic correlation (*r*)	0.79	0.31
Surface area of fine roots	Direct effect	−0.681	−0.117
	Indirect effect via root length	−3.284	−0.678
	Indirect effect via surface area	4.748	1.277
	Indirect effect via root diameter	−0.012	0.008
	Phenotypic correlation (*r*)	0.77	0.48
Root diameter	Direct effect	−0.424	0.281
	Indirect effect via root length	3.043	0.628
	Indirect effect via surface area	−2.848	−0.766
	Indirect effect via surface area of fine roots	−0.020	−0.003
	Phenotypic correlation (*r*)	−0.25	0.14
	Coefficient of determination	0.869	0.295

up to 15.17 % (*qMulti10.03* for SA2). The highest additive effect was also observed for *qMulti10.03* for SA2 (−0.403 sd) (Table 4).

LOD estimates for the MT-MIM model were higher and the confidence intervals were narrower than those for the individual MIM models, suggesting superior statistical power of MT-MIM compared with the MIM models applied to each trait individually (Fig. 2). Despite these differences, the MT-MIM and MIM models were coincident in revealing QTLs at bins 1.03, 1.07, 3.06, and 10.03, whereas QTLs at bins 1.06, 2.08, 3.04, 6.06, 8.02, and 9.04 were only revealed using the MT-MIM model. Conversely, QTLs at regions 4.05, 7.02, and 8.05 were only detected by MIM models. Therefore, combining the results of MIM and MT-MIM analyses conveyed the most accurate information regarding the genetic architecture of the traits under investigation in this particular study.

Using a simulation, Silva *et al.* [35] showed that when a QTL affects only a small subset of the traits, the MT-MIM model might have a lower power than MIM models to identify this QTL due to a greater genome-wide threshold for the MT-MIM model. This may be the reason why MT-MIM failed to identify QTLs at regions 4.05, 7.02, and 8.05. Although the MT-MIM LOD profile revealed peaks at these regions, the values were not statistically significant according to the score threshold employed.

The additive main effect of QTLs detected by MIM and MT-MIM had both positive and negative signs, confirming the contribution of favorable alleles coming from both parental lines for most of the traits analyzed (Tables 3 and 4). Additionally, five epistatic interactions were identified using the MT-MIM model, including some with magnitudes comparable to the main additive effects (Table 5). No epistatic effect was detected based on single trait analysis. Taken together, the additive and epistatic effects on the MT-MIM model explained between 23.41 % and 35.54 % of the phenotypic variance for each trait (Tables 4 and 5).

ZmPSTOL predicted proteins share a conserved serine/threonine kinase domain with OsPSTOL1

Using OsPSTOL1 [GenBank: BAK26566] as a query, six predicted proteins were selected on the maize genome, sharing more than 55 % amino acid sequence identity. The genes encoding these proteins were predicted to be located on chromosomes 3, 4 and 8, and named according to their genetic position in bin (Table 6).

Table 3 Quantitative trait loci (QTLs) identified using single trait-multiple interval mapping analysis for root length (RL), root diameter (RD), surface area of fine roots (SA2) and root:shoot ratio (R:S) under low-P

Trait	QTL[a]	Bin	cM[b]	Marker / Position (Mbp)	LOD	Flanking Markers[c] / Position (Mbp)		R^2 (%)[d]	Effect[e]	R^2_T (%)[f]
RL	*qRL8.05*	8.05	100.4	PZA00766_1	2.24	PHM934_19	*ZmPSTOL8.05_1*	6.87	−0.271**	6.87
				133.8		116.8	152.0			
RD	*qRD1.03*	1.03	94.4	umc1073	3.80	bnlg1083	PZA03742_1	9.60	0.307***	25.64
				32.9		27.5	44.5			
	qRD4.05	4.05	25.0	*ZmPSTOL4.05*	2.74	PHM15427_11	PHM3587-6	6.84	0.270***	
				39.8		33.9	59.4			
	qRD7.02	7.02	76.0	PZA01690_7	3.95	PZA01933_3	PZA01946_7	10.01	−0.331***	
				123.1		98.1	123.6			
SA2	*qSA2_10.03*	10.03	34.2	PHM2770_19	5.16	PHM1155_14	PZA01877_2	15.12	−0.393***	15.12
				72.6		62.1	77.5			
R:S	*qRS1.07*	1.07	206.0	PHM12693_8	3.76	PZA01963_15	PZA03301_2	10.85	0.377***	16.47
				223.5		203.7	240.6			
	qRS3.06	3.06	132.0	PZA02212_1	3.00	PZA00186_4	PZA01154_1	8.53	0.310***	
				174.5		165.8	216.0			

[a]QTLs are named using the trait initials followed by their genomic position in bin
[b]cM and Mbp indicate the marker position in centiMorgans and in mega base pairs at maximum LOD value
[c]Flanking markers are based on −1.5 LOD support interval
[d]R^2: Ratio of the genotypic variance of the QTL effect to the phenotypic variance, times 100
[e]Effects measured as standard deviation from the progeny mean: Positive values indicate that L3 carries the allele for an increase in the trait, and negative values indicate that L22 contributes the allele for an increase in the trait. Effect significance based on *p-values* estimated via score statistics resampling ($^+p < 0.1$, $^*p < 0.05$, $^{**}p < 0.01$, $^{***}p < 0.001$)
[f]R^2_T: genotypic variance of the full model

A phylogenetic analysis revealed that the six predicted ZmPSTOL proteins clustered together with PSTOL1 from rice, SNC4 and PR5 from *Arabidopsis* (circled in Fig. 3), which were classified as LRK10L-2 subfamily of serine/threonine receptor-like kinases by Gamuyao *et al.* [40]. In a detailed alignment of structural predictions, all maize PSTOL-like proteins shared conserved ATP-binding and serine/threonine protein kinase domains with OsPSTOL1 (Additional file 3: Figure S2). A distinct glycosyl hydrolase domain was predicted for ZmPSTOL4.05. The maize proteins ZmPSTOL4.05, ZmPSTOL8.02, ZmPSTOL8.05_1 and ZmPSTOL8.05_2 were classified as receptor-like kinases (RLKs), which are characterized by the presence of a transmembrane domain for signal perception and an intracellular kinase domain [48, 49]. In contrast, the proteins ZmPSTOL3.04 and ZmPSTOL3.06 contained the intracellular kinase domain but lacked the transmembrane domain similarly to OsPSTOL1 [40], and thus were classified as receptor-like cytoplasmic kinases (RLCKs) [49].

ZmPSTOL candidate genes have distinct expression patterns

The expression analyses revealed that *ZmPSTOL4.05*, *ZmPSTOL8.02* and *ZmPSTOL8.05_1* were highly and consistently expressed in the roots of the P-inefficient genotype (L22) under low (2.5 μM) and high (250 μM) P conditions, but were not responsive to P in either L22 or L3 (Fig. 4). *ZmPSTOL3.06* was preferentially expressed in the roots of the P-efficient line (L3) with lower expression under high-P compared to the low-P concentration, and induced by high-P in roots of L22 (Fig. 4). The expression of *ZmPSTOL3.04* and *ZmPSTOL8.05_2* was induced in the root and repressed in the shoot of L22 under high-P concentration, but were not differentially expressed in L3 (Fig. 4). Additionally, the expression pattern of *ZmPSTOL3.04* and *ZmPSTOL8.05_2* in roots may reflect the total P content in the seedling, whereas the expression in shoots could be negatively associated with the total P content in L22 (Additional file 4: Table S2).

Discussion

Complex inheritance of root traits, seedling dry weight and P content in maize

Two distinct and powerful statistical models for QTL mapping (MIM and MT-MIM) were applied to dissect root morphology traits, total seedling dry weight, root:shoot ratio and P content in tropical maize RILs. The QTLs identified using the MIM model explained from 6 to 15 % of the total phenotypic variance for each trait, which was similar to the QTLs previously mapped for root traits and P efficiency indices in maize [25–27, 29, 31]. However, the proportion of phenotypic variance explained by all QTLs and their epistatic interactions using MT-MIM ranged from 23.4 to 35.5 %, which was higher than in previous studies. To the best of our knowledge, the present study demonstrates the first QTL mapping of root

Table 4 Quantitative trait loci (QTLs) identified using multiple traits-multiple interval mapping analysis for root length (RL), root diameter (RD), root surface area (SA), surface area of fine roots (SA2), root:shoot ratio (R:S), total seedling dry weight (TDW) and total P content (Pcont)

QTL[a]	Bin	cM[b]	Marker/Position (Mbp)	LOD	Flanking markers[c]/Position (Mbp)		Main effect[d] / R^2 (%)[e]						
							RL	RD	SA	SA2	R:S	TDW	Pcont
qMulti1.03	1.03	94.4	umc1073	18.4	bnlg1083	PZA03742_1	−0.109	0.163*	−0.075	0.110	−0.168*	−0.147*	0.026
			32.9	9	27.5	44.5	1.18	2.64	0.56	1.19	2.82	2.14	0.65
qMulti1.06	1.06	183.	PZA00619_3	5.07	bnlg1598	umc1335	0.093	−0.028	−0.084	0.078	−0.054	−0.004	0.210**
		8	195.4		187.8	196.9	0.85	0.08	0.70	0.60	0.27	0.00	4.33
qMulti1.07	1.07	209.0	PHM114614_22	20.01	PZA01963_15	PHM12693_8	−0.185*	0.010	−0.231**	−0.224**	0.373***	−0.299***	−0.138^{+}
			205.6		203.7	223.5	3.03	0.01	4.73	4.41	12.28	7.89	1.67
qMulti2.08	2.08	72.7	PZA01885_2	16.10	PZA02077_1	PZA01885_2	0.116	−0.109	0.083	−0.041	−0.111	−0.049	−0.262***
			206.9		206.5	206.9	1.28	1.13	0.65	0.02	1.16	0.23	6.50
qMulti3.04	3.04	83.0	PZA00297_2	7.90	*ZmPSTOL3.04*	PHM5502_31	0.217**	−0.216**	0.192*	0.119^{+}	0.124^{+}	−0.023	−0.059
			39.9		20.2	67.2	4.28	4.25	3.34	1.29	1.40	0.05	0.31
qMulti3.06	3.06	138.	PZA01962	8.25	PZA02212_1	PZA03735_1	−0.018	−0.097	−0.049	−0.047	0.306***	−0.077	−0.025
		0	178.2		174.5	180.5	0.03	0.81	0.20	0.19	8.07	0.51	0.05
qMulti6.06	6.06	130.	PHM16607_11	6.88	PHM597_18	PZB01569_7	−0.027	0.108	0.010	0.178*	−0.064	0.111	0.045
		5	160.2		157.9	160.7	0.07	1.11	0.01	3.01	0.39	1.17	0.02
qMulti8.02	8.02	48.0	*ZmPSTOL8.02*	15.76	*ZmPSTOL8.02*	PHM1978_111	−0.252**	0.164	−0.243**	−0.184*	−0.177*	−0.095	−0.239**
			13.3		13.3	21.8	4.14	1.76	3.83	2.20	2.04	0.59	3.71
qMulti9.04	9.04	27.5	PHM13183_12	20.30	PZA0225_8	PZB01358_1	−0.022	−0.135^{+}	−0.079	−0.286***	0.083	−0.164^{+}	−0.148^{+}
			104.7		104.5	106.8	0.04	1.71	0.58	7.67	0.65	2.53	2.05
qMulti10.03	10.03	38.0	PHM1155_14	19.96	PHM1812_32	PZA01877_2	−0.180*	−0.106	−0.240**	−0.403*** 15.17	−0.047	−0.171*	−0.013
			62.1		47.7	77.5	3.03	1.06			0.21	2.74	0.02
					[f]R^2_T		26.17	35.54	24.51	33.53	34.04	23.41	27.28

[a]QTLs are named using the "multi", indicating that were detected using MT-MIM, followed by their genomic position in bin
[b]cM and Mbp indicate the marker position in centiMorgans and in mega base pairs at maximum LOD value
[c]Flanking markers are based on −1.5 LOD support interval
[d]Effect measured as standard deviation from the progeny mean: Positive values indicate that L3 carries the allele for an increase in the trait, and negative values indicate that L22 contributes the allele for an increase in the trait. Effect significance based on *p-values* estimated via score statistics resampling ($^{+}p < 0.1$, $^{*}p < 0.05$, $^{**}p < 0.01$, $^{***}p < 0.001$)
[e]R^2: Ratio of the genotypic variance of the QTL effect to the phenotypic variance, times 100
[f]R^2_T: genotypic variance of the full model (including epistasis shown in Table 4)

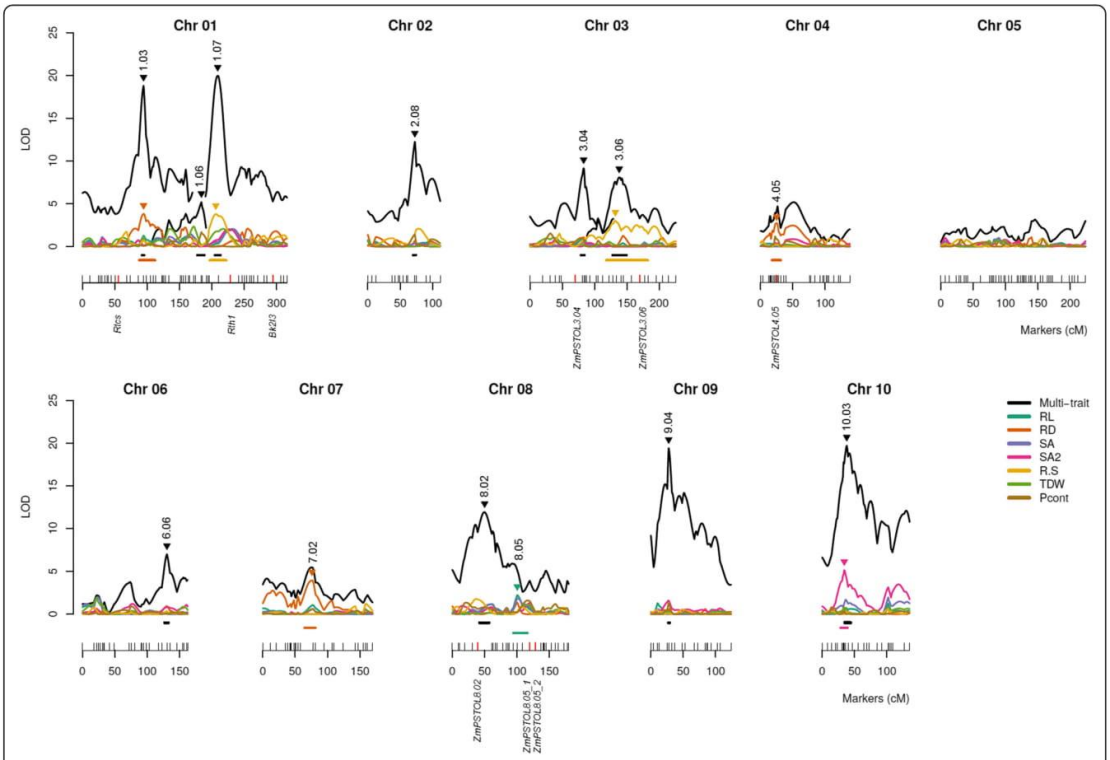

Fig. 2 QTLs identified for root traits, seedling dry weight and P content using single and multiple traits MIM analyses. The markers are represented as vertical traces along the horizontal lines, which represent the chromosomes and are numbered in centiMorgans (cM). The candidate genes are depicted below the red vertical traces. QTL profiles for single trait MIM are shown as colored lines according to the legend for root length (RL), root average diameter (RD), root surface area (SA), surface area of fine roots (SA2), root:shoot ratio (R:S), total seedling dry weight (TDW) and total P content (Pcont). Multi trait QTL profiles are shown as black line. The QTL peaks are depicted with an inverted triangle colored according to the legend followed by the bin. The confidence interval (95 %) for each QTL is represented by a horizontal line above the chromosomes colored according to the legend

Table 5 Epistatic interactions for root morphology traits, total seedling dry weight and P content evaluated in low-P conditions

Interactions	Interaction effect[a] / R^2 (%)[b]						
	RL	RD	SA	SA2	R:S	TDW	Pcont
qMulti1.03 X *qMulti1.07*	−0.060	0.067	−0.078	−0.183*	0.054	−0.053	−0.005
	0.33	0.41	0.56	3.07	0.27	0.25	0.03
qMulti1.03 X *qMulti10.03*	−0.009	−0.029	−0.029	−0.141^{+}	0.148*	−0.123	−0.235**
	0.01	0.08	0.08	1.85	2.04	1.41	5.12
qMulti1.07 X *qMulti9.04*	0.324***	−0.358***	0.280**	0.127	−0.108	0.196*	0.067
	9.02	11.00	6.76	1.38	1.00	3.31	0.39
qMulti2.08 X *qMulti10.03*	−0.071	0.179**	−0.013	0.115	0.166*	0.028	0.077
	0.45	2.86	0.02	1.18	2.47	0.07	0.53
qMulti8.02 X *qMulti9.04*	0.231**	−0.150	0.254*	0.188^{+}	−0.221*	0.307**	0.265**
	3.24	1.37	3.93	2.16	2.99	5.74	4.29

[a]Effects measured as standard deviation from the progeny mean; Positive values indicate that L3 carries the allele for an increase in the trait, and negative values indicate that L22 contributes the allele for an increase in the trait. Interaction effect significances based on *p*-values were estimated via score statistics resampling ($^{+}p < 0.1$, $^{*}p < 0.05$, $^{**}p < 0.01$, $^{***}p < 0.001$)

[b]R^2: Ratio of the genotypic variance of the QTL effect to the phenotypic variance, times 100

Traits: root length (RL), root average diameter (RD), root surface area (SA), surface area of fine roots (SA2), total seedling dry weight (TDW), root:shoot ratio (R:S) and total P content (Pcont)

Table 6 Maize candidate genes sharing more than 55 % amino acid sequence identity to OsPSTOL1

Predicted gene	Gene ID	Physical position (bp)	Identity (%)	Coverage (%)	E-value
GRMZM2G412760	*ZmPSTOL3.04*	Chr3: 20,172,140	55	99	5.1e-104
GRMZM2G448672	*ZmPSTOL3.06*	Chr3: 206,918,421	66	97	4.7e-186
AC193632.2_FG002	*ZmPSTOL4.05*	Chr4: 39,792,602	69	95	2.0e-105
GRMZM2G172396	*ZmPSTOL8.02*	Chr8: 13,267,001	55	99	9.6e-123
GRMZM2G451147	*ZmPSTOL8.05_1*	Chr8: 152,043,859	70	97	3.4e-131
GRMZM2G164612	*ZmPSTOL8.05_2*	Chr8: 152,100,275	70	97	2.3e-127

morphology traits, seedling biomass and P content in maize using the MT-MIM model, confirming that complementary information can be generated when this strategy is combined with single trait MIM analyses, as previously suggested by Silva *et al.* [35].

The genetic complexity of these traits was highlighted by the epistatic interactions among QTLs that showed effects of magnitudes comparable to those of main effects. The significant contribution of epistatic interactions was also detected by other authors for root traits in nutrient solution [25–27, 50] and for P-use efficiency indices under field conditions [30, 51].

QTL mapping revealed that both parents contributed favorable alleles for most of the traits evaluated, which possibly leads to transgressive segregation. The parents L3 and L22 were also shown to donate favorable alleles for P acquisition efficiency and P-use efficiency based on grain yield, when these RILs were backcrossed with both parental lines and evaluated in low-P soil [51]. The occurrence of segregating progenies with extreme phenotypes, out of the parental range, has been detected in plants subjected to different abiotic stresses under field or nutrient solution [50, 52, 53]. Transgressive segregation was also observed in maize RILs derived from a cross between

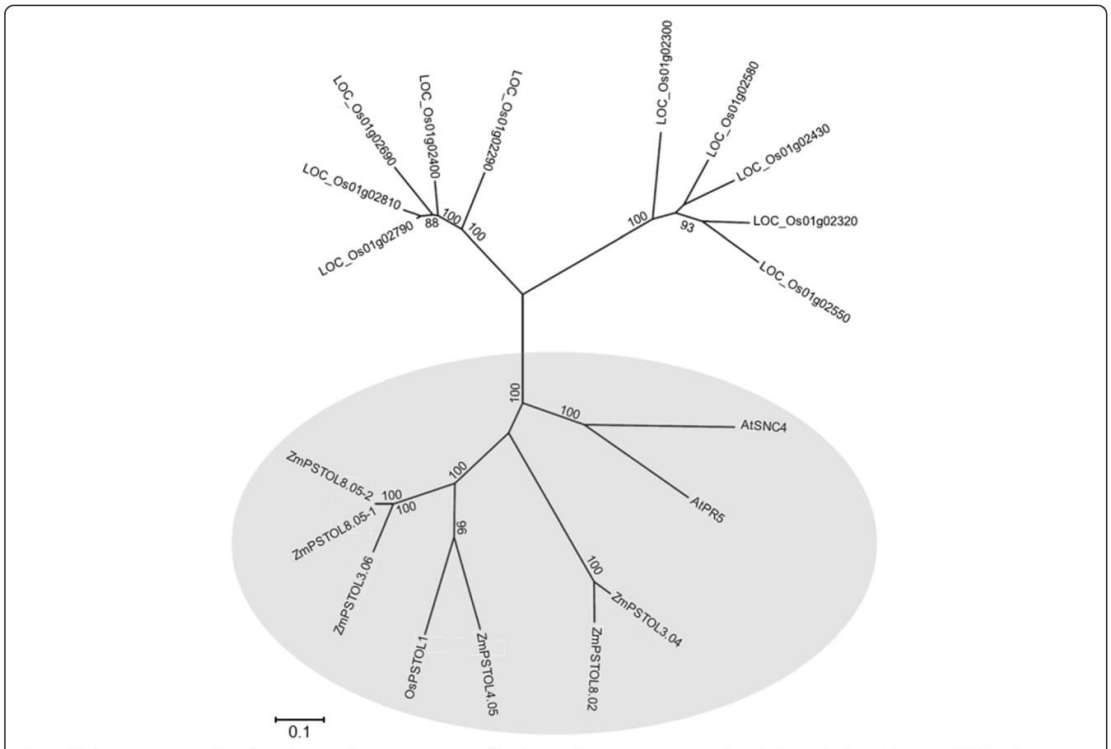

Fig. 3 Phylogenetic tree of predicted serine/theronine receptor-like kinases from maize, rice and *Arabidopsis thaliana*. The rice PSTOL1, the six maize proteins sharing more than 55 % sequence identity to OsPSTOL1, PR5K and SNC4 from *Arabidopsis thaliana* were grouped separately from other rice kinases, and are highlighted. Numbers on branches are bootstrap values for the percentage of coincidence (%) inferred from 1,000 replicates. Only percentage values higher than 50 % are shown

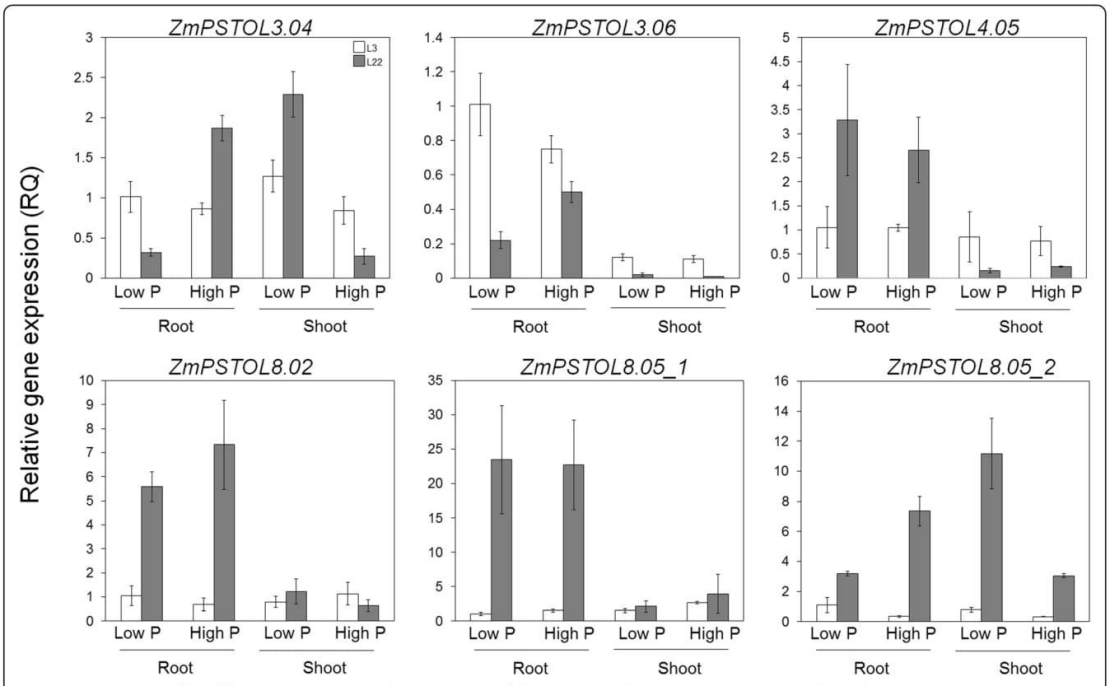

Fig. 4 Expression profiles of the *ZmPSTOL* genes. The expression of the maize candidate genes are presented as relative gene expression (RQ) evaluated in roots and shoots of maize seedlings of the two parental lines L3 (P-efficient) and L22 (P-inefficient) grown under two levels of P (2.5 and 250 μM) after 13 days of treatment. Error bars indicate the standard errors of three technical replicates composed of three seedlings each

Mo17 and B73 for the length and number of lateral and seminal roots [25, 27] and for root hair length [26].

The QTL mapping results strongly reflected the phenotypic correlations among the target traits. The high correlation between root length and root surface area ($r = 0.98$) reflected the coincidence in position and sign of the QTLs detected based on MT-MIM (*qMulti1.07, 3.04, 8.02* and *10.03*; Table 4). Additionally, two significant QTLs for root diameter were either mapped to unique regions or with opposite signs compared with other root traits, corroborating the negative correlations of these traits. Moreover, the importance of the root surface area to seedling dry weight and P content was supported by the presence of multi-trait QTLs that significantly affected these traits (*qMulti1.07*, *8.02* and *10.03*; Table 4), which could be a result of determinant genes with pleiotropic effects or the presence of linked genes.

Coincidence of QTLs for root morphology in the seedling stage with QTLs for grain yield

Three genes previously associated with root morphology in maize (*Rth1*, *Bk2l3* and *Rtcs*) were mapped to chromosome 1, but did not overlap with any mapped QTLs (Fig. 2). Even though early root growth enhancement has not always led to superior yield performance in the field [54], a large number of QTL studies have indicated that some genomic regions consistently affect root morphology traits during the seedling stage and agronomic performance under different environments. A similar situation was also found for three QTL regions on chromosome 1 in our current study, which were coincident with QTLs previously reported for early root traits and for yield components in the field.

qMulti1.03 associated with root diameter, total seedling dry weight and root:shoot ratio overlapped with the QTL influencing seminal root length and weight [50], primary axile root diameter [55], daily elongation rate of axile roots [56] and total length of second-order lateral roots [57] in nutrient solution. This region was coincident with QTLs for drought tolerance index [50], grain yield, kernel number and weight in low-P soil [58]. This genomic region was also detected in a meta-analysis for low-P tolerance in maize as the consensus cQTL1-2 [59].

qMulti1.06 was detected based on the multi-trait MIM model and was significantly associated only with the total P content in the seedling (Table 4 and Fig. 2). A major QTL at bin 1.06 was associated with root traits in nutrient solution, grain yield under well-watered and water-stressed conditions [50], and root-pulling resistance in adult plants [60]. Due to the consistency in the effects of this genomic region

on root traits and grain yields in different studies, this QTL was named *root-yield-1.06*, and validated as constitutively affecting roots, agronomic features and grain yield under different water regimens [61]. A QTL for P utilization efficiency (*qPUTIL1*) based on grain yield under low-P soil also overlapped in this region [51].

The third QTL region on chromosome 1 was mapped at bin 1.07 spanning from 214 to 223 Mbp (*qMulti1.07*), which was associated with root length, root surface area, surface area of fine roots, total seedling dry weight and root:shoot ratio. This region was coincident with a cluster of QTLs named Ax-2 that controlled the root numbers and lengths identified in a meta-analysis combining 15 QTL studies [54]. QTLs for grain yield and drought tolerance index were also mapped to this genomic region [50].

The association of root morphology QTLs in early stages of plant development with yield performance, including the validation of the *root-yield-1.06*, suggested that at least some of these genomic regions can be further used in marker-assisted selection to improve yield stability under drought and other mineral stresses in maize.

ZmPSTOL genes co-localized with QTLs for root morphology, biomass accumulation and P content

The QTL mapped using MT-MIM (*qMulti8.02*) that was associated with root length, root surface area, root:shoot ratio and P content co-localized with *ZmPSTOL8.02* (Fig. 2). This *ZmPSTOL* candidate gene was highly expressed in the roots of L22 (Fig. 4), the donor line of the favorable QTL alleles for all traits mentioned above. In rice, the overexpression of *OsPSTOL1* enhanced total root length and root surface area in transgenic seedlings in nutrient solution as well as grain yield of transgenic varieties cultivated in P-deficient soils [40]. According to these authors, the larger root system contributed to a significant increase in the uptake of nutrients such as phosphorus, nitrogen and potassium in transgenic rice lines overexpressing *OsPSTOL1*. The sequence similarity and conserved domains of these protein kinases from rice and maize combined with the evidences shown here suggest that *ZmPSTOL8.02* could be one of the genes underlying *qMulti8.02*, sharing similar functions in root development and P acquisition efficiency in maize to *OsPSTOL1* in rice. Additionally, QTLs associated with seminal root number in high-P levels [27], shoot dry weight [32] and primary root length [56] overlapped with *qMulti8.02*, confirming that genes controlling root and shoot development in this genomic region are also expressed in other genetic backgrounds.

The other three *ZmPSTOL* genes co-localized with single trait QTLs for root length (*ZmPSTOL8.05_1*), root diameter (*ZmPSTOL4.05*), and root:shoot ratio (*ZmPSTOL3.06*). These genes were preferentially expressed in the roots of the donor line that contributes positive alleles for the respective QTLs under low- and high-P conditions.

ZmPSTOL8.05_1 was mapped to 117 cM on chromosome 8, flanking *qRL8.05*. Additionally, a weak LOD peak for total P content was coincident with this candidate gene (Fig. 2). The MIM model based on score as a significance threshold was not able to detect this QTL, but a minor effect QTL was detected using the Bayesian Information Content threshold with LOD 1.8 and explaining 6.5 % of the total variance for the total P content in the seedling (data not shown). This genomic region also harbored QTLs explaining 5 to 6 % of the phenotypic variance for P acquisition efficiency based on grain yield [51], indicating that this genomic region consistently contributed to P acquisition during the seedling and adult plant stages. Additionally, QTLs in this genomic region were mapped for root length and grain yield under field conditions [32], root length and root dry weight in nutrient solution [26, 50, 62]. The coincidence of QTLs for root traits and for grain yield from different studies associated with the superior expression of *ZmPSTOL8.05_1* in roots under low-P are highly compatible with the role of its putative homolog (*OsPSTOL1*) in rice.

ZmPSTOL3.06 was mapped to 169.6 cM on chromosome 3 within the confidence interval of *qRS3.06* for root:shoot ratio (Fig. 2). This genomic region spans bin 3.06 that harbored QTLs for root traits in a meta-analysis using 15 QTL studies in nine maize mapping populations [54]. This candidate gene was highly expressed in roots cultivated with both P levels of the P-efficient line L3 (Fig. 4), which contributed with positive alleles for the root:shoot ratio QTL. *ZmPSTOL3.06* had the lowest e-value with *OsPSTOL1* (Table 6) and its predicted protein lacks the transmembrane domain, similarly to OsPSTOL1 (Additional file 3: Figure S2). This combined information makes this predicted gene also a candidate to *OsPSTOL1* homolog in maize.

ZmPSTOL4.05 was coincident with the *qRD4*.05, with L22 donating the allele that reduced the root diameter. *ZmPSTOL4*.05 was highly expressed only in roots of the donor line, L22, cultivated in both P availability. Under P starvation conditions the root diameter decreases, while the root surface area increases, enabling the root system to explore a larger volume of soil [11]. Thus, as observed in the path analysis, fine roots are an important component to improve the root surface area, which played a strong contribution to total seedling dry weight and to P content in maize seedlings cultivated in low-P conditions. A QTL controlling the plasticity of lateral root number (i.e., change in the lateral root number in response to P availability) in hydroponics [26] was also mapped at this same region, suggesting that genes harboring in this genomic region may control root traits across different populations.

The finding that *ZmPSTOL* genes were preferentially expressed in the roots of the lines that contributed the

allelic enhancing root traits, seedling dry weight and P content indicate that at least *ZmPSTOL3.06*, *ZmPSTOL4.05*, *ZmPSTOL8.02* and *ZmPSTOL8.05_1* may have a functional relationship with root morphology and/or with P acquisition in maize. Considering the role of *PSTOL1* genes in rice and sorghum, it could be expected that genes encoding important adaptive traits would be shared among rice, sorghum and maize, such as the case for the major Al tolerance gene in sorghum (*SbMATE*) [63] that was found to be functionally conserved in maize (*ZmMATE1*) [64] and rice (*OsFRDL4*) [65].

Conclusions

Comprehensive QTL analyses revealed important regions associated with root traits, seedling dry weight and P content in maize under low-P concentration. Using the multiple trait-multiple interval mapping model, these QTLs explained a larger extent of the phenotypic variance for the target traits compared with previous studies. The complementary genomic regions identified using both models jointly offered putative targets for molecular breeding aiming to improve P acquisition efficiency in maize. Additionally, this study identified new maize candidate genes sharing high identity with *OsPSTOL1* that were preferentially expressed in the roots and co-localized with QTLs for root morphology and P acquisition related traits.

Material and methods

Mapping population

The segregating population was composed by 145 maize recombinant inbred lines (RILs) derived from a bi-parental cross of lines L3 (P-efficient) and L22 (P-inefficient). F_1 plants were self-pollinated and individual F_2 plants were advanced for seven cycles of selfing by single seed descent, after which seeds were bulked for multiplication. The parental lines and the population were developed at Embrapa Maize and Sorghum (Brazil, latitude 19_270S and 716 m above sea level). The parental lines were previously characterized as contrasting for P-use efficiency under low and high P conditions in the field [45] and for root morphology traits [46].

Quantitative analysis of root traits, seedling biomass accumulation and P content using a paper pouch system

The mapping population and parents were evaluated in randomized complete block design with four biological replicates, each composed by three plants per pouch. Each biological replicate was evaluated in an identical but independent experiment performed on a seven-day interval. Maize seeds were surface sterilized with 0.5 % (v/v) sodium hypochlorite for 5 min and germinated in moistened germination paper rolls. After four days, uniform seedlings were transferred to moist blots in paper pouches after removing the endosperm to eliminate seed reserves [46]. A modified Magnavaca nutrient solution [66] containing 2.5 μM P was replaced every three days and the pH was maintained at 5.65. Each container was filled with 5 l of nutrient solution with the bottom 3 cm of the pouches immersed in the solution. The containers were maintained in a growth chamber with a 12 h photoperiod at 27/20 °C day/night temperatures and 330 μmol m^{-2} s^{-1} of light intensity. After 13 days, root images were captured using a digital photography setup and analyzed using RootReader2D (http://www.plantmineralnutrition.net/rr2d.php) and WinRHIZO (http://www.regent.qc.ca/assets/winrhizo_about.html) software according to de Sousa *et al.* [46]. The total root system, which includes all together primary, seminal and initial adventitious roots, was evaluated for total root length (RL) (cm), average root diameter (RD) (cm^3), total root surface area (SA) (cm^2) and surface area of fine roots (SA2) ($1.0 < d \leq 2.0$ mm) (cm^2).

Root and shoot tissues were dried separately at 65 °C in a forced-air oven until a constant weight was obtained to determine the root:shoot dry weight ratio (R:S) and total seedling dry weight (TDW). For P analysis, root and shoot tissues were subjected to nitric perchloric acid digestion [67]. The total P content in the seedling (Pcont) was calculated as the sum of the P content in each seedling component, which was the product of the dry weight and the P concentration in the root and shoot. As maize absorbs phosphate in its orthophosphate form (Pi), the P in the nutrient solution refers to phosphate, whereas the total P content in the seedling comprises both organic and inorganic P forms.

Analysis of variance (ANOVA), correlations between pairs of traits and path analysis were performed using the GENES software [68]. The phenotypic correlations were calculated based on the mean values. Broad sense heritability was estimated as $h^2=\hat{\sigma}^2_G/\left(\hat{\sigma}^2_G+\hat{\sigma}^2_E\right)$ with $\hat{\sigma}^2_G=(MS_G - MS_E)/r$ and $\hat{\sigma}^2_E=MS_E$, where $\hat{\sigma}^2_G$ and $\hat{\sigma}^2_E$ are the estimates of genetic and error variance, respectively; MS_G and MS_E are the genetic and error mean squares, respectively, and r is the number of replications.

For the path analysis [69], the five root traits (total root length, root average diameter, surface area and surface area of fine roots) were considered as independent variables x_i ($i = 1, 2, \ldots, 5$). The total seedling dry weight and phosphorus content were considered as dependent variables y_j ($j = 1, 2$) in two distinct path analyses. The estimated path coefficient (P_{ij}) was considered as the direct effect of variable x_i on y_j. Indirect effects of x_i on y_j mediated by variable $x_{i'}$ were calculated by multiplying the correlation between x_i and $x_{i'}$ ($r_{ii'}$) by $P_{i'j}$. Root:-shoot ratio was excluded from the analysis due to its contribution to both dependent variables.

Linkage map

DNA was isolated from young leaves using the CTAB method [70]. Initially, 60 polymorphic SSR markers were genotyped in the RIL population according to [71]. A total of 332 SNPs (Single Nucleotide Polymorphisms) were genotyped in the population using Kompetitive Allele-Specific PCR or the KASP^{TM} assay (LGC Genomics, Teddington, UK). The sequences, genetic and genomic locations of SSR and SNP markers are available at the Maize Genetics and Genomics Database (http://www.maizegdb.org/data_center/locus).

The markers were tested for the expected segregation ratio of 1:1 using chi-square statistics ($p < 0.05$) corrected for multiple tests based on Bonferroni's method. The linkage map was constructed using MapMaker/EXP 3.0 [72] considering a minimum LOD of 3.0 and a maximum frequency of recombination (r) of 0.4. The mapping function Kosambi [73] was used to convert recombination fractions into map distances. The final linkage map was drawn using Windows QTL Cartographer v 2.5 (http://statgen.ncsu.edu/qtlcart/WQTLCart.htm).

QTL mapping

Phenotypic fitted values were obtained from the following statistical model adjusted for each single trait:

$$y_{ij} = \mu + B_i + G_j + \varepsilon_{ij}$$

where y_{ij} is the phenotypic observation from the i^{th} ($i = 1, \ldots, 4$) replication on the j^{th} genotype ($j = 1, \ldots, 145$); μ is the phenotypic average; B_i is the effect of the i^{th} block; G_j is the j^{th} genotype; and ε_{ij} is the residual associated with the y_{ij} observation. We tested the fit of two models by first assuming that the residuals were normally distributed with constant variance, $\varepsilon_{ij} \sim N(0, \sigma^2)$ and by second considering the heteroscedasticity, $\varepsilon_{ij} \sim N(0, \sigma_j^2)$. Both models were fitted using the *gls* function from the *nlme* R package [74] and compared using the *ANOVA* function from the same package. For each trait, the fitted phenotypic values were extracted from the model with the best fit. Each replicate was composed by three plants that were bulked for all laboratorial analyses.

Due to the large variability in the absolute values, all phenotypic fitted values were standardized to achieve unity as standard deviations and zero means as follows:

$$z_{it} = \frac{y_{it} - \mu_t}{\sigma_t},$$

where z_{it} is the standardized observation of trait t ($t = 1, 2, \ldots, 7$) on subject i; y_{it} is the observation of trait t on subject i; μ_t is the average of trait t; and σ_t is the standard deviation of trait t.

For the joint QTL analysis, a multiple trait-multiple interval mapping (MT-MIM) model was evaluated as previously described [35]. The complete model was fitted using the following equation:

$$z_{ti} = \mu_t + \sum_{r=1}^{m} \beta_{tr} x_{ir} + \sum_{r<l}^{p} W_{trl} x_{ir} x_{il} + \varepsilon_{ti},$$

where z_{ti} is the standardized observation of trait t on subject i; μ_t is the intercept for trait t; the parameter β_{tr} has the genetic interpretation of the additive effect of QTL r on trait t ($r = 1, 2, \ldots, m$ QTLs included in the model); and the regressive variables x_{ir} represent the contrast coefficients codified according to the Cockerham model [33, 75] (i.e., x_{ir} is 1 for the dominant and −1 for the recessive homozygous). The third component on the right side of the model refers to a subset of the p pairwise interactions among QTLs previously included in the model, where w_{trl} is the epistatic effect between QTL r and QTL l on trait t and the random error ε_{ti} was assumed to be independent and identically distributed according to a multivariate normal distribution, with a mean vector of zero and a positive definite symmetric variance-covariance matrix Σ_ε, i.e., $\varepsilon_{ti} = MVN(0, \Sigma_\varepsilon)$.

Multi-trait QTL mapping was initiated with a forward search for the main effect QTL using a grid of 1 cM in the genome and a 15 % genome-wide significance level. After three rounds of QTL search, the positions of all QTLs in the model were re-estimated as along with all other parameters in the model. After the inclusion of the main effects in the model, the forward search for epistasis was performed by testing all pairwise interactions among QTLs already included in the model, employing a 5 % genome-wide significance level. Only the epistatic effects that displayed at least one significant marginal effect were kept in the final model. The Haley-Knott regression [76] was used to estimate the model parameters, and the resampled score statistics [35, 77] were employed to obtain the empirical genome-wide threshold for the QTL mapping analysis. Using this approach, a final model was selected to calculate the proportion of phenotypic variance explained by all QTLs as the ratio between the genotypic variance of the QTL effect to the phenotypic variance times 100 (coefficient of determination R^2), and the LOD profile along the chromosomes. The R^2 values were estimated using the fitted full model, including non-significant QTL effects. The QTL confidence intervals were obtained using the drop 1.5-LOD support interval method with approximately 0.95 confidence levels [78].

Multiple interval mapping (MIM) analysis was performed for each single trait [33, 79] in a similar procedure to that performed for the joint analysis, considering $t = 1$. All QTL analyses were performed using R software (version 2.15.2) and a QTL mapping package named OneQTL that is under development by L.C. Silva.

Identification of maize *PSTOL1* homologs

Using the OsPSTOL1 amino acid sequence [GenBank: BAK26566] we performed searches against the maize genome database (http://ensembl.gramene.org/Zea_mays/Info/Index) using BLASTp. Six predicted maize proteins with more than 55 % sequence identity to rice PSTOL1 were selected and aligned using ClustalX software version 1.83 [80]; the alignment included OsPSTOL1 and the Arabidopsis protein kinases SNC4 [81] and PRK5 [82]. The phylogenetic tree was constructed based on the maximum likelihood method with 1000 bootstraps [83] using MEGA software [84]. The protein domains were identified using the CDART (Conservative Domain Architecture Retrieval Tool (http://www.ncbi.nlm.nih.gov/Structure/lexington/lexington.cgi).

Mapping candidate genes

Specific primers for the maize candidate genes were designed using Primer Blast (ncbi.nlm.nih.gov/tools/primer-blast/index.cgi). PCR reactions were performed using 30 ng of DNA, 0.2 mM of each dNTP, 2 mM of $MgCl_2$, 10 pmols of each primer, 5 % (v/v) dimethyl sulfoxide (DMSO) and 1 U of Taq DNA polymerase (Invitrogen, Carlsbad, CA). The amplification profile included an initial step of 95 °C for 1 min, followed by 35 cycles of denaturing at 94 °C for 1 min, annealing at 58 to 60 °C for 30 s, depending on the primers, and extension at 72 °C for 1 min. The amplification products were treated with ExoSAP-IT reagent (USB Corporation, Cleveland, OH) and sequenced using the BigDye Terminator v3.1 cycle sequencing kit on an ABI PRISM 3100 genetic analyser (Applied Biosystems, Foster City, CA) to identify polymorphisms between the parental lines.

Sequence-tagged site (STS) markers were developed to map genes previously associated with root morphology in maize. For the *roothairless* gene (*Rth1*) [22], a 22-bp indel was amplified using the primers 5′-TTGCCCAC GGCTGGCAAGAG-3′ and 5′- GGCTCTGTAGCACG CCCCTC - 3′ and resolved on a silver-stained polyacrylamide gel [85]. The same strategy was used for the *brittle stalk-2-like protein 3* gene (*Bk2l3*) [23], which was revealed after the amplification of a 15-bp indel using the primer pair: 5′-GCTGGTTAGATCCCCCGCCCA-3′ and 5′-GCACTGGAGCCACCGACACTG-3′. The *rootless concerning crown and seminal roots* gene (*Rtcs*) [24] was genotyped as a CAPS marker obtained after digestion of the amplification product of genomic DNA with the primers 5′-CGCGCCATAGCCCGCAGTAA-3′ and 5′-GATTGGCACGGGCCGGTCAG-3′ with the restriction enzyme *Aci*I and was visualized on a silver-stained polyacrylamide gel [85].

Cleaved amplified polymorphic sequence (CAPS) markers were developed for the other candidate genes. For *ZmPSTOL3.04* the PCR product amplified using the primers 5′-ACGGGGCTTGGAGGCACATG-3′ and 5′-TGAGACCGCGTGGGGAAGGG-3′ was digested with the restriction enzyme *Stu*I. The polymorphism for *ZmPSTOL8.02* was obtained after digestion with *Rsa*I of the genomic fragment amplified with the primers 5′-TGACTGGTGCCAGAGGTACGC-3′ and 5′-TGC ATACAAGGGACTGCTTCGGA-3′. CAPS markers were resolved on silver stained polyacrylamide gels [85]. The images were digitally captured using a Nikon digital camera.

ZmPSTOL3.06 was mapped based on the presence and absence of the amplification product using the primers 5′-AAGGGCGTCCAACCGCCTTG-3′ and 5′-TTGTT GGCCGGTCCGTTGGG-3′ on a 1 % (w/v) agarose gel stained with ethidium bromide.

A G/A SNP was revealed after sequencing the amplified product obtained using the primer pair 5′-CCGCTA CGCCTTGGTTGCCA-3′ and 5′-CGCCGTAGTTAGCG GAGCCG-3′ to map *ZmPSTOL4.05*, the primer pair 5′-AGCCTCCACGATGGCCGACA-3′ and 5′-TGCA TTTGTGTGACCTGGAA-3′ to map *ZmPSTOL8.05_1*, and the primers 5′- TCCACGGCCGACAGGTAGCA-3′ and 5′-GCTCAAGAGAACTCAGGGTGGC-3′ to map *ZmPSTOL8.05_2*.

Gene expression analysis

The expression profiles of the candidate genes were assessed in the roots and shoots of the L3 and L22 genotypes harvested after 13 days in modified Magnavaca's nutrient solution containing low (2.5 μM) and high (250 μM) P. Total RNA was extracted from a bulk of three plants using the RNeasy Plant Mini kit (Qiagen, Valencia, CA), and 1 μg of total RNA pretreated with DNase I was used for cDNA synthesis using the High Capacity cDNA Reverse Transcription kit (Applied Biosystems, Foster City, CA) according to the manufacturer's instructions. Gene expression was determined by quantitative PCR (qPCR-RT) using SYBR Green I and TaqMan assays in the ABI Prism 7500 Fast System (Applied Biosystems, Foster City, CA). Primers were designed for all target genes using Primer Express Software (Applied Biosystems, Foster City, CA), and 18S rRNA was used as an endogenous constitutive control (Additional file 5: Table S3). With the exception of *ZmPSTOL4.05*, two primers pair were designed for each gene to confirm their expression pattern. However, only the expression profile obtained with the primer pairs highlighted in bold in the Additional file 5 are shown. The relative gene expression was calculated using the $2^{-\Delta\Delta CT}$ method [86], with three technical replicates and L3 roots under low-P conditions as a calibrator. Variance analysis of the gene expression and total P content was performed using GENES software [68].

Availability of supporting data

http://purl.org/phylo/treebase/phylows/study/TB2:S17800.

Additional files

Additional file 1: Table S1. Trait means, coefficients of variation (CV), genetic variances (σ^2_G), environmental variances (σ^2_E) and heritability estimates (h^2) in 145 RILs derived from a cross between maize lines L3 and L22.

Additional file 2: Figure S1. Genetic linkage map including 292 markers in a maize RIL population derived from a cross between L3 and L22. For each chromosome (chr), marker names are indicated on the right and the genetic distance in centimorgans (cM) is on the left. The colored bars indicate the position of QTLs for root traits, total plant dry weight, root:shoot ratio and P content (for details see Fig. 3, Tables 3 and 4).

Additional file 3: Figure S2. Alignment of the OsPSTOL1 and six maize serine/theronine receptor-like kinases highlighting the predicted domains. Letters in green indicate the glycosil hydrolase domain and in red, the transmembrane domain. The kinase domain is represented by a gray background, whereas the ATP-binding site is highlighted with black background with white letters and the Serine/Threonine protein kinase active site with yellow background.

Additional file 4: Table S2. Total P content in the seedling and relative expression of *ZmPSTOL* genes in shoots and roots of both parental lines in low- and high-P concentration.

Additional file 5: Table S3. Primers used for gene expression analyses.

Abbreviations

BIC: Bayesian information content; bp: Base pair; CAPS: Cleaved amplified polymorphic sequence; CDART: Conservative domain architecture retrieval tool; CI: Confidence interval; cM: centiMorgan; CTAB: Cetyl trimethyl ammonium bromide; ICP: Inductively-coupled argon; indel: Insertion/deletion; KASP: Kompetitive allele-specific PCR; LOD: Likelihood of odds; Mbp: Mega base pairs; MIM: Single trait-multiple interval mapping; MT-MIM: Multiple traits-multiple interval mapping; μM: micro Molar; mM: mili Molar; Pcont: Total phosphorus content in the seedling; PCR: Polymerase chain reaction; P: Phosphorus; PSTOL1: Phosphorus-starvation tolerance 1; qPCR-RT: Quantitative real-time PCR; QTL: Quantitative trait loci; RD: Average of root diameter; RIL: Recombinant inbred line; RL: Total root length; R:S: Root:shoot dry weight ratio; SA: Total root surface area; SA2: Surface area of fine roots; sd: Standard deviations from the progeny mean; SNP: Single nucleotide polymorphism; SSR: Simple sequence repeats; STS: Sequence-tagged site; TDW: Total seedling dry weight; v/v: Volume per volume; w/v: Weight per volume.

Competing interests

The authors declare that they have no competing interests.

Authors' contributions

Conceived and designed experiments: CTG, SMS, JVM. Performed experiments: GCA, BFN, BH, UGPL. Analyzed the data: GCA, ACG, LCS, AAFG. Wrote and revised the paper: GCA, ACG, LCS, JVM, AAFG, SMS, CTG. All authors read and approved the final manuscript.

Acknowledgments

The authors would like to acknowledge funding from the Generation Challenge Programme (project G7010.03.01), the Embrapa Macroprogram, FAPEMIG and CNPq/Embrapa REPENSA. PhD fellowship for GCA was granted by Coordenação de Aperfeiçoamento de Pessoal de Nível Superior (CAPES/Embrapa) and BH was supported by Fundação de Amparo a Pesquisa do Estado de Minas Gerais (FAPEMIG). JVM and AAFG received fellowships from Conselho Nacional de Desenvolvimento Científico e Tecnológico (CNPq). We are thankful to Dr. Sigrid Heuer (ACPFG, Australia) for sharing information about the rice *PSTOL1*.

Author details

[1]Departamento de Biologia Geral, Universidade Federal de Minas Gerais, Avenida Presidente Antônio Carlos, 6627, Belo Horizonte, MG 31270-901, Brazil. [2]Departamento de Genética, Escola Superior de Agricultura Luiz de Queiroz, Universidade de São Paulo, Caixa Postal 83, Piracicaba, SP 13400-970, Brazil. [3]Departamento de Bioengenharia, Universidade Federal de São João del-Rei, Praça Dom Helvécio, 74, São João del-Rei, MG 36301-160, Brazil. [4]Núcleo de Biologia Aplicada, Embrapa Milho e Sorgo, Rodovia MG 424, km 65, Caixa Postal 151, Sete Lagoas, MG 35701-970, Brazil.

Received: 28 May 2015 Accepted: 23 June 2015
Published online: 07 July 2015

References

1. Cordell D, Drangert J-O, White S. The story of phosphorus. Global food security and food for thought. Global Environ Chang. 2009;19:292–305.
2. Dawson CJ, Hilton J. Fertilizer availability in a resource-limited world: production and recycling of nitrogen and phosphorus. Food Policy. 2011;36:S14–22.
3. Vance C, Uhde-Stone C, Allan DL. Phosphorus acquisition and use: critical adaptations by plants for securing a nonrenewable resource. New Phytol. 2003;157:423–47.
4. Shen J, Yuan L, Zhang J, Li H, Bai Z, Chen X, et al. Phosphorus dynamics: from soil to plant. Plant Physiol. 2011;156:997–1005.
5. Lynch JP, Brown KM. New roots for agriculture: exploiting the root phenome. Phil Trans R Soc B. 2012;367:1598–604.
6. Batten GD. A review of phosphorus efficiency in wheat. Plant Soil. 1992;146:163–8.
7. Awika JM. Major cereal grains production and use around the world. In: Awika JM, Piironen V, Bean S, editors. Advances in cereal science: implications to food processing and health promotion. Washington: American Chemical Society; 2011. p. 1–13.
8. Calderón-Vázquez C, Sawers RJH, Herrera-Estrella L. Phosphate deprivation in maize: genetics and genomics. Plant Physiol. 2011;156:1067–77.
9. Parentoni SN, Souza Jr CL. Phosphorus acquisition and internal utilization efficiency in tropical maize genotypes. Pesqui Agropecu Bras. 2008;43:893–901.
10. Lambers H, Raven JA, Shaver GR, Smith SE. Plant nutrient-acquisition strategies change with soil age. Trends Ecol Evol. 2008;23:95–103.
11. Raghothama KG. Phosphate acquisition. Annu Rev Plant Phys. 1999;50:665–93.
12. Horst WJ, Kamh M, Jibrin JM, Chude VO. Agronomic measures for increasing P availability to crops. Plant Soil. 2001;237:211–23.
13. Ramaekers L, Remans R, Rao IM, Blair MW, Vanderleyden J. Strategies for improving phosphorus acquisition efficiency of crop plants. Field Crop Res. 2010;117:169–76.
14. Mollier A, Pellerin S. Maize root system growth and development as influenced by phosphorus deficiency. J Exp Bot. 1999;50:487–97.
15. Hermans C, Hammond JP, White PJ, Verbruggen N. How do plants respond to nutrient shortage by biomass allocation? Trends Plant Sci. 2006;11:610–7.
16. Silberbush M, Barber SA. Sensitivity of simulated phosphorus uptake to parameters used by a mechanistic-mathematical model. Plant Soil. 1983;100:93–100.
17. Lynch JP. Roots of the second green revolution. Aust J Bot. 2007;55:493–512.
18. Zhu J, Lynch JP. The contribution of lateral rooting to phosphorus acquisition efficiency in maize (*Zea mays*) seedlings. Func Plant Biol. 2004;31:949–58.
19. Lynch JP, Brown KM. Topsoil foraging—an architectural adaptation of plants to low phosphorus availability. Plant Soil. 2001;237:225–37.
20. York LM, Nord EA, Lynch JP. Integration of root phenes for soil resource acquisition. Fron Plan Sci. 2013;4:1–15.
21. Hochholdinger F, Tuberosa R. Genetic and genomic dissection of maize root development and architecture. Curr Opin Plant Biol. 2009;12:1–6.
22. Wen T-S, Hochholdinger F, Sauer M, Bruce W, Schnable PS. The *roothairless1* gene of maize encodes a homolog of *sec3*, which is involved in polar exocytosis. Plant Physiol. 2005;138:1637–43.
23. Brady S, Song S, Dhugga KS, Rafalski JA, Benfey PN. Combining expression and comparative evolutionary analysis. The COBRA gene family. Plant Physiol. 2007;143:172–87.
24. Taramino G, Sauer M, Stauffer Jr JL, Multani D, Niu X, Sakai H, et al. The maize (*Zea mays* L.) *RTCS* gene encodes a LOB domain protein that is a key regulator of embryonic seminal and post-embryonic shoot-borne root initiation. Plant J. 2007;50:649–59.
25. Zhu J, Kaeppler SM, Lynch JP. Mapping of QTL controlling root hair length in maize (*Zea mays* L.) under phosphorus deficiency. Plant Soil. 2005;270:299–310.
26. Zhu J, Kaeppler SM, Lynch JP. Mapping of QTLs for lateral root branching and length in maize (*Zea mays* L.) under differential phosphorus supply. Theor Appl Genet. 2005;111:688–95.
27. Zhu J, Mickelson SM, Kaeppler SM, Lynch JP. Detection of quantitative trait loci for seminal root traits in maize (*Zea mays* L.) seedlings grown under differential phosphorus levels. Theor Appl Genet. 2006;113:1–10.
28. Kaeppler SM, Parke JL, Mueller SM, Senior L, Stuber C, Tracy WF. Variation among maize inbred lines and detection of quantitative trait loci for growth at low phosphorus and responsiveness to arbuscular mycorrhizal fungi. Crop Sci. 2000;40:358–64.

29. Chen J, Xu L, Cai Y, Xu J. QTL mapping of phosphorus efficiency and relative biologic characteristics in maize (*Zea mays* L.) at two sites. Plant Soil. 2008;313:251–66.
30. Chen J, Xu L, Cai Y, Xu J. Identification of QTLs for phosphorus utilization efficiency. Euphytica. 2009;167:245–52.
31. Chen J, Xu L. The candidate QTLs affecting phosphorus absorption efficiency. Front Agric China. 2011;5:456–62.
32. Cai H, Chen F, Mi G, Zhang F, Maurer HP, Liu W, et al. Mapping QTLs for root system architecture of maize (*Zea mays* L.) in the field at different developmental stages. Theor Appl Genet. 2012;125:1313–24.
33. Kao C-H, Zeng Z-B, Teasdale RD. Multiple interval mapping for quantitative trait loci. Genetics. 1999;152:1203–16.
34. E Silva LC, Zeng Z-B. Current progress on statistical methods for mapping quantitative trait loci from inbred line crosses. J Biopharm Stat. 2010;20:454–81.
35. Silva LDCE, Wang S, Zeng Z-B. Multiple trait multiple interval mapping of quantitative trait loci from inbred line crosses. BMC Genet. 2012;13:67.
36. Wissuwa M, Wegner J, Ae N, Yano M. Substitution mapping of Pup1: a major QTL increasing phosphorus uptake of rice from a phosphorus-deficient soil. Theor Appl Genet. 2002;105:890–7.
37. Wissuwa M, Ae N. Further characterization of two QTLs that increase phosphorus uptake of rice (*Oryza sativa* L.) under phosphorus deficiency. Plant Soil. 2001;237:275–86.
38. Chin JH, Lu X, Haefele SM, Gamuyao R, Ismail A, Wissuwa M, et al. Development and application of gene-based markers for the major rice QTL *Phosphorus uptake 1*. Theor Appl Genet. 2010;120:1073–86.
39. Chin JH, Gamuyao R, Dalid C, Bustaman M, Prasetiyono J, Moeljopawiro S, et al. Developing rice with high yield under phosphorus deficiency: *Pup1* sequence to application. Plant Physiol. 2011;156:1202–16.
40. Gamuyao R, Chin JH, Pariasca-Tanaka J, Pesaresi P, Catausan S, Dalid C, et al. The protein kinase Pstol1 from traditional rice confers tolerance of phosphorus deficiency. Nature. 2012;488:535–9.
41. Hufnagel B, de Sousa SM, Assis L, Guimaraes CT, Leiser W, Azevedo GC, et al. Duplicate and conquer: Multiple homologs of PHOSPHORUS-STARVATION TOLERANCE1 enhance phosphorus acquisition and sorghum performance on low-phosphorus soils. Plant Physiol. 2014;166:659–77.
42. Schnable PS, Ware D, Fulton RS, Stein JC, Wei F, Pasternak S, et al. The B73 maize genome: complexity, diversity, and dynamics. Science. 2009;326:1112–5.
43. Parentoni SN, Magalhaes JV, Pacheco CAP, Santos MX, Abadie T, Gama EEG, et al. Heterotic groups based on yield-specific combining ability data and phylogenetic relationship determined by RAPD markers for 28 tropical maize open pollinated varieties. Euphytica. 2001;121:197–208.
44. Lu Y, Yan J, Guimaraes CT, Taba S, Hao Z, Gao S, et al. Molecular characterization of global maize breeding germplasm based on genome-wide single nucleotide polymorphisms. Theor Appl Genet. 2009;120:93–115.
45. Parentoni SN, de Souza Jr CL, de Carvalho Alves VMC, Gama EEG, Coelho AM, de Oliveira AC, et al. Inheritance and breeding strategies for phosphorus efficiency in tropical maize (*Zea mays* L.). Maydica. 2010;55:1–15.
46. de Sousa SM, Clark RT, Mendes FF, de Oliveira AC, Vasconcelos MJV, Parentoni SN, et al. A role for root morphology and related candidate genes in P acquisition efficiency in maize. Func Plant Biol. 2012;39:925–35.
47. Gardiner JM, Coe EH, Melia-Hancock S, Hoisington DA, Chao S. Development of a core RFLP map in maize using an immortalized F_2 population. Genetics. 1993;134:917–30.
48. Shiu SH, Bleecker AB. Receptor-like kinases from Arabidopsis form a monophyletic gene family related to animal receptor kinases. P Natl Acad Sci USA. 2001;98:10763–8.
49. Vij S, Giri J, Dansana PK, Kapoor S, Tyagi AK. The receptor-like cytoplasmic kinase (OsRLCK) gene family in rice : organization, phylogenetic relationship, and expression during development and stress. Mol Plant. 2008;1:732–50.
50. Tuberosa R, Sanguineti MC, Landi P, Giuliani MM, Salvi S, Conti S. Identification of QTLs for root characteristics in maize grown in hydroponics. Plant Mol Biol. 2002;48:697–712.
51. Mendes FF, Guimarães LJM, Souza JC, Guimarães PEO, Magalhaes JV, Garcia AAF, et al. Genetic architecture of phosphorus use efficiency in tropical maize cultivated in a low-P soil. Crop Sci. 2014;54:1–9.
52. Li M, Guo X, Zhang M, Wang X, Zhang G, Tian Y, et al. Mapping QTLs for grain yield and yield components under high and low phosphorus treatments in maize (*Zea mays* L.). Plant Sci. 2010;178:454–62.
53. Ruta N, Liedgens M, Fracheboud Y, Stamp P, Hund A. QTLs for the elongation of axile and lateral roots of maize in response to low water potential. Theor Appl Genet. 2010;120:621–31.
54. Hund A, Fracheboud Y, Soldati A, Frascaroli E, Salvi S, Stamp P. QTL controlling root and shoot traits of maize seedlings under cold stress. Theor Appl Genet. 2004;109:618–29.
55. Hund A, Reimer R, Messmer R. A consensus map of QTLs controlling the root length of maize. Plant Soil. 2011;344:143–58.
56. Trachsel S, Messmer R, Stamp P, Hund A. Mapping of QTLs for lateral and axile root growth of tropical maize. Theor Appl Genet. 2009;119:1413–24.
57. Burton AL, Johnson JM, Foerster JM, Hirsch CN, Buell CR, Hanlon MT, et al. QTL mapping and phenotypic variation for root architectural traits in maize (*Zea mays* L.). Theor Appl Genet. 2014;127:2293–311.
58. Cai H, Chu Q, Gu R, Yuan L, Liu J, Zhang X, et al. Identification of QTLs for plant height, ear height and grain yield in maize (*Zea mays* L.) in response to nitrogen and phosphorus supply. Plant Breed. 2012;131:502–10.
59. Zhang H, Uddin MS, Zou C, Xie C, Xu Y, Li W-X. Meta-analysis and candidate gene mining of low-phosphorus tolerance in maize. J Int Plant Biol. 2014;56:262–70.
60. Landi P, Sanguineti MC, Darrah LL, Giuhani MM, Salvi S, Conti S, et al. Detection of QTLs for vertical root pulling resistance in maize and overlap with QTLs for root traits in hydroponics and for grain yield under different water regimes. Maydica. 2002;47:233–43.
61. Landi P, Giuliani S, Salvi S, Ferri M, Tuberosa R, Sanguineti MC. Characterization of root-yield-1.06, a major constitutive QTL for root and agronomic traits in maize across water regimes. J Exp Bot. 2010;61:3553–62.
62. Liu J, Li J, Chen F, Zhang F, Ren T, Zhuang Z, et al. Mapping QTLs for root traits under different nitrate levels at the seedling stage in maize (*Zea mays* L.). Plant Soil. 2008;305:253–65.
63. Magalhaes JV, Liu J, Guimaraes CT, Lana UGP, Alves VMC, Wang YH, et al. A gene in the multidrug and toxic compound extrusion (MATE) family confers aluminum tolerance in sorghum. Nat Genet. 2007;39:1156–61.
64. Maron LG, Piñeros MA, Guimaraes CT, Magalhaes JV, Pleiman JK, Mao C, et al. Two functionally distinct members of the MATE (multi-drug and toxic compound extrusion) family of transporters potentially underlie two major aluminum tolerance QTLs in maize. Plant J. 2010;61:728–40.
65. Yokosho K, Yamaji N, Ma JF. An Al-inducible MATE gene is involved in external detoxification of Al in rice. Plant J. 2011;68:1061–9.
66. Magnavaca R, Gardner CO, Clark RB. Evaluation of maize inbred lines for aluminum tolerance in nutrient solution. In: Gabelman HW, Longhman BC, editors. Genetic aspects of plant mineral nutrition. Dordrecht: Martinus Nijhoff Publishers; 1987. p. 255–65.
67. da Silva FC. Manual de análises químicas de solos, plantas e fertilizantes. Brasília: Embrapa Informação Tecnológica; 2009.
68. Cruz CD. GENES—a software package for analysis in experimental statistics and quantitative genetics. Acta Sci. 2013;35:271–6.
69. Wright S. Correlation and causation. J Agric Res. 1921;20:557–85.
70. Saghai-Maroof MA, Soliman KM, Jorgensen RA, Allard RW. Ribosomal DNA spacer length polymorphisms in barley: Mendelian inheritance, chromosomal location, and population dynamics. P Natl Acad Sci USA. 1984;81:8014–8.
71. Ninamango-Cárdenas FE, Guimaraes CT, Martins PR, Parentoni SN, Carneiro NP, Lopes MA, et al. Mapping QTLs for aluminum tolerance in maize. Euphytica. 2003;130:223–32.
72. Lander ES, Green P, Abrahamon J, Barlow A, Daly M, Lincoln SE, et al. MAPMAKER: an interactive computer package for constructing primary genetic linkage maps of experimental and natural populations. Genomics. 1987;1:174–81.
73. Kosambi DD. The estimation of map distances from recombination values. Ann Eugenic. 1944;12:172–5.
74. Pinheiro J, Bates D, Debrov S. R-CORE-TEAM: nlme: Linear and nonlinear mixed effects models. 2014. http://cran.r-project.org/package=nlme.
75. Kao C-H, Zeng Z-B. Modeling epistasis of quantitative trait loci using Cockerham's model. Genetics. 2002;160:1243–61.
76. Haley CS, Knott SA. A simple regression method for mapping quantitative trait loci in line crosses using flanking markers. Heredity. 1992;69:315–24.
77. Zou F, Fine JP, Hu J, Lin DY. An efficient resampling method for assessing genome-wide statistical significance in mapping quantitative trait loci. Genetics. 2004;168:2307–16.
78. Lynch M, Walsh B. Genetics and analysis of quantitative traits. Sunderland: Sinauer Associates; 1998.
79. Zeng ZB, Kao CH, Basten C. Estimating the genetic architecture of quantitative traits. Genet Res. 1999;74:279–89.
80. Thompson JD, Gibson TJ, Plewniak F, Jeanmougin F, Higgins DG. The CLUSTAL_X windows interface: flexible strategies for multiple

sequence alignment aided by quality analysis tools. Nucleic Acids Res. 1997;25:4876–82.
81. Bi D, Cheng YT, Li X, Zhang Y. Activation of plant immune responses by a gain-of-function mutation in an atypical receptor-like kinase. Plant Physiol. 2010;153:1771–9.
82. Wang X, Zafian P, Choudhary M, Lawton M. The PR5K receptor protein kinase from *Arabidopsis thaliana* is structurally related to a family of plant defense proteins. P Natl Acad Sci USA. 1996;93:2598–602.
83. Jones DT, Taylor WR, Thornton JM. The rapid generation of mutation data matrices from protein sequences. Comput Appl Biosci. 1992;8:275–82.
84. Tamura K, Peterson D, Peterson N, Stecher G, Nei M, Kumar S. MEGA5: molecular evolutionary genetics analysis using maximum likelihood, evolutionary distance, and maximum parsimony methods. Mol Biol Evol. 2011;28:2731–9.
85. Creste S, Neto AT, Figueira A. Detection of single sequence repeat polymorphisms in denaturing polyacrylamide sequencing gels by silver staining. Plant Mol Biol Rep. 2001;19:299–306.
86. Schmittgen TD, Livak KJ. Analyzing real-time PCR data by the comparative C_T method. Nat Protoc. 2008;3:1101–8.